

**GENETIC PORE TYPING AS A MEANS OF CHARACTERIZING RESERVOIR
FLOW UNITS: SAN ANDRES, SUNFLOWER FIELD, TERRY COUNTY,
TEXAS**

A Thesis

by

AUBREY HUMBOLT

Submitted to the Office of Graduate Studies of
Texas A&M University
in partial fulfillment of the requirements for the degree of
MASTER OF SCIENCE

December 2008

Major Subject: Geology

**GENETIC PORE TYPING AS A MEANS OF CHARACTERIZING RESERVOIR
FLOW UNITS: SAN ANDRES, SUNFLOWER FIELD, TERRY COUNTY,
TEXAS**

A Thesis

by

AUBREY HUMBOLT

Submitted to the Office of Graduate Studies of
Texas A&M University
in partial fulfillment of the requirements for the degree of

MASTER OF SCIENCE

Approved by:

Chair of Committee,	Wayne M. Ahr
Committee Members,	David S. Schechter
	Yuefeng Sun
Head of Department,	Andreas Kronenberg

December 2008

Major Subject: Geology

ABSTRACT

Genetic Pore Typing as a Means of Characterizing Reservoir Flow Units: San Andres,
Sunflower Field, Terry County, Texas. (December 2008)

Aubrey Humbolt, B.S., Oklahoma State University

Chair of Advisory Committee: Dr. Wayne M. Ahr

Carbonate reservoirs are characteristically heterogeneous in reservoir quality and performance owing to the variety of processes that influence pore formation.

Additionally, porosity and permeability do not conform to depositional facies boundaries in carbonate reservoirs affected by diagenesis or fracturing; consequently, conventional methods of petrophysical characterization of flow units based on depositional facies are unreliable as predictors of reservoir behavior.

We provide an integrated stratigraphic, petrographic, and petrophysical study of the San Andres reservoir at Sunflower field that identifies and quality-ranks flow units on the basis of genetic pore types. A total of 12 full-diameter cores were analyzed revealing three primary depositional facies and cyclical patterns of deposition identified as parasequences. From the cores, 73 samples were chosen for thin sections. Through petrographic analysis, pores were classified using the Ahr 2005 method and four distinct, genetic pore types were identified. Petrophysical rock types were established by identifying which genetic pore types correspond to high poroperm values, and where they occur within the stratigraphic framework of the reservoir.

Sixteen coherent plugs were also subjected to mercury injection capillary pressure analysis in order to quantify pore – pore throat relationships. The data were then evaluated by facies, porosity type, and cycle position using graphical methods, such as k/ϕ , Winland R35, and Lorenz plots. The results of this study reveal that the most effective way of characterizing petrophysical flow units is the combination of k/ϕ ratio analyses and genetic pore typing.

This thesis is dedicated to the loving memory of Samuel and Joan Landwehr whose
spirit inspires me everyday.

ACKNOWLEDGEMENTS

First and foremost, I would like to thank my advisor, Dr. Wayne Ahr, for his guidance and encouragement throughout my time at Texas A&M University. Thank you for serving not only as my academic mentor, but also as my trusted friend. I will always be proud that I was one of your “kids”! Special thanks also go to my dedicated research assistant and friend Jonathan Funk.

I would also like to extend my gratitude to committee members Dr. Yuefeng Sun and Dr. David Schechter, as well as Texland Petroleum of Fort Worth, TX who sponsored this project. Sincere thanks are due to Texland geologist Keith Davis for his assistance and generous support. Thanks also go to my friends and colleagues for making my time at Texas A&M University such a wonderful experience.

Lastly, I would like to acknowledge my amazing family. Thanks to my mother and father who have always motivated me in my personal and professional life, and to my brother who has taught me the meaning of dedication and hard work. Most of all I would like to thank my husband Daniel for his continuing patience, support, and love.

NOMENCLATURE

BBL	Barrels
MBBL	Thousand barrels
BBL/D	Barrels per day
HPMI	High pressure mercury injection
K	Permeability in millidarcies (md)
Φ	Phi, porosity as a fraction or as a percent
PSIA	Pounds-force per square inch absolute
SMLP	Stratigraphic modified Lorenz plot

TABLE OF CONTENTS

	Page
ABSTRACT	iii
DEDICATION	v
ACKNOWLEDGEMENTS	vi
NOMENCLATURE.....	vii
TABLE OF CONTENTS	viii
LIST OF FIGURES.....	xi
LIST OF TABLES	xii
INTRODUCTION.....	1
Definition of Problem.....	2
Purpose of Study	3
Regional Geologic Setting	4
Sunflower Field.....	8
PREVIOUS WORK	10
San Andres Formation.....	10
Carbonate Porosity Classification	11
Carbonate Reservoir Characterization.....	14
METHODS.....	17
Materials for Study.....	17
Core Analysis	18
Petrographic Analysis	18
High Pressure Mercury Injection	22
Graphical Analysis	23

	Page
RESULTS.....	27
Reservoir Lithofacies	27
Wackestone Facies	28
Spiculiferous Wackestone Sub-Facies	29
Mudstone Facies.....	30
Packstone/Grainstone Facies.....	30
Occurrence of Anhydrite.....	31
Stratigraphic Architecture	32
Parasequence Structure	34
Sunflower Cycles	36
H1 Genetic Pore Types	38
Enhanced H1 Pores	38
Reduced H1 Pores	40
Relationship with Reservoir Lithofacies	42
HPMI Capillary Properties.....	43
Well Comparison.....	47
DISCUSSION AND INTERPRETATION.....	49
Petrophysical Relationships with Facies	49
Petrophysical Relationship with Genetic Porosity Type.....	51
Petrophysical Characterization.....	53
K Φ Ratio Analysis	54
Winland R ₃₅ Analysis	56
Petrophysical Rock Type Identification.....	58
Evaluation of Reservoir Capacity to Flow	62
Distribution of Flow Units Within Sunflower Field	65
SUMMARY AND CONCLUSIONS.....	67
Summary	67
Conclusions	68
REFERENCES CITED.....	70
APPENDIX A	75
APPENDIX B	101
APPENDIX C	105

	Page
APPENDIX D	166
VITA	175

LIST OF FIGURES

	Page
Figure 1 Map area of West Texas.....	5
Figure 2 Facies distribution map for the lower San Andres of West Texas	7
Figure 3 Ahr genetic classification of carbonate porosity	13
Figure 4 Idealized Winland plot	15
Figure 5 Adapted Ahr porosity classification	20
Figure 6 Example SMLP plot for Muldrow 11	26
Figure 7 Sunflower parasequences	33
Figure 8 Shallowing-upward model for carbonate parasequences	35
Figure 9 P37-2 drainage curves	45
Figure 10 M2 drainage curves	47
Figure 11 Poroperm relationship with facies.....	50
Figure 12 Poroperm relationship with thin section facies	51
Figure 13 Poroperm relationship with genetic pore type.....	53
Figure 14 K/Φ ratio analysis.....	56
Figure 15 Winland R_{35} analysis	58
Figure 16 Sunflower Petrophysical rock types.....	60
Figure 17 M2 SMLP plot.....	63
Figure 18 P37-2 SMLP plot.....	64

LIST OF TABLES

	Page
Table 1 Porosity classification scheme	39
Table 2 Pore type occurrence and poroperm relationship	42
Table 3 Summary table of HPMI capillary properties of M2 and P37-2	44
Table 4 Quick-look table of petrophysical rock type attributes	59

INTRODUCTION

The Permian Basin of West Texas and New Mexico is a prominent hydrocarbon rich provenance that accounted for nearly 17% of the United States production in 2002. After the Gulf Coast and Alaska, it is the third largest oil-producing region within the United States, containing 22% of the nation's proved oil reserves, some 5 billion bbl (Dutton, 2005). Carbonate reservoirs account for 75% of total oil production within the Permian Basin. Of the Permian Basin carbonate reservoirs, a significant portion produce from the San Andres formation.

Although carbonate reservoirs hold more than 60% of the world's oil and 40% of the world's gas reserves, inherent complexities present many technical risks. Carbonate reservoirs are characterized by heterogeneities in reservoir quality and performance owing to the wide variety of processes that influence pore formation. Unlike siliciclastic rocks, carbonates are primarily biogenic in origin and largely composed of skeletal and chemical grains. They are highly susceptible to diagenetic alteration, which together with the effects of depositional and fracture mechanisms results in complex porosity systems. Sandstone reservoir porosity and permeability are typically fabric and facies selective, and depositional intergranular porosity dominates (Ahr, 2006). However, carbonate reservoirs commonly exhibit a variety of porosity types such as interparticle, intercrystalline, moldic, vuggy, fracture, and fenestral. These carbonate pore types have been classified by Ahr et al. (2005) into three end-member genetic types: depositional,

This thesis follows the style of the American Association of Petroleum Geologists Bulletin.

diagenetic, and fracture with hybrids between end member types. Because of the variability among carbonate genetic pore types, corresponding petrophysical and reservoir performance characteristics can be more challenging to predict than in sandstone reservoirs.

In carbonate reservoirs affected by diagenesis or fracturing, porosity and permeability do not conform to depositional facies boundaries; consequently it is essential to: 1) classify genetic pore types by mode of origin; 2) determine which of the major genetic pore types contribute to high, moderate, and low combined values of porosity and permeability; 3) find tell-tale clues that help identify rock properties that serve as proxies, or correlatable markers, for the major genetic pore types; and 4) correlate the pore-proxy rock properties between wells to visualize the 3-D spatial distribution of pore types and corresponding flow units at reservoir scale. Flow units are defined as continuous reservoir zones with high, intermediate, and low values of porosity and permeability with correspondingly lower capillary resistance to fluid flow. Discontinuous zones characterized by lower poroperm values and indirect fluid flow around low poroperm segments are referred to as baffles. True barriers to flow do not allow fluid to flow vertically or horizontally. It is the distribution and connectivity of these three reservoir zones that determines performance in carbonate reservoirs.

Definition of Problem

Sunflower field, in Terry County, Texas, is an anhydritic dolomite reservoir in the San Andres Formation. Although the field is in stages of secondary recovery, little is

known about the spatial distribution and the lateral continuity of flow units in the field. The dominant genetic pore types and their association with flow units and the stratigraphic architecture of the field were also unknown. Additionally, a method of carbonate reservoir characterization that integrates genetic carbonate pore type had not previously been established.

Purpose of Study

Although the San Andres is a very productive formation, diagenetic alteration and complex stratigraphic architecture makes it very heterogeneous. Porosity and permeability distribution is often difficult to predict on the field-reservoir scale. For this reason typical recovery efficiencies for San Andres reservoirs are quite low, 30% or less, and residual oil saturations are high, about 30% (Kerans et al., 1994).

Ultimately, the purpose of this study is to establish an improved method of carbonate reservoir characterization that integrates reservoir petrophysical properties with genetic porosity classification. This new system will provide a superior means of identifying and ranking carbonate petrophysical flow units, thus improving recovery efficiencies within carbonate fields. Poroperm values, measured petrophysical data, stratigraphic architecture, lithofacies, and genetic pore types from Sunflower field will be used to test pre-existing and modified techniques of reservoir characterization. From the resulting analysis, a method of carbonate characterization will be proposed and recommendations regarding further development of Sunflower field will be made.

Regional Geologic Setting

Origins of the West Texas and New Mexico Permian Basin trace back to Pennsylvanian tectonism that asymmetrically deformed Precambrian basement and adjacent pre-Pennsylvanian sedimentary rocks (Major and Holtz, 1997; Ward et al., 1986). Sedimentation during the Permian took place in two basins; Midland Basin in the east and Delaware Basin in west (Figure1). These two basins were separated by the northwest-southeast trending Central Basin Platform. The northern extent of the Permian basin is defined by the Northern and the Northwestern shelves in Texas and eastern New Mexico. Along the Texas/New Mexico border, the contact between the Northern Shelf and the more southern Central Basin Platform and Midland basin is paralleled by the Abo Reef trend. The Abo trend is composed of a long, narrow, dolomitized reef complex that was deposited during the Early Permian (Ramondetta, 1992a).

Thick shelf carbonate accumulations in the northern Delaware Basin began in the Middle Pennsylvanian, but intense tectonism and associated siliciclastic sedimentation precluded significant Midland carbonate deposition. By Middle Wolfcampian time, tectonism subsided allowing a carbonate shelf and margin system to form around both the Midland and Delaware Basin (Ward et al., 1986). Through Guadalupian time, central portions of the two basins were primarily areas of siliciclastic sedimentation, although shelves and platforms remained carbonate. The Central Basin Platform was dominated by shallow water carbonates with minor siliciclastic input from Wolfcampian to Guadalupian time, but during the Ochoan both the Central Basin Platform and the Midland Basin became the site of cyclically deposited siliciclastics and evaporites.

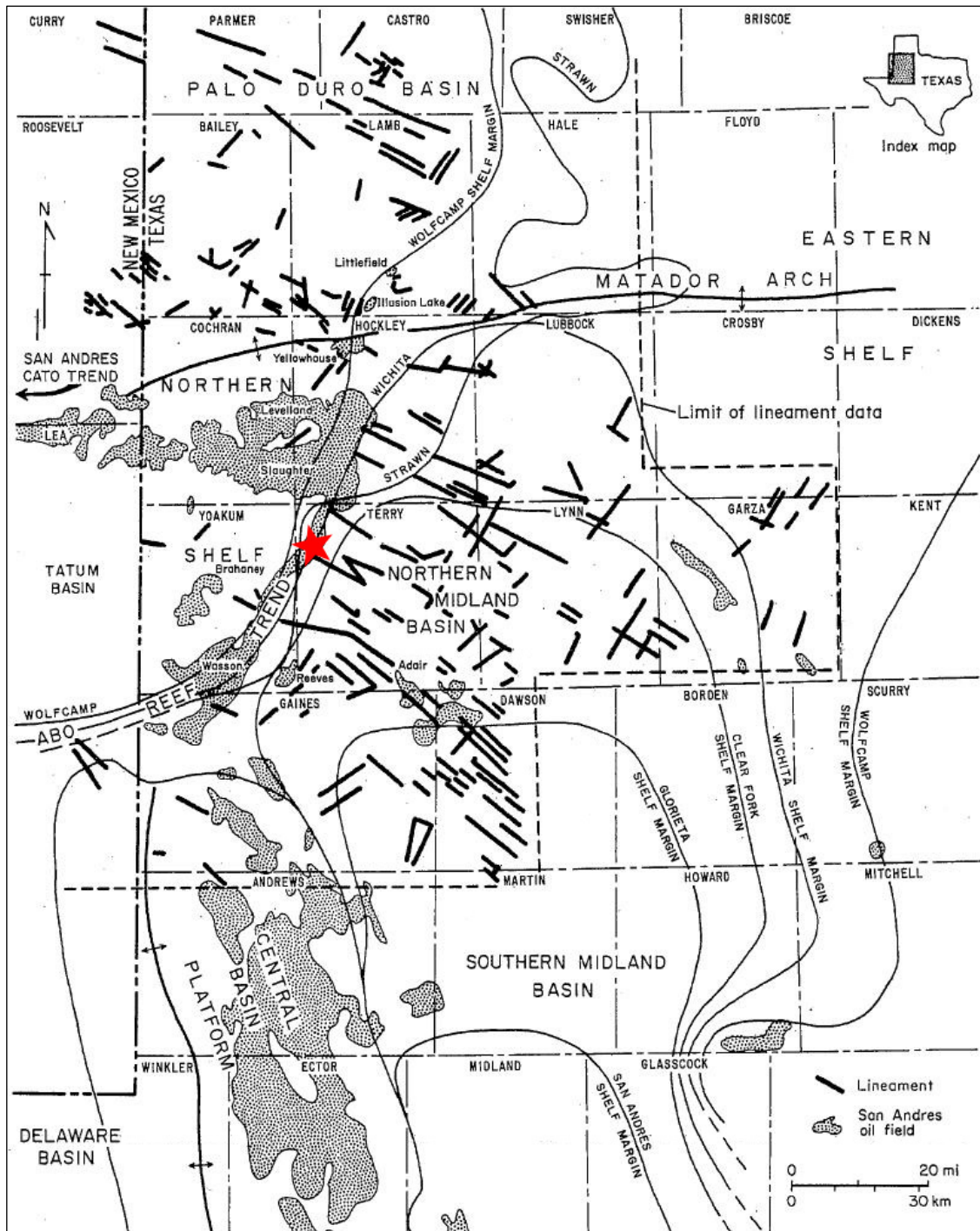


Figure 1: Map area of West Texas. Illustrates San Andres oil production, shelf margins, and the location of Sunflower field indicated by a red star. Modified from Ramondetta (1982a).

(Major and Holtz, 1997). The Late Permian (Leonardian-Ochoan) was characterized by tectonic quiescence, thus observed anticlinal structures are the result sediment drapes of pre-Permian hills, anticlines, or shelf margins (Hills, 1970).

During Leonardian to Guadalupian times, an eastward prograding sequence was deposited in the Delaware and Midland Basins, the San Andres Formation. In West Texas, the San Andres is underlain by the sandy, anhydritic dolomites of the Leonardian Glorieta and Yeso formations, and overlain by the evaporitic dolomites of the Guadalupian of the Grayburg Formation. The San Andres is a large scale shoaling upward depositional cycle consistent with a carbonate ramp depositional model. Open-marine shelf deposits are overlain by more restricted, shallow shelf and tidal flat deposits, which are topped by supratidal sabkha deposits (Cowan and Harris, 1986). Dominant lithofacies include dolomite and anhydritic dolomite with less common limestone, bedded evaporites, and siliciclastic red beds. Distribution of these facies in the lower San Andres of West Texas is illustrated in Figure 2. The San Andres is commonly divided into upper and lower parts using a siltstone marker bed π that is regionally correlatable over the Northwest Shelf.

Shelf and tidal flat cycles within the lower San Andres are strongly vertically stratified by high frequency, parasequence scale, shoaling upward successions of subtidal, intertidal, and supratidal deposits. The cyclic nature of these deposits has separated the lower San Andres into alternating zones of high and low reservoir quality (Pranter, 1999). Cyclic bedded anhydrites and tight dolomites, as well as updip porosity pinch outs from evaporite plugging serve as stratigraphic traps (Ward et al., 1986).

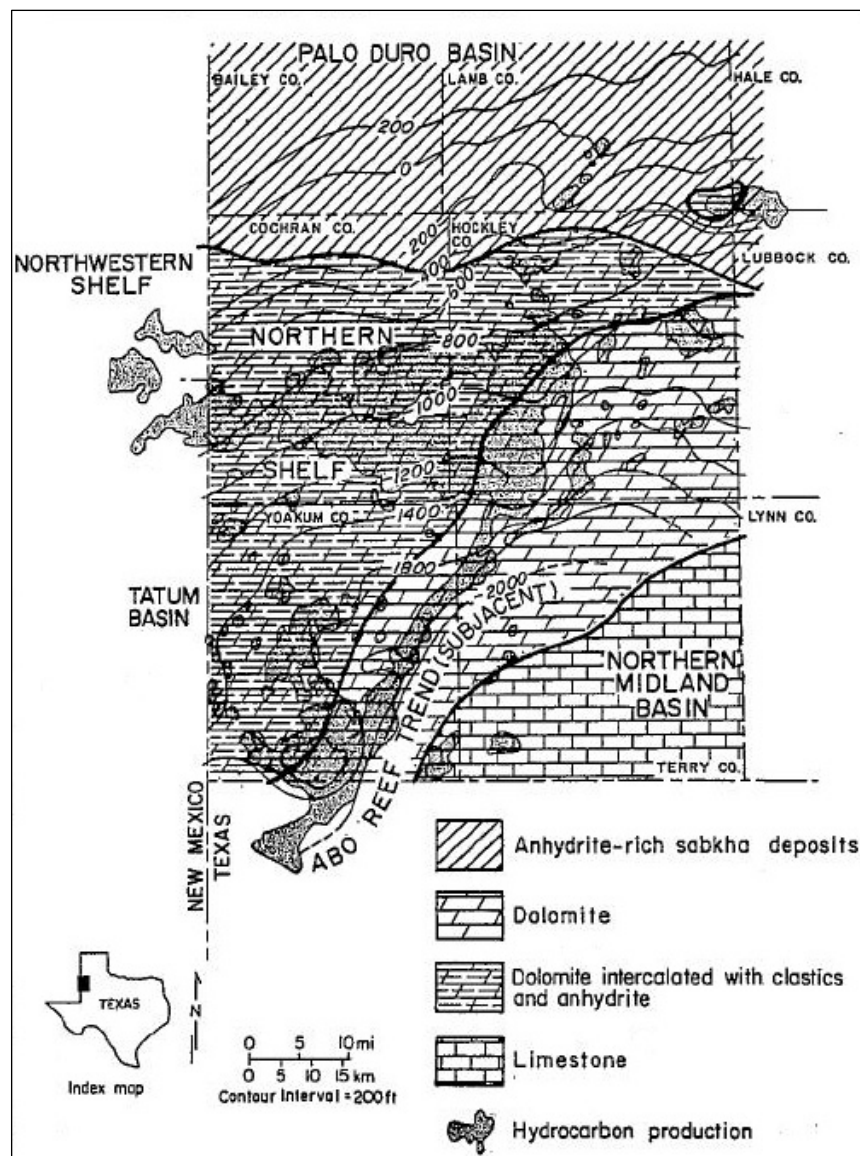


Figure 2: Facies distribution map for the lower San Andres of West Texas. Structure on the π marker is illustrated with contours. From Ramondetta (1982b).

Previously mentioned, basement seated anticlinal structures also serve as traps within portions of the San Andres reservoir.

More than 80% of the total oil production from the Northern Shelf of the Midland Basin comes from the San Andres formation (Ramondetta, 1982b). Northern

Shelf San Andres oils originated in Wolfcampian basinal deposits in the Midland Basin. Migration occurred from the basin towards the Abo Reef trend where vertical fractures allowed the oil to migrate into stratigraphically higher units. Porosity was created during times of periodic subaerial exposure of the carbonate platform and subsequent leaching by meteoric waters (Ramondetta, 1982b). It is theorized that subaerial exposure of the San Andres during the Late Permian was the result of eustatic sea level changes related to recurring glaciation in Gondwanaland (Hills, 1972).

Sunflower Field

South Sunflower field produces from the top of the lower San Andres Formation in the Northwest Shelf of the Permian Basin. The field is located in the northwestern corner of Terry County, Texas, along the Abo Reef trend (Figure 1). Within the South Sunflower field, π is expressed as a thin, shaley to silty zone located directly above the pay zone, typically around a depth of 5,300 feet. Sunflower pay is composed of several stacked, laterally continuous, high frequency cycles defined herein as parasequences. Dolomite, anhydritic dolomite, and thin bedded anhydrite serve as dominant facies although minor lime and silt can be found. Depositional facies indicate an arid tidal flat environment with relatively shallow subtidal (possibly lagoonal), channelized intertidal, and evaporitic supratidal components.

Texland Petroleum, Inc. of Fort Worth, TX, operates a portion of the South Sunflower field with an area of approximately 5 miles. This study focuses Texland controlled sections, specifically the Muldrow section in the central portion of Sunflower

field. The first well was drilled in the Sunflower area in 1986, however the South Sunflower was not drilled by Texland until 2004. A low relief anticlinal structure striking northeast to southwest bisects the South Sunflower. Structural strike and dip are believed to be the same as depositional strike. Poroperm trends tend to follow the structure but do not always conform to its boundaries. Cyclically repeated successions of tight evaporites and dolomites, as well as lateral facies change and anhydrite plugging are the most likely trapping mechanisms. The reservoir was initially produced via solution gas drive, but stages of secondary recovery have been initiated with the emplacement of 13 injection wells evenly spaced across the field.

PREVIOUS WORK

San Andres Formation

Many studies have been undertaken to define the stratigraphic framework of the San Andres Formation in New Mexico and West Texas. Elliot and Warren (1989), Kerans et al. (1992, 1993, 1994), Hovorka et al. (1993), Harris et al. (1993), Grant et al. (1994), and others have conducted regionally extensive outcrop studies along the Guadalupe Mountains. These studies have defined multiple scales of cyclicity and associated facies and porosity trends within the San Andres. Kerans et al. (1994) identified six rock fabric assemblages and developed a fabric-based flow unit model that followed the sequence framework and depositional facies architecture within the cycle framework. Parasequence-scale cycles were described and further related to the distribution of porosity and permeability trends by Hovorka et al. (1993). Observations resulting from these outcrop studies show that the San Andres is composed primarily of carbonate ramp facies with subsurface reservoir equivalents.

San Andres depositional environments and diagenetic sequences have been widely studied and described. Ramondetta (1982a) provided a detailed analysis of facies occurrence and distribution within the San Andres of the Northern and Northwestern Shelves. Subsurface stratigraphic and environmental observations were tied to equivalent outcrop analogs by Elliot and Warren (1989). Other studies including Silver and Todd (1969), Milner (1976), Meissner (1972), Chuber and Pusey (1985), Cowan and

Harris (1986), Keller (1993) recognized the highly cyclic, shoaling nature of the Northern and Northwestern Shelf San Andres.

Although research is prevalent in the San Andres of West Texas, no studies have been published, to date, that focus on reservoirs within Terry County. Work has been conducted within the lower San Andres of adjacent Yoakum (Chuber and Pusey, 1969, 1985; Amare, 1995), Cochran, and Hockley (Cowan and Harris, 1986) counties. Again, the cyclic nature of low to high energy deposits was observed and the spatial distribution of porosity was analyzed. Post-depositional diagenetic processes such as dolomitization, anhydrite and gypsum cementation, and leaching were found to have reversed depositional porosity patterns on both the cyclic and regional scale.

Carbonate Porosity Classification

A variety of carbonate porosity classification schemes have been proposed through the years. Many group pores according to pore geometry, pore size, petrophysical characteristics, or pore origin. However, most conventional classification schemes do not illustrate the relationships between petrophysical reservoir and rock characteristics (Ahr, 2006).

Archie (1952) devised one of the first carbonate porosity classification schemes that attempted to relate rock fabric to petrophysical rock properties. Archie recognized that not all carbonate pores are observable with petrographic microscopy and thus divided pore space into *visible* and *matrix*. *Matrix* porosity was estimated based upon its texture (chalky, sucrosic, or compact) while *visible* porosity was described in terms of

size. Petrophysical parameters such as permeability and capillary pressure characteristics were also related back to these textures. Archie's method of classification proved difficult to relate with geologic models because no distinction was made between depositional and diagenetic fabrics (Lucia, 1995).

Perhaps the most recognizable method of carbonate porosity classification is that of Choquette and Pray (1970). Choquette and Pray organized pores into three groups depending on whether they are *fabric selective*, *not fabric selection*, or *fabric selective or not*. The primary shortcoming of this classification is that no correlation is made between pore type and resulting petrophysical characteristics. For instance, moldic and interparticle porosity are both classified as *fabric selective* but have significantly different effects on petrophysical rock properties.

A new method of classification was developed by Lucia (1983) that emphasized petrophysical characteristics of carbonate pores and divided pores into *interparticle* (between grains or crystals) and *vuggy* (separate or touching). Although Lucia's method relates pore type to capillary pressure characteristics, Archie *m* values, permeability, and porosity, it offers no genetic modifiers or categories for diagenetically altered pores.

A simplified but comprehensive classification of carbonate pores was proposed by Ahr et al. (2005). The Ahr system focuses on the origin and timing of reservoir porosity allowing correlations to be drawn between rock and reservoir properties. Pores are classified based on end-member processes: *depositional*, *diagenetic*, or *fracture*, and can be displayed on a ternary diagram (Figure 3). Depositional pores are closely related to original rock texture and fabric, and include interparticle, intraparticle, shelter,

fenestral, and reef porosity. Diagenetic porosity is formed through dissolution, recrystallization, cementation, compaction, replacement, and pressure solution processes. Fracture porosity results from brittle failure of the rock under differential stress (Ahr et al., 2005). By linking pore geometry and pore genesis, the Ahr method of carbonate pore classification can be used for subsurface mapping and the evaluation of petrophysical flow units.

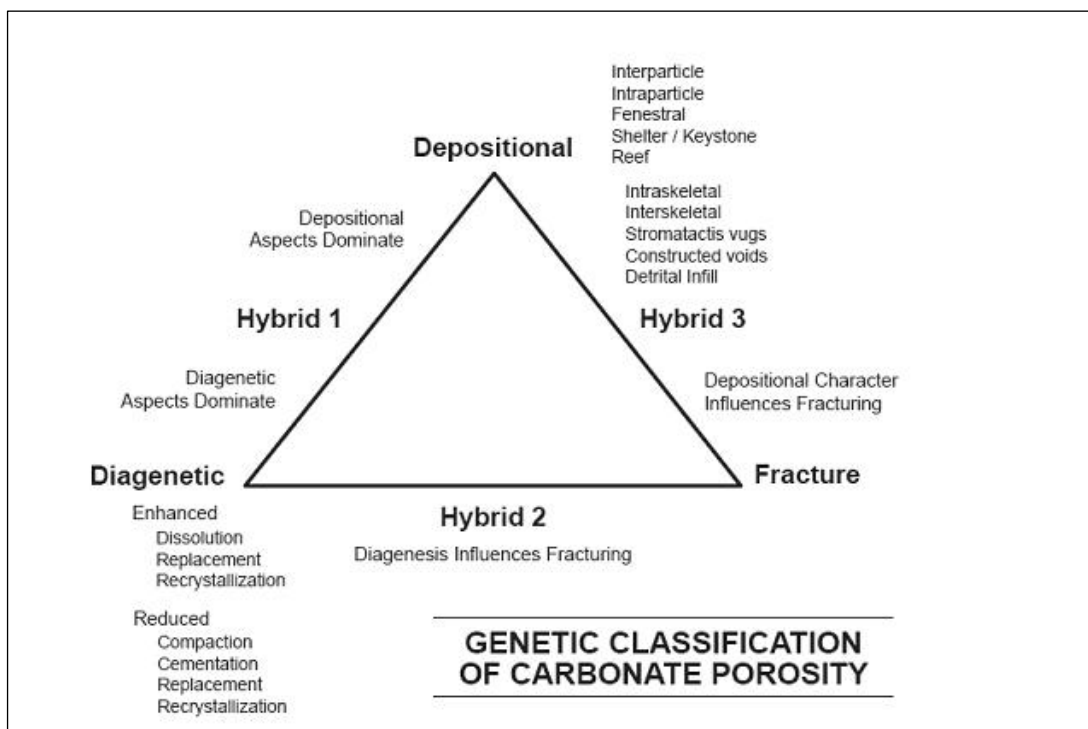


Figure 3: Ahr genetic classification of carbonate porosity. From Ahr et al., (2005).

Carbonate Reservoir Characterization

While working with the Amoco Research Department, Dale Winland devised a system of estimating the average pore throat size of a core sample. Using 322 sandstone and carbonate specimens, Winland developed an empirical relationship among porosity, air permeability, and pore throat aperture at a mercury saturation of 35% (Pittman, 1992). The resulting Winland equation was first published by Kolodzie (1980):

$$\text{Log } R_{35} = 0.732 + 0.588 \text{ Log } K_{air} - 0.864 \text{ Log } \Phi$$

where R_{35} is the pore aperture radius corresponding to 35% mercury saturation, K_{air} is uncorrected air permeability in millidarcies, and Φ is porosity entered as a percent.

Kolodzie (1980) and later publications of Hartmann and Coalson (1990) and Pittman (1992) characterized petrophysical flow units in sandstone reservoirs through a series of interrelated R_{35} , porosity, permeability, and capillary pressure crossplots. However, Pittman argued that the measurement of pore throat radius at the 25th percentile of mercury saturation (R_{25}) is a more accurate estimator of permeability in sandstones.

Winland's R_{35} method flow unit characterization was applied to carbonate reservoirs by Martin et al., (1997). Martin found that R_{35} characteristics for a specific carbonate flow unit reflect both the depositional environment and diagenetic fabric of the rock and resulting flow performance. Using the Winland Plot, a semi-log crossplot of permeability (md) versus porosity (%) with R_{35} isopore throat lines (Figure 4), Martin was able to use R_{35} as a means of identifying and characterizing flow unit types in four different carbonate reservoirs. Gunter et al., (1997) also demonstrated the effectiveness

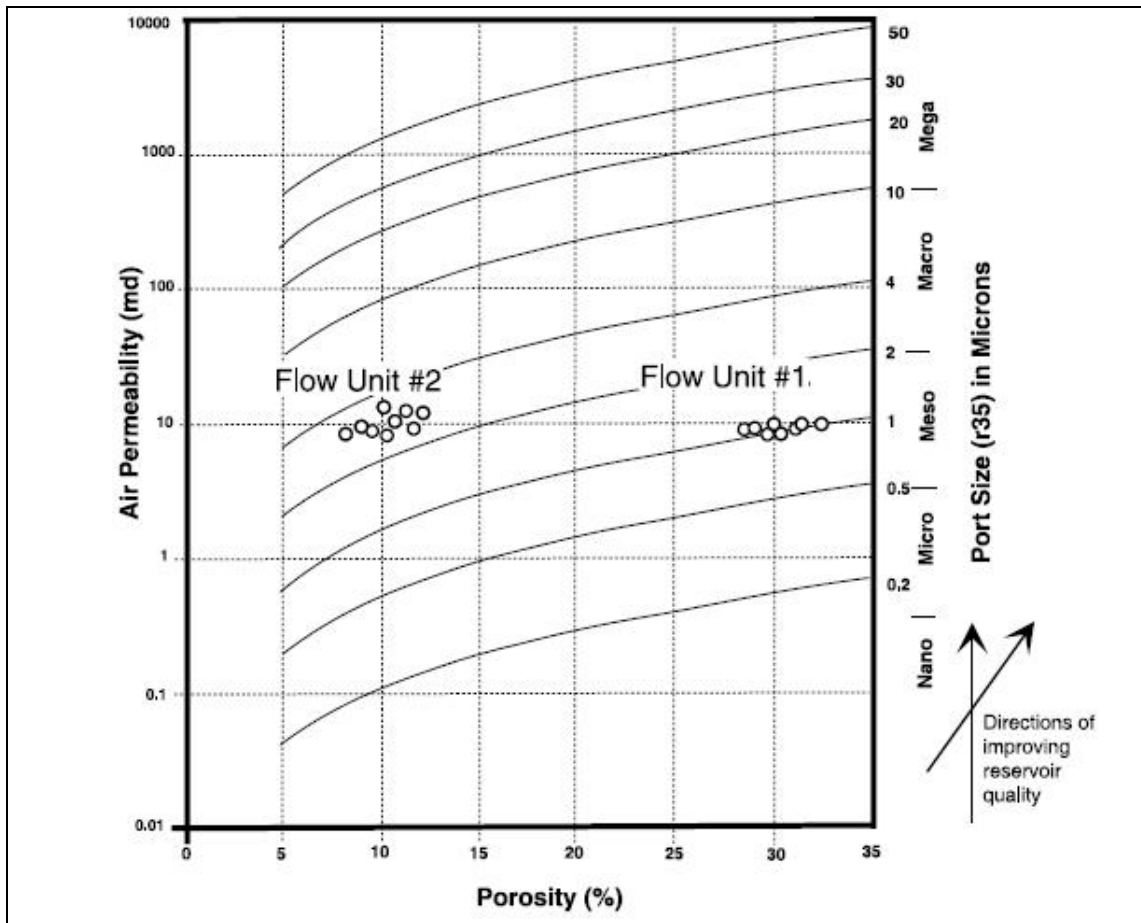


Figure 4: Idealized Winland plot. Illustrates how flow units can be identified using R_{35} isopore throat lines. From Hartmann (1999).

of the Winland plot when used in conjunction with other graphical tools such as modified Lorenz plots to characterize carbonate flow units.

More recent publications have proposed higher mercury saturations for carbonate reservoir characterization. Rezaee et al. (2006) found that characteristics of carbonate reservoirs with high pore network complexity are better estimated by pore throat apertures at higher mercury saturation percentiles. Their research revealed that best correlation coefficients for permeability, porosity, and pore throat radii for carbonates

are obtained using a pore throat radius measured at 50% mercury saturation (R_{50}). The large discrepancy between R_{50} and the previously mentioned sandstone permeability estimators of Winland's R_{35} and Pittman's R_{25} is most likely explained by pore network complexity. Sandstones pore networks are typically intergranular and homogenous, whereas diagenesis in carbonates can create a wide variety of complex pore/pore throat systems.

METHODS

Materials for Study

This study provides an integrated stratigraphic, petrographic, and petrophysical study of the San Andres reservoir at Sunflower field that identifies and quality-ranks flow units on the basis of genetic pore types. A total of 12 wells were sampled throughout Sunflower field. From each of the wells, 30 to 45 foot continuous, full-diameter cores were used to identify and correlate depositional facies and parasequences. Cores were accompanied by conventional core analysis data that was obtained by Core Laboratories Inc., Houston, Texas, at an earlier date. Data sets for each well include vertical and horizontal permeability, porosity, grain density, water saturation, and oil saturation measurements taken in one foot intervals from core. Core analysis permeability values used in this study refer to horizontal permeability (K90) values.

Seventy-three thin sections were taken from carefully selected, representative rock and pore types in the cores in order to identify reservoir facies and genetic pore types from various positions within parasequences. Special attention was given to two wells, M2 and P37-2, which exhibit strongly contrasting reservoir characteristics. From these two wells, sixteen samples were chosen and subjected to high pressure mercury injection (HPMI) capillary analysis and coherent petrographic thin section examination.

Core Analysis

A total of 12 full-diameter cores were analyzed revealing three primary depositional facies and cyclical patterns of deposition identified as parasequences. Observations were made and recorded in one inch intervals using a low-zoom stereo microscope. Descriptions follow the AAPG Sample Examination Manual format and are found in Appendix A. Facies were classified using the traditional Dunham classification, which emphasizes depositional texture: grain supported versus mud supported. Wells P37-1 and Muldrow 14 only received cursory descriptions due to their apparent similarity with adjacent wells.

In this study, parasequences are defined as shoaling-upward sedimentary successions that are bounded by marine flooding surfaces after Van Wagoner et al. (1990). These successions were identified in cores as transitions from subtidal to supratidal depositional facies and maximum exposure surfaces were defined based on evidence of subaerial exposure such as desiccation cracks or bedded evaporate deposits.

Petrographic Analysis

From of the core, 73 samples were chosen for thin section analysis. In order to identify the spatial distribution of genetic pore types within the stratigraphic framework, cores were sampled from the bottom, middle, and top of each correlatable parasequence from multiple wells across Sunflower field. Well selections were made on the basis of individual well performance as well as their position along depositional strike and dip. Thin sections were also taken from carefully selected examples of representative rock

and pore types that exhibit characteristic diagenetic and depositional patterns found throughout the field. Four of the twelve wells that were analyzed were not represented in the thin section analysis due to their strong correlation with neighboring well lithology, porosity, and stratigraphic architecture.

After sample locations were selected from core analysis, billets were cut using a slab saw. Billets were processed by National Petrographic Service, Inc. in Houston, Texas. Samples were impregnated with blue epoxy to assist in porosity identification and stained with alizarin red to define any occurrence of calcite. However, coherent thin sections taken from MICP plugs were not subject to blue epoxy impregnation or staining. In these 16 samples, porosity was identified on the basis of isotropic epoxy extinction and lack of crystal form. Calcite was found to be a negligible mineralogical component throughout the sampling area. For this reason, the differentiation between calcite and dolomite in these samples was not made.

Through petrographic analysis, pores were classified using an adapted form of the Ahr et al., (2005) method, which emphasizes the origins of porosity: deposition, diagenesis, and fracturing. Significant fracturing has not been observed in Sunflower field, thus the genetic porosity classification used in this study focuses on the ratio of depositional to diagenetic pores in each sample. Pores that conform to original rock texture and fabric are classified as depositional pores and are considered to be facies selective. Depositional pores that have been altered by some form of diagenesis are classified as Hybrid 1 pores. Hybrid 1 pores are subdivided into three categories: H1-A, H1-B, and H1-C (Figure 5).

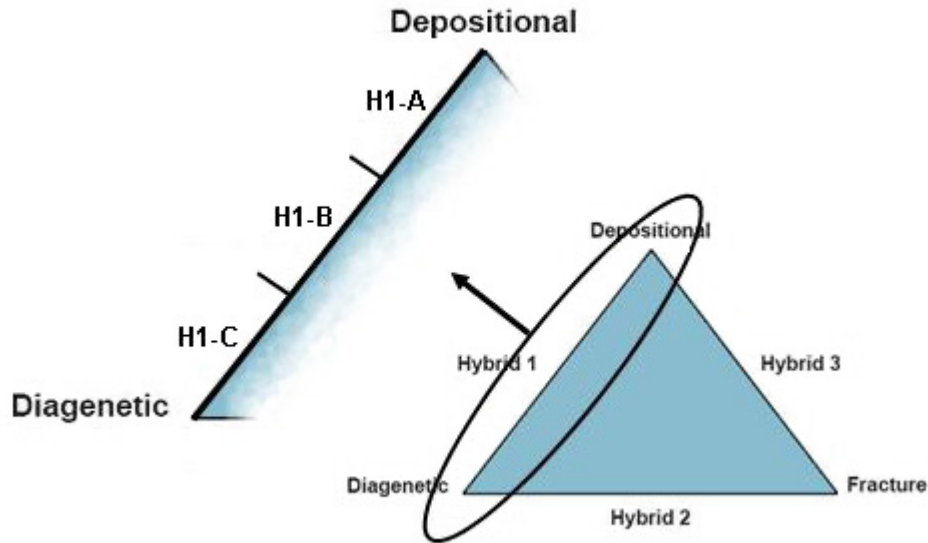


Figure 5: Adapted Ahr porosity classification. Based on the Ahr genetic classification of carbonate porosity. Modified from Ahr et al., (2005).

If depositional characteristics dominate but are somewhat altered by diagenesis, the porosity is classified as Hybrid 1-A (H1-A). In the case of H1-A, facies is still a reliable proxy for porosity. Appendix D, Figure D.7 depicts a spiculiferous dolowackestone dominated by skel-moldic porosity. Although porosity was generated by a diagenetic process, it is closely linked to the original texture of the rock due to its dependence on grain dissolution and not mud matrix dissolution.

If porosity exhibits equivalent depositional and diagenetic control, then the porosity is classed as H1-B. H1-B pores still retain most depositional texture and fabric controls, but diagenesis has made facies a less reliable predictor of porosity. Appendix D, Figure D.9 also displays a spiculiferous dolowackestone with skel-moldic porosity, but diagenetic intercrystalline porosity is equally significant in this example. Again,

porosity is greatly influenced by the original texture of the wackestone, but additional diagenesis in the form of recrystallization and crystal dissolution has weakened the correlation with facies.

When the diagenetic overprint overrides relict depositional texture and fabric, facies can not be used as a proxy for porosity. Pores of this nature are classified as H1-C. If diagenetic alteration dissects and destroys original depositional characteristics, then the porosity is classified as purely diagenetic. H1-C porosity was only found in isolated, irregular beds and is not considered to be significant pore type within the studied Sunflower interval. No examples of purely diagenetic or depositional pores were found.

Diagenetic and hybrid pores are further segregated into two classes: enhanced or reduced. Determination of porosity reduction versus enhancement was determined by developing a diagenetic history for each sample using petrographic analysis. The type of diagenesis is simply denoted by the letters “r” and “e” following the pore type. For example, a H1-A pore that has been enhanced would be denoted H1-Ae.

Some forms of diagenesis, such as cementation, replacement, compaction, or recrystallization can reduce existing porosity. In some cases, diagenetic porosity reduction can reduce a flow unit to a baffle or even a barrier. Alternatively, diagenesis can enhance porosity through dissolution and some forms of replacement and recrystallization. Appendix D, Figure D.15 illustrates the difference between the two forms of diagenetic modification. Lower portions of the sample illustrate a dissolution enhanced skeletal wackestone with H1-Ae porosity. Conversely, the upper portion exhibits obvious porosity reduction through mechanical compaction of a peloidal

wackestone creating H1-Br porosity. The two different lithofacies and pore types were likely brought into contact with one another through pressure solution associated with stylolitization.

High Pressure Mercury Injection

Special attention was given to two wells which exhibit contrasting reservoir characteristics. M2, located in the central portion of the Muldrow drilling area, has an average porosity of 11.2%, average permeability of 2.981 md and has produced over 21.5 mbbls since discovery. Well P37-2 lies at the northeastern edge of the Texland study area in the Pool 37 section. It exhibits an average porosity of 9.8%, average permeability .691 md. P37-2 cumulative production is less than two thirds of M2 production, only 7.1 mbbls since discovery. From these two wells, 16 core plugs were obtained and subjected to high pressure mercury injection analysis (HPMI) in order to quantify pore to pore throat relationships. Core derived plugs were taken from the bottom, middle, and top of multiple parasequences within the two wells. Samples were also selected to represent typical reservoir facies and poroperm trends, and to avoid large anhydrite accumulations and positions that fall below the oil/water contact. Coherent thin sections were also obtained in order to determine genetic pore and lithofacies type.

HPMI measurements were conducted by Core Laboratories Inc., Houston Texas. Preceding the injection testing, core plug samples were evacuated with toluene to extract residual hydrocarbons and other pore-filling compounds. After cleaning, the plugs were dried in a vacuum oven to remove the toluene. Samples were tested using the high

pressure injection Micromeritics Autopore. Pressures were incrementally increased from 0 to 55,000 psia, allowing time for saturation equilibrium to be reached at each incremental pressure. Injected mercury data was recorded at 85 pressure points from 1.04 psia to 54,900 psia. Results from the HPMI testing includes: 1) drainage curves for each sample based on mercury saturation at each incremental pressure point, 2) mercury derived porosity, 3) permeability measured to air and using the Swanson equation, 4) R_{35} and R_{50} median pore throat calculations for each sample, 5) pore throat distribution based on fraction of intruded pore space, 6) pore throat size histograms for each sample, and 7) J-function values at each incremental pressure point.

Graphical Analysis

Data from the 17 HPMI samples were then evaluated by facies, porosity type, and cycle position using graphical methods, such as K/Φ ratio graphs, Winland R_{35} plots, and Lorenz plots in order to determine the most effective way of characterizing carbonate petrophysical flow units. Several methods of petrophysical rock typing were explored in this study. Petrophysical rock types are classified according to the petrophysical attributes that influence reservoir performance: porosity, permeability, capillary pressure, saturations, etc. Petrophysical rock types are defined independent of facies.

First, traditional porosity and permeability semi-log crossplots were constructed in order to evaluate the relationship, if any, between poroperm values, facies, and genetic porosity type. $K/$ ratio lines were used to illustrate the comparative 'value' of ratios

corresponding to the K/Φ data points. Second, the R_{35} Winland plot was tested against the K/Φ ratio method. Winland's method consists of a permeability versus porosity semi-log plot with isopore throat (R_{35} Ports) lines. Again the relationships between poroperm values, facies, and genetic pore types, were evaluated using R_{35} isopore lines as a quality gauge. Ultimately, petrophysical rock types were established by identifying which genetic pore types correspond to high and low poroperm values. Their occurrence within parasequences and distribution across the reservoir was then established.

The Lorez plot is a petrophysical plot that was devised in order to define a measure of reservoir heterogeneity, the Lorenz coefficient (Jensen et al., 1997). Lorenz plots graphically display the relationship between the transmissivity or flow capacity (the permeability thickness product, Kh) and the storage capacity (the product of porosity and thickness, Φh) of a reservoir rock. From it, the distribution of pore throat sizes can be related to fluid capacity.

In homogenous reservoirs pore-throats are uniformly distributed and contribute evenly to flow. Therefore, flow and storage capacity are relatively balanced and data plot along a diagonal at roughly 45 degrees. Reservoir heterogeneity is represented by a departure from this diagonal, and can be quantified using the Lorenz coefficient. The coefficient is a number between 0 and 1 that illustrates how unevenly flow capacity is distributed in a rock when compared to storage capacity. Homogenous reservoirs are represented with a coefficient of 0; heterogeneity increases with increasing coefficients with 1 indicating that only a small percentage is responsible for the majority of the flow.

By plotting data points in stratigraphic order on a Lorenz plot it becomes possible to identify zones with the greatest capacity to flow within a reservoir. Stratigraphic Modified Lorenz Plots (SMLP) were constructed after Gunter et al., (1997), in order to define petrophysical flow units within wells M2 and P37-2. SMLP illustrate cumulative flow capacity (cumulative %Kh) versus the cumulative storage capacity (cumulative %K Φ) ordered in the stratigraphic sequence of the reservoir. Figure 6 illustrates a SMLP derived from M11 core analysis data. Inflection points indicate changes in flow or storage capacity, allowing for the evaluation of reservoir flow. Steeper slopes indicate faster rates of flow; similarly, horizontal trends indicate little to no flow. The relatively constant 45 degree trend of the storage capacity line indicates that storage capacity is uniformly distributed throughout the reservoir. Where the two lines overlap or plot closely together, all pores are contributing equally to flow; intercrystalline or interparticle porosity could yield such a trend. Where separation occurs, different pores are contributing more to flow than others; moldic or vuggy porosity could plot in this manner.

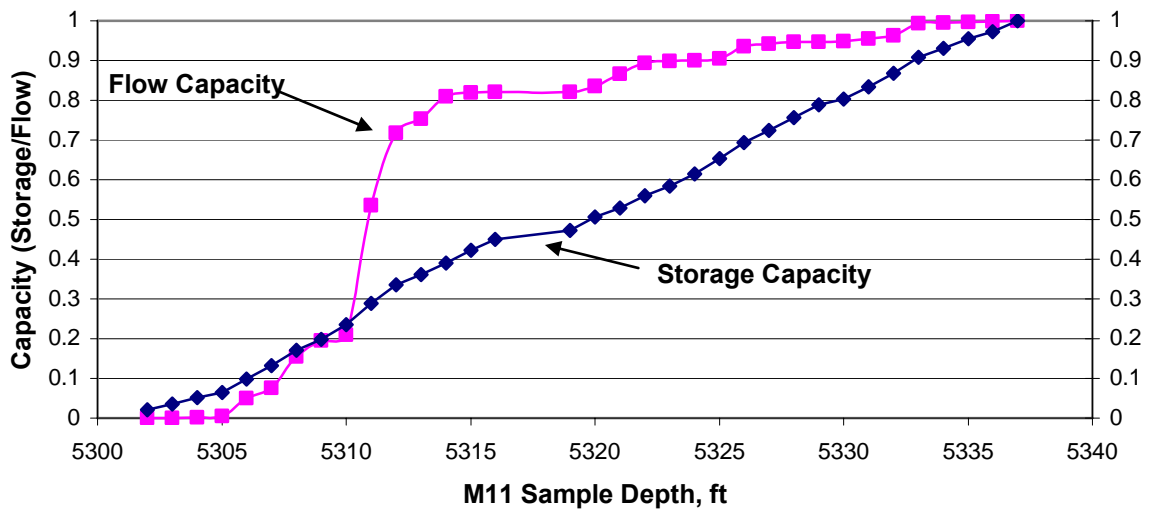


Figure 6: Example SMLP plot for Muldrow 11. Storage capacity is evenly distributed across M11 with the exception of depth 5314.5 ft. At this point flow and storage capacity are reduced, which is indicated by the horizontal trend. Highest flow is associated with the vertical trend from 5310 to 5313 ft. The steep slope of the flow capacity line indicates that a large portion of M11 flow (roughly 50%) comes from this three foot interval which is associated with H1-Ae/Be porosity.

RESULTS

Results from core evaluation and petrographic analysis will be discussed in this section. This includes the identification and illustration of four common reservoir facies, three complete parasequence cycles (numbered C1 to C3, from bottom to top respectively), and four primary genetic pore types. Relationships among facies, porosity, and position within the stratigraphic architecture will then be drawn. Capillary property measurements from HPMT pressure testing will also be discussed and related back to facies and porosity type.

Reservoir Lithofacies

Core evaluation and petrographic analysis of Sunflower field has led to the identification of three major, pervasively dolomitized facies: dolomudstone, dolowackestone, and dolopackstone/dolograinstone. Additionally, a spiculiferous sub-facies of dolowackestone was found to be regionally extensive and petrophysically significant. For ease of description, the prefix dolo is dropped in further discussions. Relationships among lithofacies, textures, and sedimentary structures are consistent with shallow subtidal, intertidal, and supratidal depositional environments. These environments and their corresponding facies are found vertically stacked in cyclic parasequences which will be discussed in the following section.

Small framework grains (averaging 250 μm or less), pervasive dolomitization, and abundant anhydrite precluded definitive facies identification from core analysis.

Many core described packstone intervals were found to be spiculiferous wackestones whose moldic porosity resembled peloidal and interparticle pores at the core scale. For this reason, facies were primarily defined petrographically. Porosity and permeability values given in this section come from core analysis and capillary measurements of samples whose facies were definitively identified through petrographic analysis.

Wackestone Facies

Three major facies, mudstone, wackestone, packstone/grainstone, and a spiculiferous wackestone sub-facies were identified in cores and thin sections from Sunflower field. Wackestone serves as the primary reservoir facies, accounting for 35% of the core analyzed. Wackestones are typically composed of a mixture of peloidal and skeletal grains. The facies is dominated by micritic peloidal grains averaging 100-250 μm in diameter and various skeletal fragments including benthic foraminifera, sponge spicules, green algae, ostracods, gastropods, crinoids, and mollusks. Skeletal fragments average around 250 μm but can vary greatly in size, from less than 100 μm to greater than 500 μm .

Skeletally dominated wackestones are typically found in the middle portions of depositional cycles and are interpreted as subtidal environments. Fossil assemblages indicate a relatively shallow depth. Peloidal dominated wackestones are usually found near the top of depositional cycles associated with nodular anhydrite, muddy wavy laminations, channel scours, rip-up clasts, and occasionally algal laminations. These textural characteristics indicate an intertidal depositional environment. Skeletal and

peloidal wackestones exhibit similar petrophysical characteristics and have been grouped into a single lithofacies (W) for the purpose of this study (Appendix D, Figures D.1, D.10, and D.11).

Spiculiferous Wackestone Sub-Facies

Within some wackestone facies, sponge spicules account for greater than 50% of the total framework grains (Appendix D, Figures D.2, D.7, and D.9). These spiculiferous wackestones exhibit distinctive petrophysical properties, and for this reason are categorized into a wackestone sub-facies (SW). SW sub-facies accounts for nearly 26% of the reservoir facies and is found concentrated in the middle to upper portions of parasequence Cycle 1 in beds ranging in thickness from 5 to 15 ft. Spicules are detrital but do not display any preferred orientation, thus these thick accumulations represent a low energy, subtidal sediment sink. The well preserved elongate nature of the spicules indicates that they were transported over relatively short distances. Spiculiferous carbonates have been described from a wide range of water depths making them poor environment indicators (Bein and Land, 1982).

The spiculiferous sub-facies is characterized by extensive leaching of siliceous spicule grains yielding skel-moldic porosity. However, less than 10% of the spiculiferous beds exhibit siliceous cementation and replacement of the surrounding dolo-mud matrix (Appendix D, Figures D.13 and D.14). These spiculiferous wackestones/packstones are found in irregular 1 to 3 inch gray bands that exhibit little to

no visible porosity. Similar deposits were noted by Bein and Land (1982) in their study of the San Andres in the Palo Duro Basin.

Mudstone Facies

Mudstone (M) facies account for roughly 23% of the total reservoir facies and are typically found at the base of depositional cycles. Shaley, organic rich laminations and detrital siliciclastic silt often accompany mudstone facies (Appendix D, Figure D.3). Such mudstones are interpreted as shallow subtidal or lagoonal depositional environments. Occasional mudstone facies are found associated with desiccation features and anhydrite accumulations at the top of depositional cycles. These mudstones are attributed to intertidal and supratidal environments.

Packstone/Grainstone Facies

The least prevalent lithofacies in Sunflower field is the packstone/grainstone facies (P/G). Grainstones account for less than 2% of the reservoir facies thus they have been grouped with the packstone facies for the purpose of this study. The packstone/grainstone facies constitutes 12% of the reservoir and is typically found at the top of depositional cycles. P/G facies is dominated by micritic peloids, pellets, oncoids, and other undifferentiated coated grains. Oncoidal accumulations indicate a high energy regime, possibly a shoal crest environment (Appendix D, Figure D.4). However, peloidal and pelletal dominated P/G facies could be attributed to deposition in intertidal channels and ponds (Appendix D, Figure D.5).

Unusual 1 to 4 foot skeletal P/G intervals are found in Cycle 1, directly below the SW bed (Appendix D, Figure D.6). The contact between the P/G and surrounding wackestones is gradational with no indication erosion or subaerial exposure, thus it is not considered to be a parasequence top. In wells M3 and M13 the interval contains a localized, 2 to 3 foot algal packstone/grainstone deposit composed primarily of dolomitized phylloid algal fragments and undifferentiated coated peloids. This mid-cycle P/G could possibly have been deposited as part of a barrier complex that allowed for the low energy accumulations of SW.

Occurrence of Anhydrite

The remaining 3% of the reservoir area is composed of .5 to 1 ft. anhydrite accumulations. The anhydrite is not internally bedded but composed of concentrations of nodular, chicken-wire, and mosaic anhydrite textures. Such anhydrite accumulations are considered to be subtidal evaporitic deposits, possibly from a sabkha or salina environments.

Anhydrite is commonly found as moldic, interparticle, poikilotopic, and intercrystalline pore filling cement throughout the reservoir. Cement is typically blocky or bladed in nature averaging 100 to 250 μm in size. However, poikilotopic anhydrite crystals can reach several millimeters in diameter. Extensive anhydrite replacement, moldic, and poikilotopic cement is often associated with subtidal and intertidal wackestone facies. Intertidal facies also exhibit finely bladed anhydrite nodules, some of which may be burrow filling. Wackestones often find anhydrite cement filling moldic

pores. Packstone/grainstone facies typically display interparticle pore filling anhydrite cement and localized replacement of framework grains. Common chalcedony and occasional gypsum, halite, and pyrite are found replacing anhydrite accumulations.

Stratigraphic Architecture

Van Wagoner et al. (1988, 1990) defined cyclic deposits in the San Andres as parasequences: relatively conformable shoaling-upward sedimentary successions that are bounded by marine flooding surfaces and their correlative conformities. For this study, Van Wagoner's definition will be used to identify parasequences. Parasequences will also be considered equivalent to the fifth-order cycles of Goldhammer et al. (1991), upward-shallowing cycles of James (1984), and cycles as defined by Wilson (1975). For this reason, the terms parasequence and cycle are used interchangeably in this discussion.

Sunflower field exhibits several shoaling upward parasequence-scale cycles that are characteristic of the lower San Andres. Thick cored intervals, such as well M3, reveal as many as six complete cycles, but only three could be correlated regionally across Sunflower field. These three correlatable parasequences are stacked vertically and numbered sequentially C1, C2, and C3, from bottom to top respectively (Figure 7).

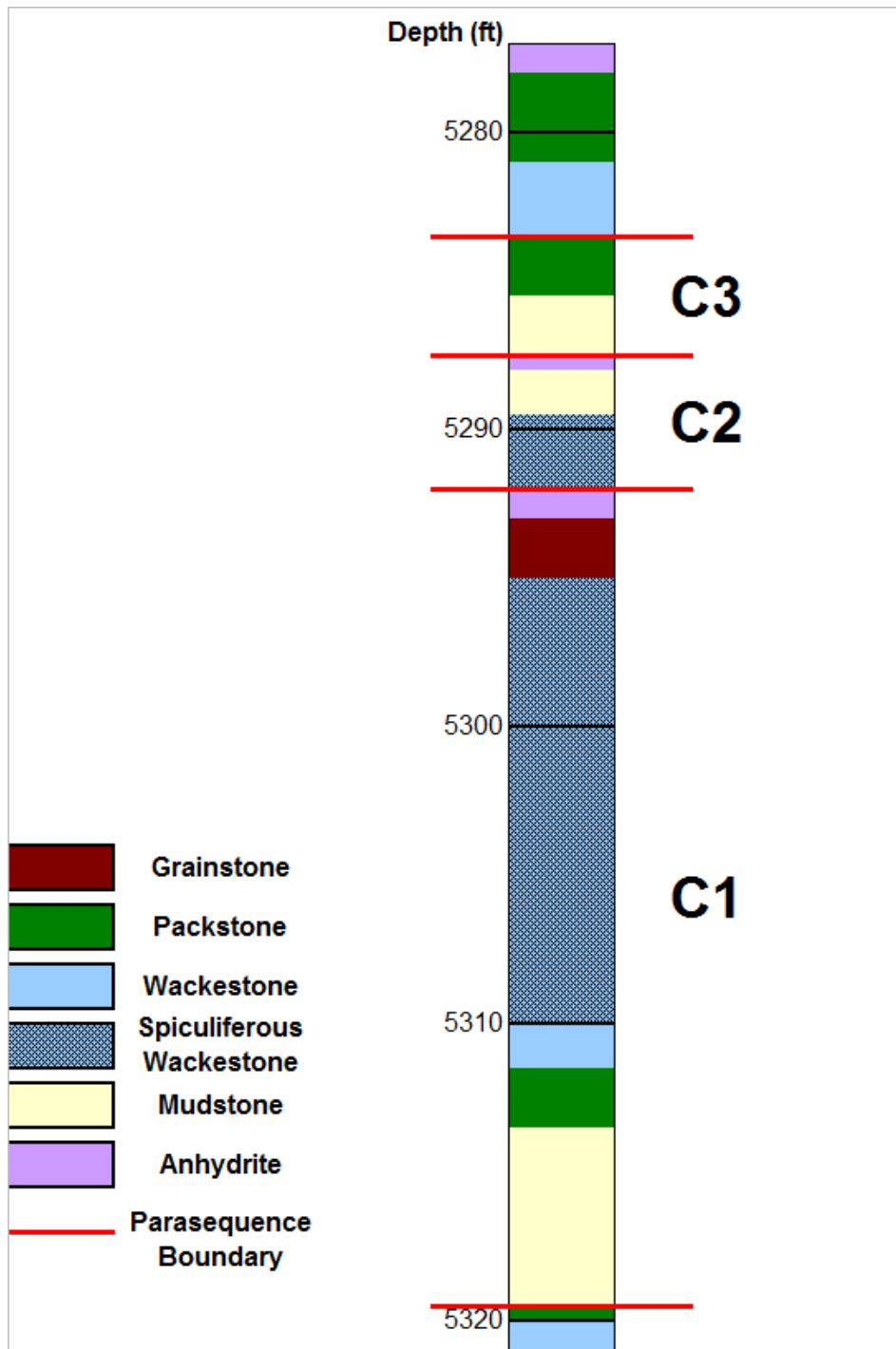


Figure 7: Sunflower parasequences. Cored interval of M2 illustrating Sunflower parasequences C1, C2, and C3 with associated facies succession.

Parasequence Structure

Parasequences were identified in cores as transitions from subtidal to supratidal depositional facies (Figure 8) and maximum exposure surfaces were defined based on evidence of subaerial exposure such as desiccation cracks or bedded evaporite deposits. Contacts between parasequences are sharp and often associated with texture and color changes. Parasequences are correlatable throughout the field and should not be confused with depositional facies boundaries. Depositional facies are rock units that possess a distinctive set of characteristics that are unique to a specific environment. Parasequences are typically composed of several shoaling upward depositional facies, but unlike parasequence boundaries, depositional facies boundaries are typically gradational and may not be correlatable throughout the field. The continuity of depositional facies is especially erratic in shallow carbonate depositional settings where there can be discontinuous depositional environments such as tidal channels or ponds.

Parasequences can be subdivided into three basic sections: bottom, middle and top. In idealized Sunflower San Andres parasequences, the bottom section coincides with subtidal deposits, the middle with intertidal, and top of cycles correspond with supratidal facies. Parasequences also tend to grade from mud to grain supported facies, from bottom to top.

Subtidal deposits are typically found in the bottom to middle portions of parasequences. They are characterized by mud dominated facies grading into more grain rich wackestone facies. Mudstones are typically light gray to light brown, and are found associated with dark brown shaley laminations (typically less 1 inch) and stringers

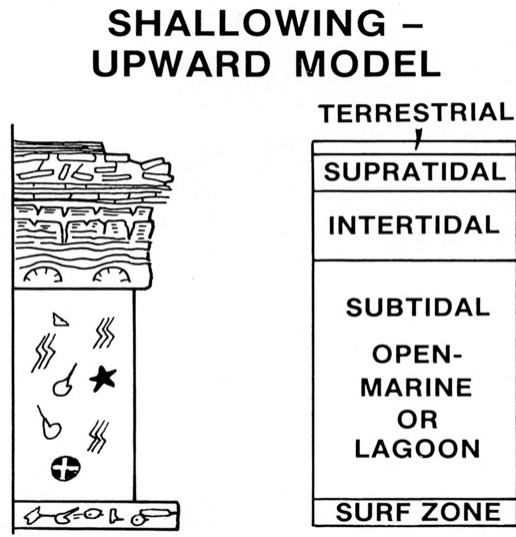


Figure 8: Shallowing-upward model for carbonate parasequences (James, 1984).

(Appendix B, Figure B.1). Anhydrite is minor to absent in subtidal mudstones. Subtidal wackestone framework material is composed primarily of assorted skeletal grains with accessory peloidal grains. Sponge spicules, foraminifera, green algae, ostracods, and miscellaneous mollusk fragments are common subtidal skeletal constituents across the field. Skel-pel wackestones commonly exhibit light brown color, bioturbation, and anhydrite cementation/replacement of grains (Appendix B, Figures B.2-B.4).

Intertidal deposits are found in the middle to upper sections of parasequences and are primarily composed of peloidal wackestone and mudstone facies. Intertidal environments are characterized by channel scour surfaces, rip-up clasts, fenestrae, algal laminations, desiccation cracks, concentrations of anhydrite nodules, and scarcity of skeletal fossils (Appendix B, Figures B.5-B.7). Intertidal deposits are typically grade from cream to light gray in color, becoming more laminated upwards.

Packstone/grainstone facies are less abundant in intertidal zones, but are present in the form of discontinuous peloidal/pelletal packstone deposits.

Supratidal deposits are only found at the top of parasequence cycles. They are easily identified by their high concentrations of anhydrite, desiccation cracks, and absence of fossils. Supratidal facies are composed primarily of white to light gray anhydrite with locally discontinuous peloidal-oncoidal wackestone and packstone/grainstone facies (Appendix B, Figure B.8).

Although idealized Sunflower parasequences find supratidal deposits capping parasequences, this is not always the case. Some cycles in Sunflower field are capped by intertidal and subtidal deposits. The lack of supratidal and intertidal facies in some cycles could be caused by local variations in depositional topography or possible erosion of the intertidal and supratidal deposits by storms or subaerial exposure.

Sunflower Cycles

Parasequences thickness and composition vary considerably in Sunflower field, but three distinct cycles can be correlated regionally. C1 is the deepest and thickest of the three cycles. C1 has an average thickness of 26.4 ft. but ranges from 17 ft. in M19-4 to 36.5 ft. in well M14. These major differences in thickness are attributed to depositional paleotopography. Thinner cycle accumulations were deposited on structurally high areas while thicker deposits are found in low areas, specifically down dip of the anticlinal structure. In most wells, C1 represents a complete, idealized parasequence transitioning from subtidal to intertidal and finally supratidal deposits.

Mudstone facies are typically found at the base of C1 and are overridden by an anomalous P/G facies ranging from 1 to 4 ft. in thickness. The P/G facies is primarily composed of skeletal fragments with variable peloidal content. Facies then grade into wackestone followed immediately by spiculiferous wackestone sub-facies. SW intervals are 5 to 15 ft. in thickness and represent a low energy sediment sink. The mid-cycle transition from P/G to SW sub-facies could be explained by a regressive system tract where shallow subtidal deposits of a bay or lagoon are found stepping over older barrier deposits.

Intertidal wackestones and mudstones are typically next in succession with intertidal P/G and supratidal anhydrite found capping C1. As a whole C1 averages 10.7% porosity and 1.617 md of permeability; the SW facies of C1 averages 12.3% porosity and 2.434 md of permeability.

Parasequence C2 lies directly above the capping C1 facies and appears to be a lower magnitude cycle. C2 averages only 4.25 ft. in thickness and ranges from 3 to 6.5 ft. throughout South Sunflower. Subtidal to intertidal mudstone facies are found at the base of C2 grading into intertidal peloidal wackestones and mudstone. C2 is capped by locally occurring .5 to 1 inch supratidal anhydrite accumulations or peloidal/oncoidal packstone facies. Petrophysically, C2 exhibits an average porosity of 7.5% and permeability of .0936 md. This could be attributed to the lower abundance of SW sub-facies and the overall muddy and anhydritic nature of C2. However, it must be noted that data is limited. Core analysis porosity and permeability was not measured for C2 in most wells.

Similarly, C3 averages 4.25 ft. and ranges 3 to 5.5 ft. in thickness. C3 overlies C2 and also exhibits a gradual transition from subtidal/intertidal mudstone to wackestone facies. A regionally extensive 1 to 2 ft. peloidal packstone is found capping C3. This P/G facies displays desiccation features and has a sharp, erosional contact with the overlying cycle. Due to the thin, muddy nature of C3, no core analysis was performed in this cycle. Visible porosity is scattered in C3 and is not expected to exceed 5-10%.

H1 Genetic Pore Types

As stated in the methods portion of this study, porosity from 73 thin sections were classified using the genesis based method of Ahr et al., (2005). No observed pore system within Sunflower field was found to be purely depositional or diagenetic, thus samples were identified as hybrid type 1 pore systems (H1). H1 pores were further subdivided based on the ratio of depositional to diagenetic pores as well as whether porosity was reduced or enhanced (Table 1). Of the 73 samples analyzed, the following pore types were observed: H1-Ae, H1-Be, H1-Ar, H1-Br, and localized occurrences of H1-Cr.

Enhanced H1 Pores

Porosity enhancement occurs through two methods in Sunflower field, the primary type being dissolution of framework grains, cements, and matrix crystals. The secondary mode of enhancement is dolomite replacement and subsequent neomorphism of matrix material.

Table 1: Porosity classification scheme. Method subdivides hybrid pore types on the basis of depositional to diagenetic porosity ratio.

H1	Enhanced	Depositional porosity dominate	Ae
		Equal ratio of depositional to diagenetic	Be
		Diagenetic porosity dominate	Ce
	Reduced	Depositional porosity dominate	Ar
		Equal ratio of depositional to diagenetic	Br
		Diagenetic porosity dominate	Cr

Partial to complete dissolution of framework grains is extremely common in Sunflower field, specifically in skeletally dominated wackestone facies. The dissolution of grains appears to have occurred post dolomitization and pre-anhydrite cementation and replacement. Siliceous skeletal grains were not affected by dolomitization, but have undergone leaching. This is especially evident in the spiculiferous wackestone sub-facies, which is dominated by spicule-moldic porosity. To a lesser extent the cements and dolo-micrite matrix have also been affected by dissolution. Microporosity after differential dissolution of dolo-micrite crystals is the leading cause of porosity in mudstone facies.

Enhancement through replacement is relatively minor but observable in Sunflower field. This phenomenon is most evident in dolomite replacement of framework grains. In some instances peloidal and skeletal grains, specifically algal grains, have been replaced by a mosaic of 10 to 35 μm dolomite rhombs yielding

intercrystalline porosity. Dolomitization of micrite in some mud dominated rocks has also yielded accessory, micro-intercrystalline porosity.

Genetic porosity type H1-Ae is defined as a porosity system in which depositional characteristics dominate but have been somewhat altered by diagenesis. In the case of H1-Ae, facies is still a reliable proxy for porosity. Although original framework grains may be partially to completely dissolved, their boundaries are still clearly visible (Appendix D, Figures D.7 and D.8). However, when the boundaries of dissolved framework grains are compromised by additional dissolution, the pores are classified as a H1-Be system (Appendix D, Figure D.9).

Reduced H1 Pores

Porosity reduction is attributed to three main processes in Sunflower field, replacement, cementation, and compaction. The most common process through which porosity is reduced is anhydrite replacement. Anhydrite is often found replacing portions of original framework grains, matrix, and/or pore space thereby reducing storage and flow capacity of the reservoir. Replacive anhydrite accumulations typically occur as nodules or localized clusters, thus increasing the heterogeneity of a given unit. Siliceous replacement of framework grains and surrounding matrix is also observed as irregular bands associated with some spiculiferous wackestones and packstones.

Cementation is the secondary mode of porosity reduction and is often found associated with anhydrite replacement, however cementation exhibits a more uniform distribution across the sample. Cements are typically found filling moldic pores or

coating grain boundaries. Stages of dolomite and anhydrite cementation are both found in Sunflower field, but the latter is much more prevalent. Relict dolomite cement is typically isopachous and appears to have precipitated in conjunction with reservoir dolomitization. Anhydrite cementation clearly occurred sometime after dolomitization and subsequent leaching of the reservoir. Anhydrite cement is widespread throughout the field and can be found filling moldic, interparticle, intercrystalline, and fracture porosity.

The final mode of porosity reduction is compaction. Much of the porosity lost in carbonate reservoirs can be attributed to burial diagenesis and the resulting mechanical and chemical compaction. Mechanical compaction can be recognized in Sunflower field by the plastic and brittle deformation of grains, and concavo-convex grain contacts. Solution seams and stylolites, which are common throughout Sunflower field, hint to chemical compaction and dissolution of carbonate material.

For H1-Ar pore systems, porosity is primarily controlled by depositional characteristics but has been somewhat reduced by diagenesis. As previously stated, in H1-A pores facies is still a reliable proxy for porosity. H1-Ar pore systems often exhibit moderate replacement, cementation, or compaction, but porosity is still strongly controlled by depositional attributes (Appendix D, Figure D.10 and D.11). If porosity is moderately to extensively reduced and the depositional porosity controls are diminished, then porosity is classified as H1-Br (Appendix D, Figure D.12). When extensive diagenesis precludes a definitive relationship between porosity and depositional characteristics, the pore system is classified as H1-Cr. Analyzed portions of Sunflower field do not display extensive H1-Cr pore systems, but irregular siliceous

wackestone/packstone laminations do illustrate this pore type (Appendix D, Figure D.13 and D.14).

Relationship with Reservoir Lithofacies

Distribution of hybrid pore types within Sunflower field appears to be somewhat controlled by reservoir facies composition. 73% of grain-dominated packstone/grainstone samples exhibit reduced hybrid pore systems, and 84% of mud-dominated facies (mudstone, wackestone, and spiculiferous wackestone sub-facies) display enhanced hybrid porosity (Table 2). Nearly 95% of all diagenetically enhanced hybrid pores are found in mud-dominated rocks. Thus there is a strong correlation between porosity enhancement and muddy lithofacies. This association could be attributed to the high original permeability of muddy facies which allowed for early fluid movement at high rates resulting in porosity enhancement through dissolution.

Table 2: Pore type occurrence and poroperm relationships. Table illustrating facies and pore type correspondence and petrophysical trends by facies and pore types.

Pore Type Occurrence by Facies

	M	W	SW	P/G
H1-Ae	21	17	8	2
H1-Be	---	---	6	1
H1-Ar	2	2	---	2
H1-Br	---	4	2	6

Average Petrophysical Properties

	Average Φ (%)	Average K (md)
Facies:		
M	9.2	0.301
W	9.9	0.947
SW	13	3.174
P/G	8.6	1.119
Pore Type:		
H1-Ae	10.7	0.806
H1-Be	16.4	6.346
H1-Ar	5.1	0.194
H1-Br	7.6	0.698

Although porosity enhancement is most prevalent in mud-dominated facies, this does not always equate to high poroperm values for mudstones, wackestones, and enhanced hybrid pore systems. Table 2 illustrates this point. Mudstones samples are commonly subject to differential dissolution of dolo-micrite and scattered grains yielding enhanced porosity. Sunflower mudstones average a considerable 9.2% porosity, but only .301 md of permeability. This is likely due to the irregular and scattered nature of mudstone dissolution.

On average, the spiculiferous wackestone sub-facies exhibit the most favorable properties for reservoir storage and flow. 87.5% of the SW samples display porosity enhancement, primarily through the dissolution of siliceous sponge spicules. Due to the elongate nature and random orientation of these grains, spicule molds often intersect creating permeability. Similarly, spicule molds can be connected by intercrystalline porosity formed through the dolomitization and subsequent recrystallization of the wackestone micrite matrix. These enhanced SW systems average 14% porosity and 3.652 md of permeability, but observed measured properties reach 18.6% porosity and 18.131 md permeability. Spiculiferous wackestones exhibiting porosity reduction from anhydrite and siliceous replacement pull the total average for SW porosity and permeability down to 13% and 3.174 md, respectively.

HPMI Capillary Properties

As outlined in the methods portion of this study, 16 samples from two wells, P37-2 and M2, exhibiting contrasting reservoir characteristics were subjected to high

pressure mercury injection analysis (HPMI) in order to quantify pore to pore throat relationships. Eight capillary sample locations were chosen from the bottom, middle, and top portions of the productive C1 parasequence in each well. Special attention was given to areas of facies change and variations in core analysis petrophysical properties.

Resulting data include: 1) drainage curves for each sample based on mercury saturation at each incremental pressure point, 2) mercury derived porosity, 3) permeability measured to air and using the Swanson equation, 4) pore throat distribution based on fraction of intruded pore space, and 5) median pore throat radii from r_{35} and r_{50} (Table 3).

Table 3: Summary table of HPMI capillary properties of M2 and P37-2.

Well ID	Depth	Facies	Pore Type	Core Φ (%)	Core K (md)	HPMI Φ (%)	HPMI K air (md)	Threshold Pressure (psi)	R35 (μm)	R50 (μm)
M2	5293.6	P/G	1Br	6.1	0.147	7.1	0.034	780.8	0.052	0.045
M2	5296.4	M	1Ae	9.1	0.881	8.0	0.126	230.7	0.19	0.152
M2	5297.7	SW	1Ae	12.5	2.150	12.6	2.04	53.9	1.32	1.07
M2	5299.3	W	1Ae	7.9	1.334	12.5	0.914	59.9	0.469	0.366
M2	5302.4	SW	1Be	18.6	18.131	24.0	24.6	43.1	1.6	1.37
M2	5308.3	SW	1Be	17.3	3.745	23.1	25.6	37.2	1.49	1.25
M2	5313.4	P/G	1Br	7.9	1.635	7.6	0.928	46.8	1.15	0.872
M2	5321	M	1Ae	10.5	0.107	12.2	0.211	229.2	0.24	0.198
P37-2	5299.9	M	1Ae	12.4	0.272	9.8	0.1	336.7	0.128	0.109
P37-2	5300.3	W	1Ae	15.1	1.278	15.9	1.87	68.2	0.88	0.677
P37-2	5302.3	M	1Ae	11.2	0.827	10.8	0.563	60.5	0.87	0.671
P37-2	5305	SW	1Ae	11.2	1.412	14.7	0.399	141.0	0.331	0.236
P37-2	5306.7	SW	1Ae	12.2	2.074	13.3	3.66	42.3	1.77	1.45
P37-2	5311.8	M	1Ar	2.9	0.123	0.7	0.123*	259.0	0.018	0.009
P37-2	5315.3	M	1Ae	9.7	0.143	13.6	0.565	126.8	0.33	0.238
P37-2	5320.2	SW	1Br	8.8	0.551	9.9	1.000	53.9	1.26	1.04

* Core analysis K; unable to measure K air from plug

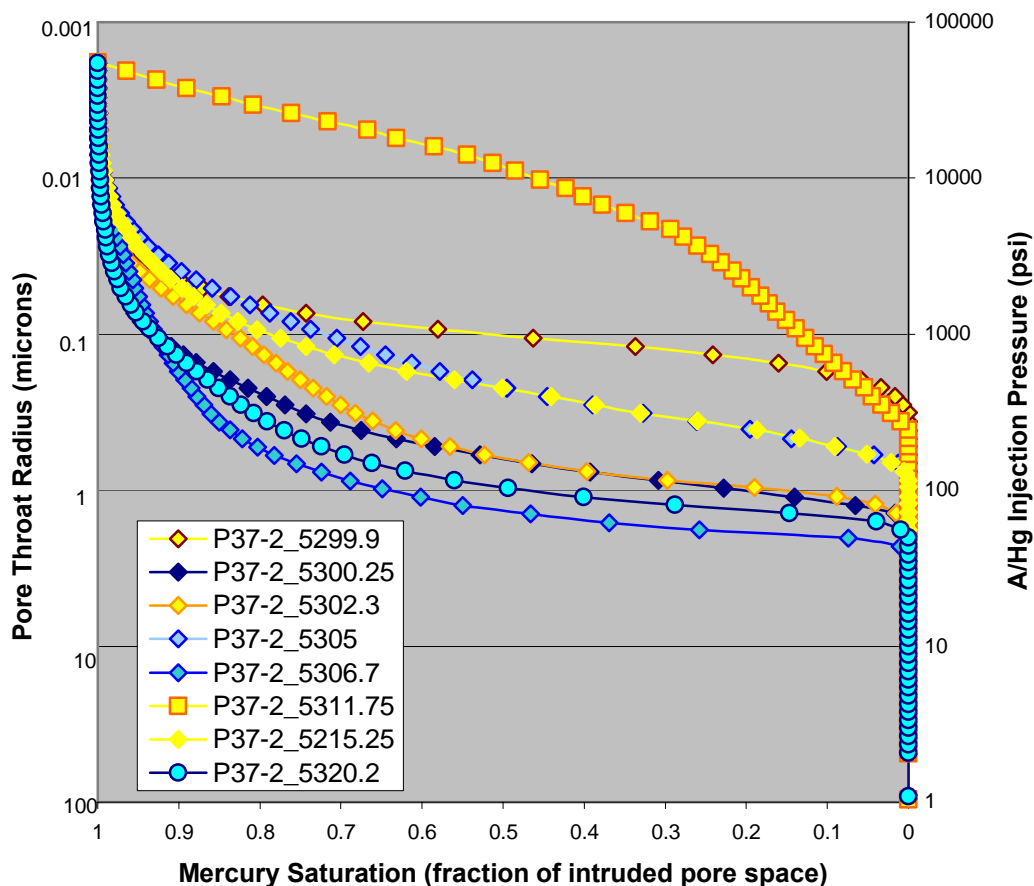


Figure 9: P37-2 drainage curves. Samples categorized by facies (mudstone – yellow, wackestone – blue, packstone/grainstone – green) and pore type (H1-AE with diamonds, H1-Be with triangles, H1-Ar with squares, and H1-Br with circles).

Well Pool 37-2 is located in the northeastern portions of the Sunflower study area and is oriented along strike. It is considered a moderate to poor producer despite its close proximity and lithologic similarity with productive wells. As of April 2008, P37-2 generated 13.8 bbl/d of oil. Drainage curves categorized by facies and pore type are given for P37-2 samples in Figure 9. Note that P37-2 mudstone facies are distributed throughout C1 and exhibit entry pressures typically above 100 psi. H1-Ar mudstone

sample 5311.75' has extremely high entry pressures and negligible porosity and permeability. Its central position in C1 may preclude fluid communication between upper and lower portions of C1. Lowest entry pressures and highest poroperm trends correspond to wackestone facies, specifically spiculiferous samples (light blue data points).

Figure 10 displays the drainage curve for well Muldrow 2 categorized by facies and pore type. M2 is centrally located in the Sunflower study area along strike. It is considered to be of good reservoir quality, producing 37.2 bbl/d of oil as of April 2008. Unlike P37-2, M2's tightest intervals requiring the highest threshold pressures are located at the base and top of C1. Tight muds exhibiting less than .2 md and threshold pressures above 200 psi are found above and below a relatively continuous, enhanced wackestone facies dominated by spiculiferous wackestone sub-facies. C1 is capped oncoidal/peloidal grainstone facies requiring 780.8 psi for threshold pressure. The two drainage curves representing the best reservoir conditions are the product of spiculiferous samples exhibiting H1-Be pore types.

Median pore throat sizes were calculated for each of the samples using both the R_{35} and R_{50} methods. For both calculations, the largest median pore throat sizes are found associated with enhanced pores, specifically H1-Be. The smallest median pore throat apertures observed from the 16 samples were taken from reduced pore systems. However, it should be noted that some reduced pore systems, such as the H1-Br of sample M2, 5313.4 ft. exhibit considerable median pore throat radii.

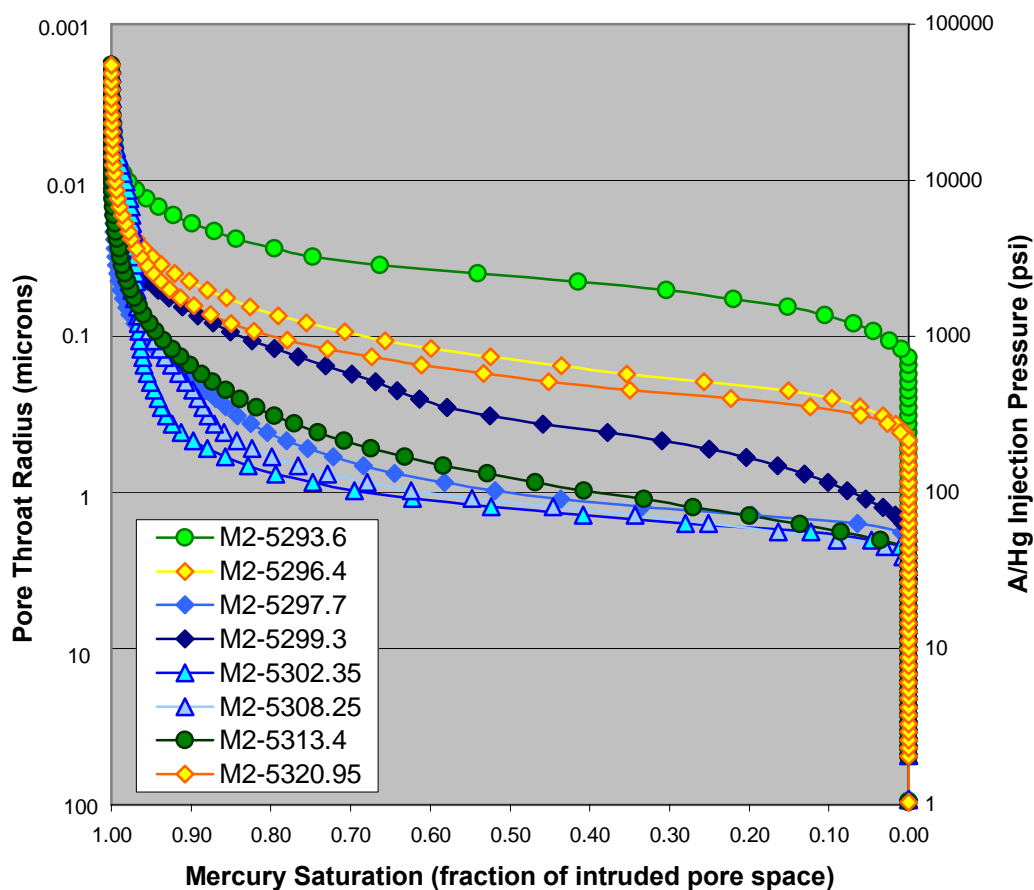


Figure 10: M2 drainage curves. Samples categorized by facies (mudstone – yellow, wackestone – blue, packstone/grainstone – green) and pore type (H1-AE with diamonds, H1-Be with triangles, H1-Ar with squares, and H1-Br with circles).

Well Comparison

Capillary data supports the notion that wackestones, specifically spiculiferous intervals with H1-Be porosity provide the most favorable flow conditions in Sunflower field. Conversely, tight mudstone and grainstone intervals present the worst. Overall, capillary data reveals much more favorable reservoir in well M2 over P37-2. This finding agrees with previously discussed production data for the two wells. Reservoir

quality differences are likely related to the distribution of tight intervals. Alternating enhanced wackestone and tighter mudstone facies limits fluid communication and overall flow capacity of C1 in P37-2. The relatively continuous enhanced wackestone interval of M2 is encompassed by tighter mudstone and grainstone intervals allowing for more uniform flow.

It should also be noted that core and thin section analysis reveal a significant difference in facies and cycle thickness between M2 and P37-2. Cycle 1 is found to be 27.5 ft. thick in M2 and slightly less in P37-2, 23 ft. More significantly, spiculiferous sub-facies accumulations are 13.5 ft. thicker in M2 than P37-1. P37-2 contains more mudstone and assorted skeletal and peloidal wackestones in place of SE. Thicker intervals could be attributed to structural paleo-lows that served as sediment sinks for detrital spicules as opposed to paleo-highs that would exhibit less prominent accumulations.

DISCUSSION AND INTERPRETATION

Petrophysical Relationship with Facies

Results of this study show that there is a tenuous relationship between facies and reservoir performance characteristics in Sunflower field. On average wackestone facies, specifically the spiculiferous wackestone sub-facies exhibit the highest poroperm values but this is not always the case. Figure 11 illustrates the relationship between facies and poroperm values for 336 core samples taken from Sunflower field. Each of the three primary lithofacies from Sunflower field displays an extensive range of petrophysical characteristics creating a widely scattered “shotgun” distribution of data points. Again the wackestone facies yields the highest poro/permeability values in Sunflower field; however wackestones also produce some of the lowest values. As a result, no substantial relationship can be drawn between petrophysical characteristics and facies on the reservoir scale.

Similarly, Figure 12 displays the relationship between facies and reservoir characteristics, but the data set has been restricted to the 67 thin section samples, which have corresponding core analysis poroperm data. Spiculiferous wackestone sub-facies have also been designated with a lighter shade of blue. Again, generalizations can be made, but no solid correlation between facies and petrophysical properties can be drawn.

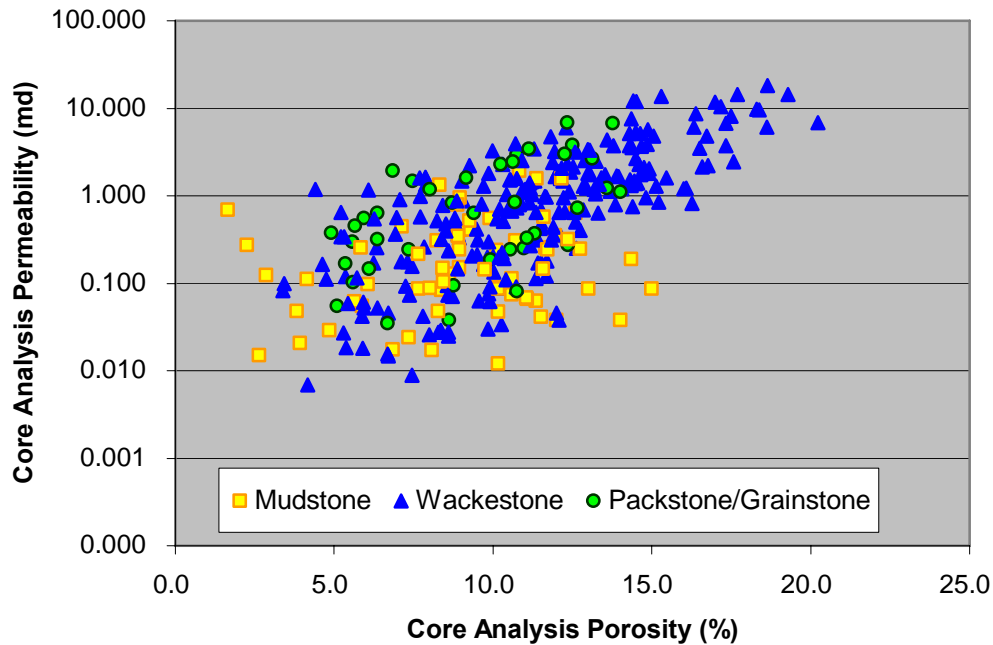


Figure 11: Poroperm relationship with facies. Semi-log crossplot of core analysis permeability versus porosity for 366 core samples taken from throughout Sunflower field. Note the widely scattered “shotgun” distribution of facies.

These findings suggest that traditional, facies-dependent methods of reservoir characterization may not be applicable in all carbonate reservoirs. As previously stated, porosity and permeability do not conform to depositional facies boundaries in carbonate reservoirs affected by diagenesis or fracturing. Consequently, conventional methods of petrophysical characterization based on depositional facies are unreliable as predictors of carbonate reservoir behavior. Unlike characterization by facies, genetic pore typing accounts for diagenetic enhancement and reduction of flow units by evaluating the origins of porosity. For this reason, this study proposes a new method of carbonate

reservoir characterization that emphasizes the genetic pore type of a reservoir rather than the facies.

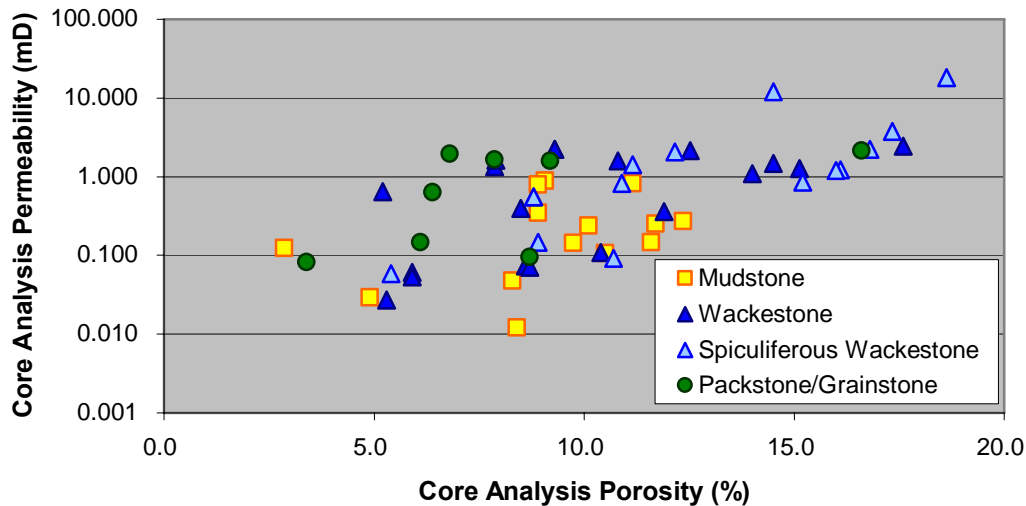


Figure 12: Poroperm relationship with thin section facies. Semi-log crossplot of core analysis permeability versus porosity for 67 thin section samples. Again, individual facies exhibit a wide variety of poroperm values yielding widely distributed data points.

Petrophysical Relationship with Genetic Porosity Type

Results of this study suggest a stronger relationship exists between the petrophysical properties of a reservoir and genetic pore type than with facies. cursory analysis of thin sections and capillary data implies higher poroperm values and larger median pore throat apertures are associated with enhanced pores, with H1-Be serving as the best unit for flow. Similarly, reduced hybrid pore systems produced the smallest median pore throat estimates from HPMT analysis, the highest threshold pressures, and often times the lowest poroperm values.

Figure 13 again illustrates 67 of the original 73 thin section samples analyzed in this study on a semi-log plot of permeability versus porosity. However, Figure 13 has been categorized on the basis of genetic pore type rather than facies. When divided by hybrid 1 pore type, reduced and enhanced pores plot in clusters rather than the wide “shotgun” patterns of Figures 11 and 12. There is some overlap between enhanced and reduced pore type data points, but overall it appears that genetic pore type is a more reliable predictor of flow properties than facies and may be used to define petrophysical rock types.

Although data do exhibit better grouping when categorized by genetic pore type, facies plots and pore type plots have some similarities and overlap. This is possibly because the number of pore types is limited by the number of depositional textures that can be modified by diagenesis. Because different pore types vary so closely with facies this is not an unreasonable conjecture. More defined separation between pore type and facies plots would be expected if the data set included a wider range of grain supported facies, genetic porosity types (purely depositional or diagenetic), or more variable porosity fabrics like vuggy or intergranular.

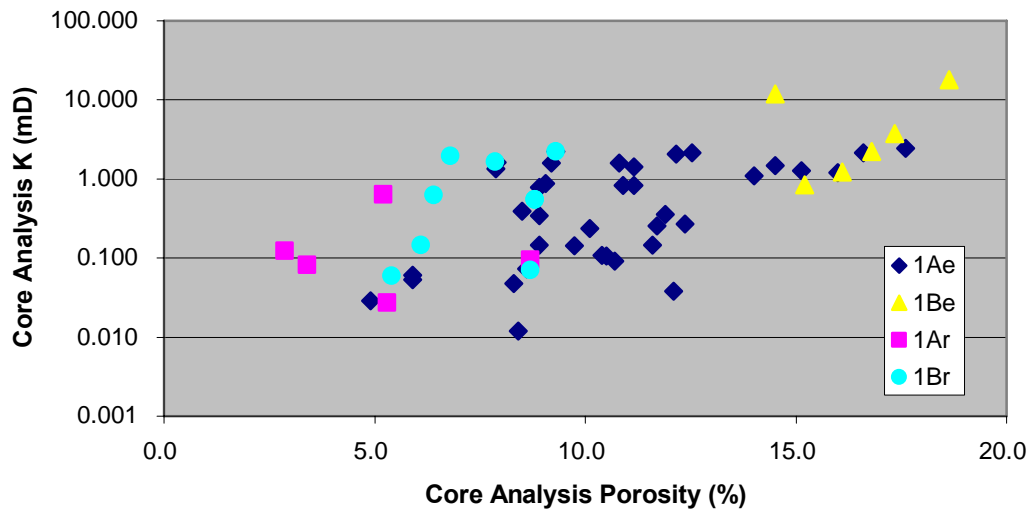


Figure 13: Poroperm relationship with genetic pore type. Semi-log crossplot of core analysis permeability versus porosity categorized by hybrid 1 genetic pore type. Note the tighter grouping of data when organized by pore type than by facies in Figure 12.

Petrophysical Characterization

Two graphical methods of petrophysical evaluation were utilized to illustrate effectiveness of characterization using facies and genetic pore type: K/Φ crossplots and Winland R_{35} plots. The usefulness of K/Φ crossplots for reservoir characterization can be enhanced by adding contours representing constant K/Φ ratios. Data points that plot along a constant K/Φ ratio exhibit similar flow quality across a wide range of poroperm values. Thus, these ratio lines can be used as a scale to evaluate and rank petrophysical rock types by quality. Using the Winland equation, R_{35} isopore throat lines can be derived and applied to traditional K/Φ semi-log plots. The resulting graph is known as a Winland plot. Similar to K/Φ ratio lines, data points that plot along constant isopore throat lines represent similar flow quality, and may be used to rank flow units.

These two methods of petrophysical evaluation were applied to the 16 HPMI capillary pressure samples of wells M2 and P37-2. Due to facies and porosity variability observed in core foot intervals, plug porosity and permeability measured from HPMI were deemed more accurate and used in place of core analysis values, with the exception of P37-2, 5311.5'. The tight nature of the mudstone sample precluded determination of capillary K_{air} , thus core analysis permeability values for the 5311' interval were used.

Data points were categorized on the basis of facies and hybrid genetic pore type in each of the graphs. The following standard was utilized to highlight sample facies: the mudstone facies is yellow, wackestone is blue, spiculiferous wackestone sub-facies is light blue, and the packstone/grainstone facies is displayed as green. Genetic pore type is displayed by data point shape and uses the following standard: H1-Ae pores are diamonds, H1-Be are triangles, H1-Ar are squares, and H1-Be pores are displayed as circles. These standards apply to the graphs discussed under K/Φ ratio and Winland R_{35} analysis.

K/Φ Ratio Analysis

Figure 14 illustrates the K/Φ semi-log crossplot of HPMI measured K_{air} and porosity for wells M2 and P37-2. Equal K/Φ ratio lines are given at values of .5, 5, 50, and 500. These contour lines serve as a scale for evaluating the quality of flow units. As previously noted, individual facies exhibit a wide range of poroperm values thus complicating characterization by facies. This is especially true for the wackestone facies, including the spiculiferous sub-facies. Measured wackestone values range from 10 to

24% porosity and .399 to 25 md of permeability, and K/Φ ratios of less than five to greater than 50. This wide range of variability again implies that facies is not a direct indicator of reservoir quality in carbonates, and is likely not an effective means of reservoir characterization.

When evaluated on the basis of genetic pore types, data shows better grouping and trends become more evident. For instance, data points that were before grouped as the widely variable wackestone facies are now divided into multiple, more clustered pore types. H1-Be pores represent the best flow properties and are the only pore types to plot above the 50 K/Φ ratio line. H1-Ae pores are the most variable, with porosity values ranging from 8 to 16% and permeabilities from .1 to 3.66 md. This range is much smaller than that given by wackestones when categorized by facies.

Although genetic pore type appears to be a stronger basis for carbonate reservoir characterization, the influence of facies on flow quality can not be ignored. For instance, wackestone facies that exhibit H1-Ae porosity cluster above the 5 K/Φ ratio line while mudstones with H1-Ae porosity cluster below the same ratio. From this, it can be assessed that the most favorable flow units in South Sunflower field are characterized by wackestones, specifically spiculiferous intervals that exhibit enhanced hybrid porosity. From this observation, it is evident that a more precise means of reservoir characterization may be obtained by combining both genetic pore type and facies.

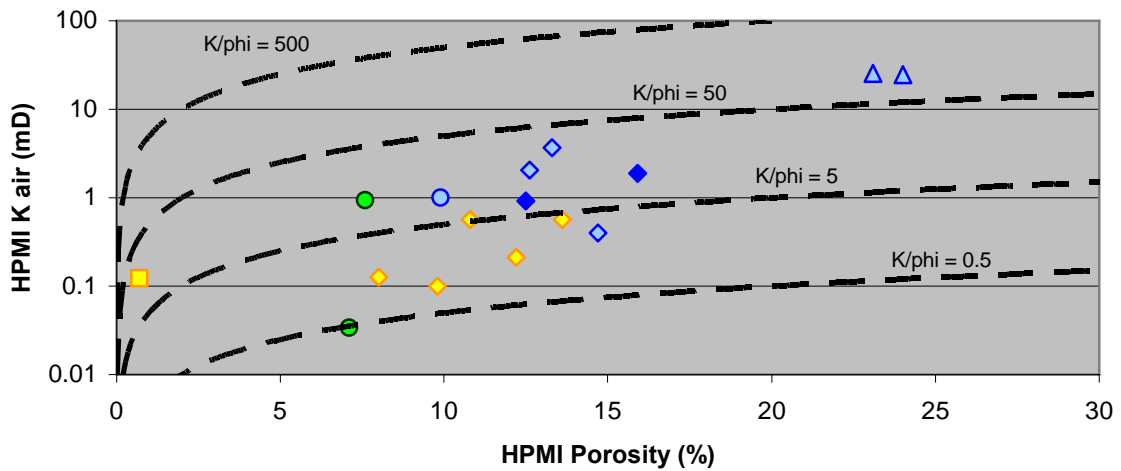


Figure 14: K/Φ ratio analysis. Semi-log crossplot of HPMI derived permeability versus porosity with K/Φ ratio contours. Data is categorized by facies (mudstone – yellow, wackestone – blue, spiculiferous sub-facies – light blue, packstone/grainstone – green) and pore type (H1-AE with diamonds, H1-Be with triangles, H1-Ar with squares, and H1-Br with circles).

Winland R_{35} Analysis

Figure 15 displays the same M2 and P37-2 data points on a semi-log permeability versus porosity crossplot but with contours representing isopore lines of R_{35} pore port sizes, given in microns. Note that both graphs use log scale permeability versus porosity axes, thus data points are plotted identically. There is no difference in the distribution, ranges, or clustering of data for either facies or pore type. With the Winland plot, pore/pore throat size ratios are assumed to be relatively uniform and R_{35} port sizes are used to represent 'cutoff values' for good and bad flow unit quality. This differs from the K/Φ method which uses K/Φ ratio lines as estimators of flow quality.

Although R_{35} port size is a good estimator of flow quality in clastic reservoirs, it is inconsistent and often inaccurate in carbonate reservoirs. The Winland method uses

uniform pore/pore throat size as the primary criterion for defining flow units using R_{35} pore sizes. This is valid in clastic reservoirs which typically exhibit homogenous interparticle porosity and uniform pore/pore throat size ratios. However, carbonate reservoirs display highly variable pore/pore throat geometry. This is especially true in reservoirs affected by diagenesis and fracturing.

Lucia (1999) supports this argument and states that pore size varies in deposition and diagenetic rock fabrics, thus uniform pore size is not the fundamental link between facies and petrophysical properties. Lucia goes on to point out that permeability varies greatly on the inch to foot scale within depositional rock types, and due to R_{35} pore sizes' close correlation with permeability, it is reasonable to assume that R_{35} pore size is also highly variable. Thus uniform pore size is unable to characterize depositional facies. The Winland method also fails to identify pore type; therefore it can not define different flow units by geological origin. These apparent shortcomings illustrate the ineffectiveness of R_{35} analysis in carbonate reservoirs and promote the K/Φ ratio method of petrophysical characterization.

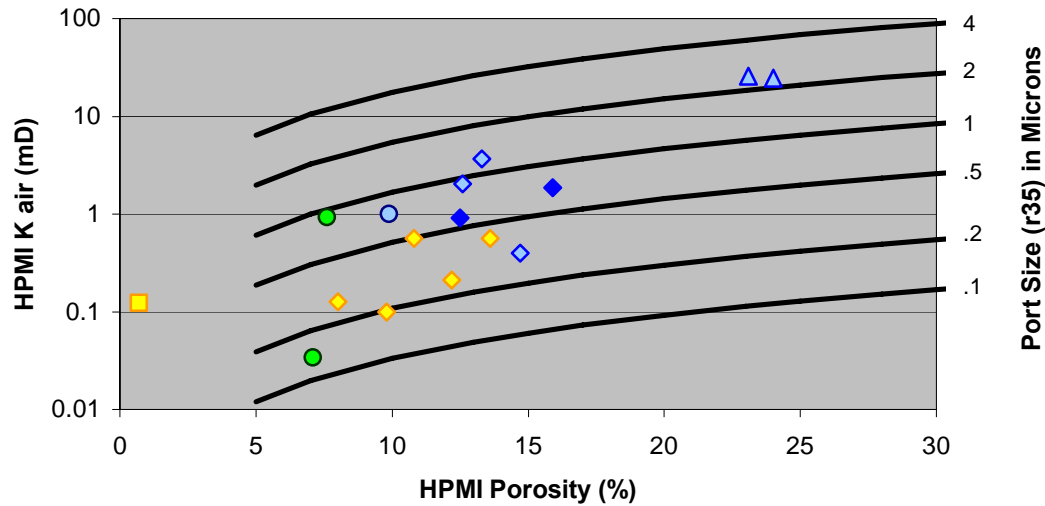


Figure 15: Winland R_{35} analysis. Semi-log crossplot of HPMI derived permeability versus porosity with R_{35} isopore lines. Data is categorized by facies (mudstone – yellow, wackestone – blue, spiculiferous sub-facies – light blue, packstone/grainstone – green) and pore type (H1-AE with diamonds, H1-Be with triangles, H1-Ar with squares, and H1-Br with circles).

Petrophysical Rock Type Identification

From previous discussion, it has been concluded that the most accurate means of characterizing petrophysical rock types within carbonate reservoirs is through K/Φ ratio analysis on the basis of genetic pore type. Using these parameters, four distinct petrophysical rock types can be assigned to South Sunflower field. Rock types have been numbered consecutively from lowest to highest quality (Figure 16). Table 4 summarizes the attributes of each petrophysical rock type. Again, it should be noted that petrophysical rock types are classified according to the petrophysical attributes that influence reservoir performance and are defined independent of facies.

Table 4: Quick-look table of petrophysical rock type attributes.

** Ranges are approximations from core and HPMI data and corresponding K/ ϕ ratio graphs*

Petrophysical Rock Type	Dominant Pore Type	Dominant Facies	K/ ϕ Ratio Range*	ϕ Range* (%)	K Range* (mD)
R1	H1-Ar	None	0.5 to 4	< 5	< .125
R2	H1-Br	P/G	.5 to 20	5 to 10	.05 to 2
R3	H1-Ae	W and M	1 to 30	8 to 15	1 to 4
R4	H1-Be	SW	5 to 100	15 to 25	> 1

Petrophysical rock type 1 (R1) is found to have the least favorable petrophysical flow properties. R1 is dominated by H1-Ar porosity but has no strong association with facies. In other words, multiple facies contribute to petrophysical rock type 1. K/ Φ ratios rarely exceed 4 and range as low as .5. Petrophysical rock type 2 (R2) exhibits slightly better petrophysical properties with average porosity ranges of 5 to 10% and permeability up to 2 md. R2 is dominated by the H1-Br genetic pore type and is closely associated with the packstone/grainstone facies. K/ Φ ratios for R2 range from .5 to 20.

It is logical to assume that H1-Br rocks would have lower poroperm values than that of H1-Ar; however, this is not what is observed in Sunflower field. Several explanations of this counterintuitive finding have been proposed. First, many rocks in which H1-Br porosity exist appear to have had higher original poroperm values than H1-Ar, thus after extensive reduction H1-Br poroperm values still exceed those of H1-Ar. Secondly, H1-Br pore systems are sometimes found associated with localized porosity enhancement which increases poroperm values.

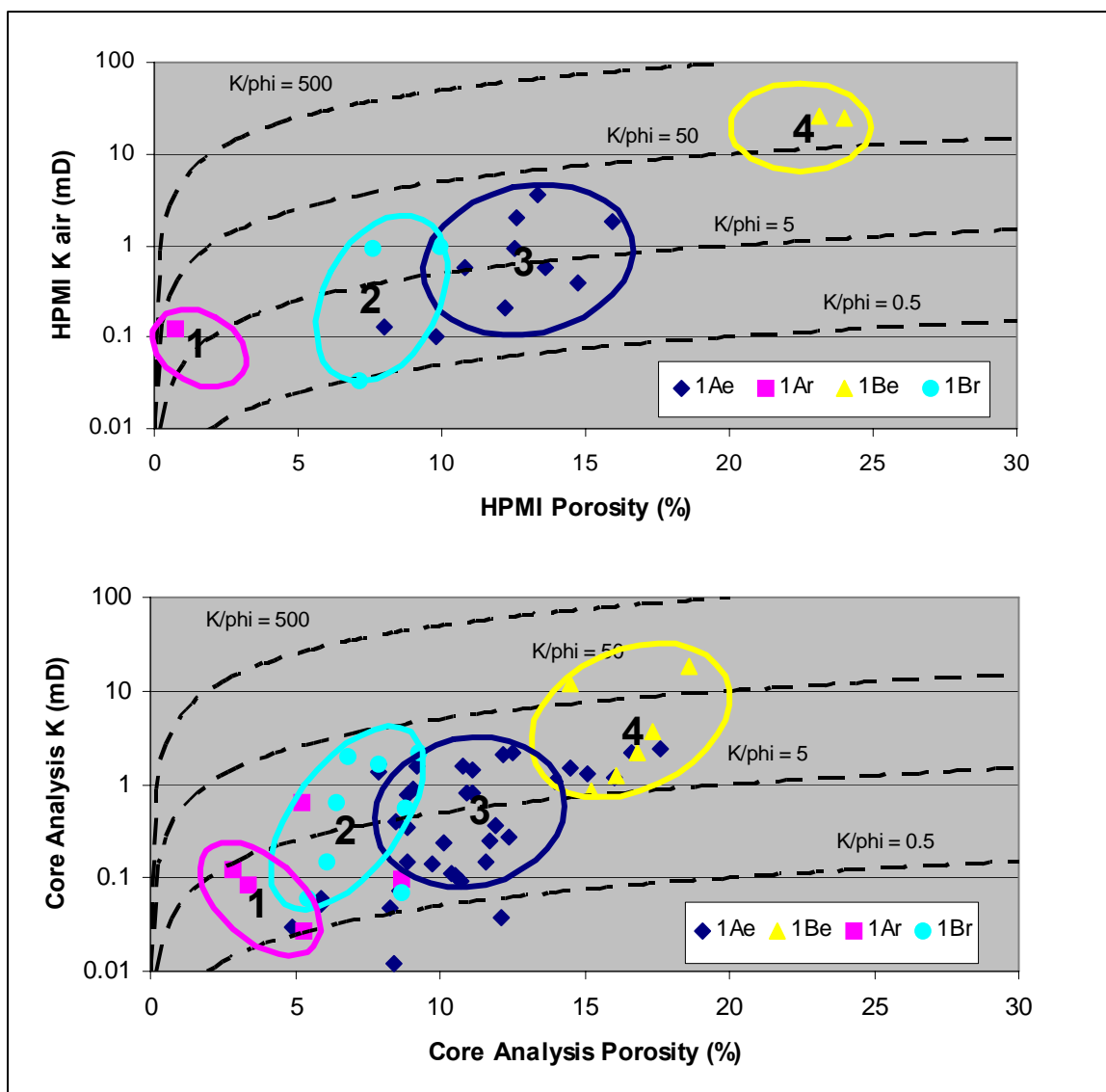


Figure 16: Sunflower petrophysical rock types. Semi-log crossplots of permeability versus porosity for both HPMI samples and core analysis data. Data are categorized by hybrid 1 genetic pore type and petrophysical rock types are highlighted by associated circles and numbers. Petrophysical rock type 4 exhibits the best flow properties and correlates to H1-Be pores.

For example, M2, 5293.6' is an oncoidal grainstone that has undergone extensive mechanical compaction, reducing originally high interparticle porosity, but subsequent dissolution created vuggy porosity (7%). Although some porosity enhancement has occurred, the porosity of M2, 5293.6' is primarily the product of diagenetic reduction, and little relationship remains between facies and porosity. Lastly, porosity and permeability can vary greatly on the inch to foot scale; thus foot interval, core analysis poroperm values may include several different hybrid pore types, as evidenced by Appendix D, Figure D.15.

Petrophysical rock type 3 (R3) is characterized by pore type H1-Ae and is dominated by mudstone and wackestone facies, including spiculiferous sub-facies. K/Φ ratios for R3 range from 1 to 30 with associated porosity and permeability ranges of 8 to 15% and .1 to 4 md. This petrophysical rock type could be further divided on the basis of facies. Mudstone facies of R3 typically fall below a ratio of 10 K/Φ and the majority of wackestones plot above the 5 K/Φ ratio. However, the overlap between the two is sufficient enough to make such generalizations uncertain.

H1-Be genetic pore types dominate petrophysical rock type 4 (R4). This enhanced pore type is only found associated with spiculiferous wackestone sub-facies in Sunflower field. Several wackestones and a single packstone/grainstone facies also plot within R4. R4 exhibits the most favorable petrophysical flow properties and is found to be associated with the highest flow in Sunflower field. R4 plots between 5 and 100 K/Φ ratios with porosities greater than 15% and permeabilities over 1 md.

Evaluation of Reservoir Capacity to Flow

Stratigraphic modified Lorenz plots (SMLP) were constructed after Gunter et al., (1997), in order to evaluate petrophysical flow within parasequence C1 of Sunflower field. SMLP illustrate cumulative flow capacity and cumulative storage capacity ordered in the stratigraphic sequence of the reservoir. Inflection points indicate changes in flow or storage capacity, and allow for the evaluation of reservoir flow. By combining SML plots, facies and genetic pore type distribution, Sunflower flow was characterized and correlated on the reservoir scale. Discussion will continue to focus on wells M2 and P37-2 however, SML plots were generated for additional Sunflower wells.

Figure 17 displays the SMLP for parasequence C1 of well M2. Storage capacity is evenly distributed throughout the reservoir as evidenced by the diagonal, 45 degree trend. Reservoir flow capacity is divided into multiple zones of varying flow quality. Separation between reservoir flow and storage capacity indicates that not all pores contribute equally to flow.

The most favorable flow conditions are found in the middle portion of parasequence C1, from 5300 to 5312 ft., and are represented by highly sloped trends on the flow capacity line. This zone is responsible for 70% of the flow capacity in M2 and is found associated with the spiculiferous and enhanced R3 and R4 petrophysical rock type. Within this productive zone, 5300 to 5302 ft. exhibits the most dramatic flow, contributing 30% of the total flow capacity in just two feet. C1 flow is encased by tighter, low flow zones. These areas of poor flow are found associated with H1-Br (R2) dominated packstone/grainstone facies and H1-Ar/Ae mudstone (R1/R3 respectively).

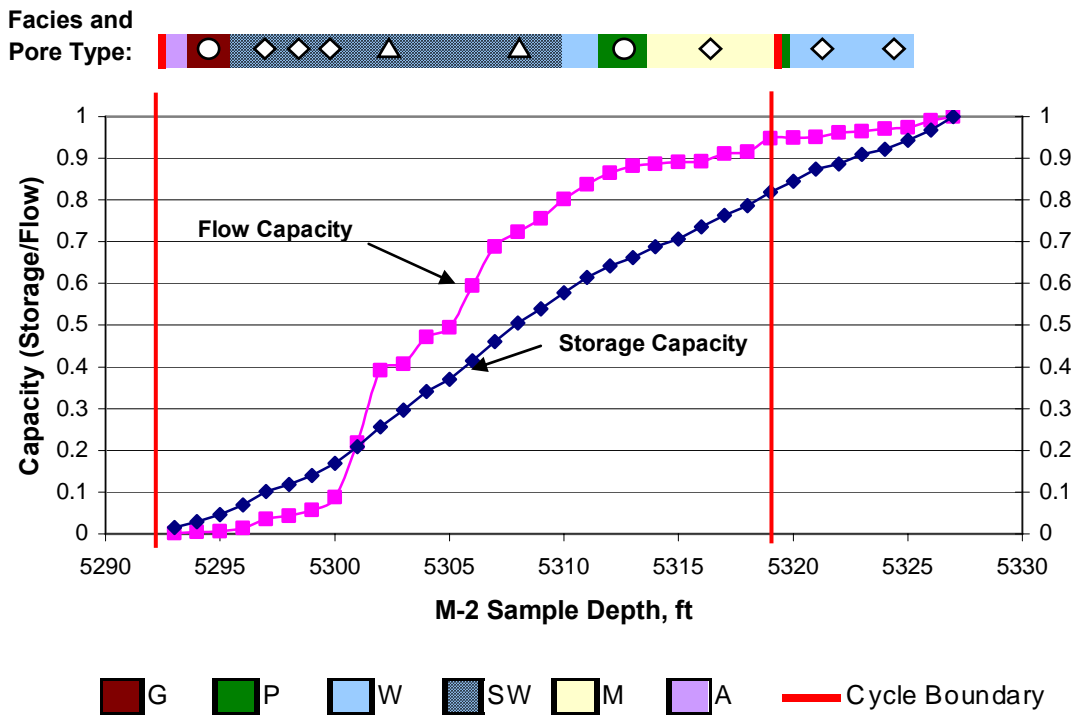


Figure 17: M2 SMLP plot. Illustrates reservoir flow and storage capacity of well M2. C1 boundaries are represented by red lines with the cycle top being located on the left hand portion of the graph. Corresponding reservoir facies and pore type (H1-Ae – diamonds, H1-Be – triangles, H1-Ar – squares, H1-Br – circles) are given at the top of the graph.

Figure 18 displays the distribution and quality flow in parasequence C1 from well P37-2. Again, storage capacity is relatively uniform throughout the reservoir with the exception of a low flow R1 interval from 5310 to 5312 ft. Reservoir flow capacity within C1 illustrates two distinct flow units separated by the previously mentioned tight R1 zone. Reservoir flow and storage capacity are closely associated indicating most pores are contributing equally to flow.

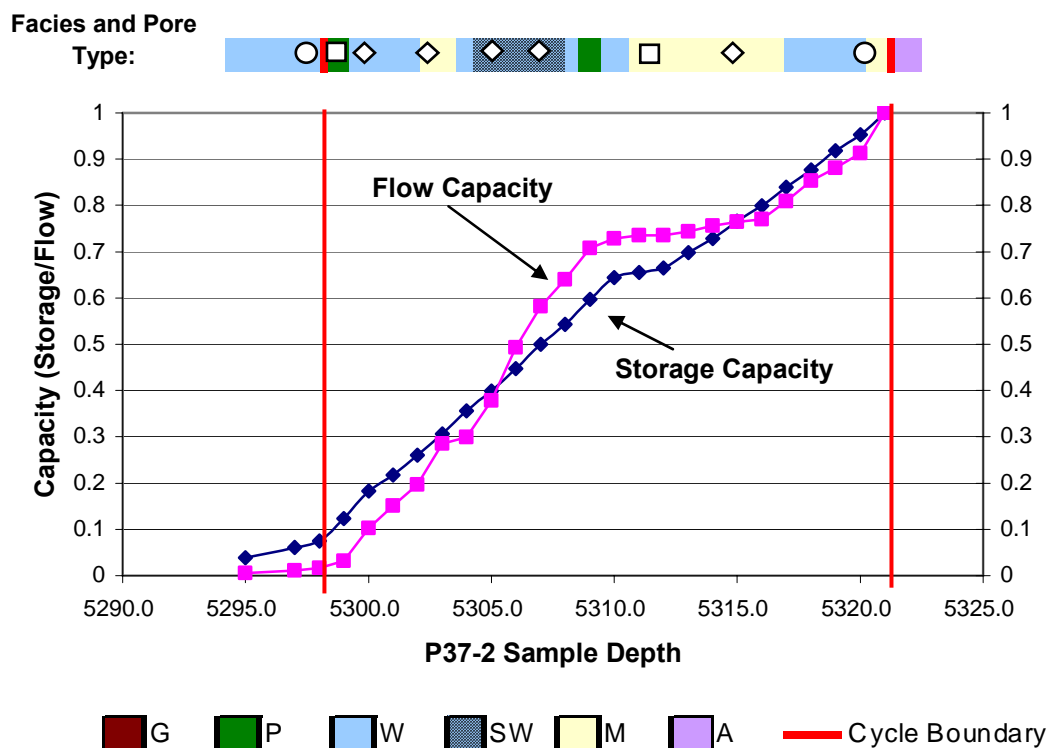


Figure 18: P37-2 SMLP plot. Illustrates reservoir flow and storage capacity of well P37-2. C1 boundaries are represented by red lines with the cycle top being located on the left hand portion of the graph. Corresponding reservoir facies and pore type (H1-Ae – diamonds, H1-Be – triangles, H1-Ar – squares, H1-Br – circles) are given at the top of the graph.

Flow conditions in well P37-2 are most favorable between 5299 to 5309 ft. which is responsible for 70% of the total flow capacity, and 5316 to 5321 ft. which contributes 10%. Both zones appear to be R3 rock types, are characterized by H1-Ae porosity, and are associated with wackestone and spiculiferous facies. A tight R1 mudstone interval exhibiting poor flow conditions is found separating these two R3 zones and may serve as a barrier or baffle to vertical flow.

From the SML plots of M2, P37-2, and additional Sunflower wells, several observations can be made. First, Sunflower field flow is characterized by petrophysical

rock types R3 and R4. These rock types are defined by pore types H1-Ae and H1-Be, respectively. These favorable flow conditions are typically found in association with the spiculiferous wackestone interval of parasequence C1. This strong relationship allows the spiculiferous sub-facies and enhanced pore types (R3 and R4 rock types) to serve as pore-proxy rock properties that can be correlated across the field. Therefore, Sunflower flow can be correlated on the reservoir scale by mapping the distribution of the C1 spiculiferous zone.

Distribution of Flow Units Within Sunflower Field

As discussed in the previous section, flow within Sunflower field is closely associated with the spiculiferous wackestone sub-facies of parasequence C1. Spiculiferous wackestone accounts for nearly 26% of all reservoir facies and is found concentrated in the middle to upper portions of parasequence C1, typically 4 feet below the cycle top. A three-dimensional fence diagram constructed for Sunflower field, (Appendix E, Figure E.2) displays the distribution of the SW interval and associated reservoir flow. The SW interval is believed to have been deposited in quiet waters behind a barrier complex. If this is the case, the deposit would be expected to be elongate along strike.

Appendix E, Figure E.2 reveals C1 spiculiferous wackestone deposits range in thickness from 4 to 15 ft. Accumulations appear to thin along strike with wells M19-4 and P37-2 containing the thinnest intervals, approximately 4 ft. However, it should not be assumed that the SW interval pinches out laterally. Observations made within the

limited extent of the study area can not definitively determine lateral extent of facies.

No constant thickness trends were observed along dip, but it should be noted that there is little dip control in this study. Additionally, in some down-dip wells, like B48-4, C1 falls below the oil/water contact (Figure 3) and water is produced.

Despite the considerable accumulations of SW sub-facies and associated high poroperm values, structurally down-dip locations that fall along the oil/water contact should not be considered for development. SW deposits are likely found up-dip within Muldrow and Pool-Hannes sections, but are expected to pinch out abruptly. Although the SW interval thins along strike, this study recommends further exploratory drilling along strike to determine the lateral extent of the deposit and corresponding flow unit.

SUMMARY AND CONCLUSIONS

Summary

The primary objectives of this study are: to conduct an integrated stratigraphic, petrographic, and petrophysical analysis of the San Andres, Sunflower field, test pre-existing methods of reservoir characterization with resulting data, and establish an improved method of carbonate reservoir characterization that integrates reservoir petrophysical properties with genetic porosity classification.

Core analysis led to the identification of three correlatable, vertically stacked, shallowing upward parasequences composed of subtidal, intertidal, and supratidal successions. Within these cycles, three primary facies and a sub-facies were identified: mudstone, wackestone, spiculiferous wackestone sub-facies, and packstone/grainstone facies. Petrographic analysis revealed four hybrid genetic pore types in Sunflower field, H1-Ae, Be, Ar, and Br.

High pressure mercury injection capillary data and graphical analysis methods of Winland R_{35} and K/Φ ratio illustrated that petrophysical properties share a stronger relationship with genetic pore types than with facies. Therefore, genetic pore typing is a more accurate means of carbonate reservoir characterization than traditional facies dependent methods. Ultimately, the results of this study reveal that the most effective way of characterizing petrophysical flow units is the combination of K/Φ ratio analyses and genetic pore typing.

From this development, four petrophysical rock types were defined, characterized, and related to flow distribution in Sunflower field using SMLP. Petrographic rock types corresponding with the most favorable flow conditions, R3 and R4, were found to be closely associated with the spiculiferous wackestone interval typically found 4 feet below the top of parasequence Cycle 1. Therefore, the spiculiferous wackestone sub-facies may be used as a pore-proxy rock property for the determination of pore type distribution and corresponding flow units at the reservoir scale.

Conclusions

- In carbonate reservoirs affected by diagenesis, petrophysical properties share a closer relationship with genetic pore type than with facies.
- The most effective way of characterizing petrophysical flow units in carbonate reservoirs is the combination of K/Φ ratio analyses and genetic pore typing.
- In South Sunflower field four hybrid genetic pore types define four distinct petrophysical rock types: R1 from H1-Ar pores, R2 from H1-Br pores, R3 from H1-Ae pores, and R4 from H1-Be pores. R4 petrophysical rock types present the most favorable flow conditions followed by R3, while R2 and R1 yield the least desirable petrophysical characteristics.
- Distribution of R4 and R3 petrophysical rock types in Sunflower field closely follow the spiculiferous wackestone interval of parasequence C1, thus the sub-

facies can be used to determine pore type distribution and corresponding flow units at the reservoir scale.

REFERENCES CITED

Ahr, W. M., D. Allen, A. Boyd, H. N. Bachman, T. Smithson, et al, 2005, Confronting the carbonate conundrum: Schlumberger Oilfield Review, Spring 2005, p. 18-29.

Ahr, W. M., 2006, GEOL-624 Carbonate Reservoir, Course Notes, Texas A&M University, 109 p.

Amare, K., 1995, Mapping flow units in a heterogeneous carbonate reservoir: Reeves field, Yoakum County, Texas: Ph.D. dissertation, Texas A&M University, College Station, Texas, 144 p.

Archie, G.E., 1952, Classification of carbonate reservoir rocks and petrophysical considerations: AAPG Bulletin, v. 36, p. 278-298.

Bein, A. and Land, L., 1982, San Andres carbonates in the Texas panhandle: sedimentation and diagenesis associated with magnesium-calcium-chloride brines; Bureau of Economic Geology, The University of Texas at Austin, Report of Investigations, no. 121, 48 p.

Choquette, P. W., and L. C. Pray, 1970, Geologic nomenclature and classification of porosity in sedimentary carbonates: American Association of Petroleum Geologists Bulletin, v. 54, p. 207-250.

Chuber, S., and W. C. Pusey, 1969, Cyclic San Andres facies and their relationship to diagenesis, porosity, and permeability in the Reeves field, Yoakum County, Texas, *in* J. G. Elam and S. Chuber, eds., Cyclic Sedimentation in the Permian Basin-A Symposium: West Texas Geological Society, Publ., p. 136- 151.

Chuber, S., and W. C. Pusey, 1985, Productive Permian carbonate cycles, San Andres Formation, Reeves Field, West Texas, *in* P. O. Roehl and P. W. Choquette, eds., Carbonate Petroleum Reservoirs: Springer-Verlag, New York, p. 290-307.

Cowan, P. E. and P. M. Harris, 1986, Porosity distribution in San Andres Formation (Permian), Cochran and Hockley Counties, Texas: AAPG Bulletin, v. 70, p. 888-897.

Dutton, S. P., Kim, E. M., Broadhead, R. F., Raatz, W. D., Breton, C. L., Ruppel, S. C., and Kerans, Charles, 2005, Play analysis and leading-edge oil-reservoir development methods in the Permian basin: increased recovery through advanced technologies: AAPG Bulletin, v. 89, no. 5, p. 553–576.

Elliot, L. A., and J. K. Warren, 1989, Stratigraphy and depositional environment of Lower San Andres Formation in subsurface and equivalent outcrops: Chaves, Lincoln, and Roosevelt Counties, New Mexico: AAPG Bulletin, v. 73, p. 1307-1325.

Goldhammer, R. K., E. J. Oswald, and P. A. Dunn, 1991, Hierarchy of stratigraphic forcing: example from Middle Pennsylvanian shelf carbonates of the Paradox Basin, *in* E. K. Franseen, W. L. Watney, C. G. Kendall, and W. Ross, eds., Sedimentary modeling: computer simulations and methods for improved parameter definition: Kansas Geological Survey Bulletin, v. 233, p. 361-413.

Grant, C. W., D. J. Goggin, and P. M. Harris, 1994, Outcrop analog for cyclic-shelf reservoirs, San Andres Formation of Permian Basin: stratigraphic framework, permeability distribution, geostatistics and fluid-flow modeling; AAPG Bulletin, v. 78, p. 23-54.

Gunter, G. W., J. M. Finneran, D. J. Hartmann, and J. D. Miller, 1997, Early determination of reservoir flow units using an integrated petrophysical method: SPE Paper 38679, 8 p.

Harris, P. M., C. Kerans, and D. G. Bebout, 1993, Ancient outcrop and modern examples of platform carbonate cycles-Implications for subsurface correlation and understanding reservoir heterogeneity, *in* R. G. Loucks and J. F. Sarg, eds., Carbonate Sequence Stratigraphy: AAPG Memoir no. 57, p. 475-492.

Hartmann, D. J., and E. B. Coalson, 1990, Evaluation of the Morrow Sandstone in Sorrento Field, Cheyenne County, Colorado, *in* S. A. Sonnenberg, L. T. Shannon, K. Rader, W. F. Von Drehle, and G. W. Martin, eds., Morrow Sandstones of Southeast Colorado and Adjacent Areas, The Rocky Mountain Association of Geologists, Denver, Colorado, p. 91-100.

Hartmann, D. J., and E. A. Beaumont, 1999, Predicting reservoir system quality and performance, *in* E. A. Beaumont and N. H. Foster, eds., *Exploring for oil and gas traps: AAPG Treatise of Petroleum Geology, Handbook of Petroleum Geology*, p. 9-1-9-154.

Hills, J. M., 1970, Late Paleozoic structural directions in southern Permian Basin, west Texas and southeastern New Mexico: *AAPG Bulletin*, v. 54, p. 1809-1827.

Hills, J. M., 1972, Late Paleozoic sedimentation in West Texas Permian Basin: *AAPG Bulletin*, v. 56, p. 2303-2322.

Hovorka, S. D., H. S., Nance, and C. Kerans, 1993, Parasequence geometry as a control on permeability evolution: examples from the San Andres and Grayburg Formations in the Guadalupe Mountains, New Mexico, *in* R. G. Loucks and J. F. Sarg, eds., *Carbonate Sequence Stratigraphy: AAPG memoir no. 57.*, p. 493-514.

James, N.P., 1984, Shallowing-upward sequences in carbonates, *in* R.G. Walker, ed., *Facies Models: Geoscience Canada, Geological Association of Canada Publications*, Toronto, Canada, p. 213-228.

Jensen, J. L., L. W. Lake, P. W. M. Corbett, and D. J. Goggin, 1997, *Statistics for petroleum engineers and geoscientists: Englewood Cliffs, New Jersey, Prentice Hall*, 390 p.

Keller, D. R., 1993, Evaporite geometries and diagenetic traps, Lower San Andres, Northwest Shelf, New Mexico: *AAPG Bulletin Southwest Section Meeting*, p. 183-193.

Kerans, C., W. M. Fitchen. M. H. Gardner, M. D. Sonnenfeld, S. W. Tinker, and B. R. Wardlaw, 1992, Styles of sequence development within uppermost Leonardian through Guadalupian strata of the Guadalupe Mountains, Texas and New Mexico, *in* D. H. Mruk and B. C. Curran, eds., *Permian Basin Exploration and Production Strategies: Applications of Sequence Stratigraphic and Reservoir Characterization Concepts: West Texas Geological Society Symposium, no. 92-9 1*, p. 1-7.

Kerans, C., W. M. Fitchen, M. H. Gardner, and B. R. Wardlaw, 1993, A contribution to the evolving stratigraphic framework of middle Permian strata of the Delaware Basin, Texas and New Mexico: *New Mexico Geological Society Guidebook, 44th Field*

Conference, Carlsbad Region, New Mexico and West Texas, p. 175- 184.

Kerans, C., F. J. Lucia, and R. K. Senger, 1994, Integrated characterization of carbonate ramp reservoirs using Permian San Andres Formation outcrop analogs: AAPG Bulletin, v. 78, no. 2, p. 181-216.

Kolodzie, S., Jr., 1980, Analysis of pore throat size and use of the Waxman-Smiths equation to determine OOIP in Spindle Field, Colorado: Society of Petroleum Engineers, 55th Annual Fall Technical Conference, Paper SPE-9382, 10 p.

Lucia, F. J., 1983, Petrophysical parameters estimated from visual description of carbonate rocks: a field classification of carbonate pore space: Journal of Petroleum Technology, March, v. 35, p. 626-637.

Major, R.P., and M.H. Holtz, 1997, Predicting reservoir quality at the development scale: methods for quantifying remaining hydrocarbon resource in diagenetically complex carbonate reservoirs, *in* J.A. Kupecz, J. Gluyas, and S. Bloch, eds., Reservoir quality prediction in sandstones and carbonates: AAPG Memoir 69, p. 231-248.

Martin, A. J., S. T. Solomon, and D. J. Hartmann, 1997, Characterization of petrophysical flow units in carbonate reservoirs: AAPG Bulletin, v. 81, no. 5, p. 734-759.

Meissner, F. F., 1972, Cyclic sedimentation in middle Permian strata of the Permian Basin, West Texas and New Mexico, *in* J. G. Elarn and S. Chuber, eds., Cyclic Sedimentation in the Permian Basin: West Texas Geological Society, Midland, Texas, p. 203-232.

Milner, S., 1976, Carbonate petrology and syndepositional facies of the Lower San Andres Formation (Middle Permian), Lincoln County, New Mexico: Journal of Sedimentary Petrology, v. 46, p. 463-482.

Pittman, E. D., 1992, Relationship of porosity and permeability to various parameters derived from mercury injection-capillary pressure curves for sandstone: AAPG Bulletin, v. 76, p. 191-198.

Pranter, M. J., 1999, Use of a petrophysical-based reservoir zonation and multicomponent seismic attributes for improved geologic modeling, Vacuum field, New Mexico: Ph.D. dissertation, Colorado School of Mines, Golden, Colorado, 366 p.

Ramondetta, P. J., 1982a, Facies and stratigraphy of the San Andres Formation, Northern and Northwestern Shelves of the Midland Basin, Texas and New Mexico: Bureau of Economic Geology, The University of Texas at Austin, Report of Investigations No.128, 56 p.

Ramondetta, P. J., 1982b. Genesis and emplacement of oil in the San Andres Formation: Bureau of Economic Geology, The University of Texas at Austin, Report of Investigations, no. 116, 39 p.

Rezaee, M. R., A. Jafari, and E. Kazemzadeh, 2006, Relationships between permeability, porosity and pore throat size in carbonate rocks using regression analysis and neural networks: Journal of Geophysics and Engineering, v. 3, p. 370-376.

Silver, B. A., and R. G. Todd, 1969, Permian cyclic strata, northern Midland and Delaware Basins, West Texas and southeastern New Mexico: AAPG Bulletin, v. 53, p. 2223-2251.

Van Wagoner, J. C., H. W. Posamentier, R. M. Mitchum Jr., P. R. Vail, J. F. Sarg. T. S. Loutit, and J. Hardenbol, 1988, An overview of the fundamentals of sequence stratigraphy and key definitions, *in* Sea-Level Changes-An Integrated Approach: SEPM Special Publication, no. 42, p. 39-45.

Van Wagoner, J. C., R. M. Mitchum, K. M. Campion, and V.D. Rahmanian, 1990, Siliciclastic sequence stratigraphy in well logs, cores and outcrops: AAPG Methods in Exploration Series, no. 7, 55 p.

Ward, R. F., G. St. C. C. Kendall, and P. M. Hams, 1986, Upper Permian (Guadalupian) facies and their association with hydrocarbons-Permian Basin, West Texas and New Mexico: AAPG Bulletin, v. 70, p. 239-262.

Wilson, J. L., 1975, Carbonate Facies in Geologic History: New York, Springer-Verlag, 471 p.

APPENDIX A
CORE DESCRIPTION

Table A.1
Well list with name abbreviations

Lease Name	Well Number	Well ID
Muldrow	2	M2
Muldrow	3	M3
Muldrow	6	M6
Muldrow	7	M7
Muldrow	11	M11
Muldrow	13	M13
Muldrow	14	M14
Muldrow 19	4	M19-4
Muldrow 50	1	M50-1
Pool 37	1	P37-1
Pool 37	2	P37-2
Beasley 48	4	B48-4

LITHOFACIES

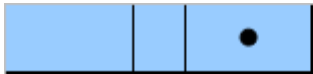
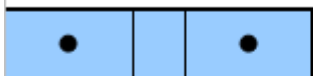


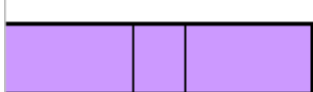

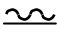
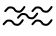

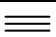

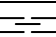
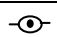
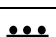
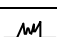
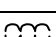

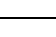
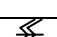





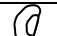

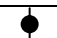


	Mudstone
	Wackestone
	Packstone
	Grainstone
	Anhydrite

Figure A.1: Facies key for core description.

Structures (Stratification, Sedimentary, Diagenetic)

	Irregular bedding		Current produced laminations
	Discontinuous irregular bedding		Burrowed
	Parallel bedding		Churned
	Discontinuous parallel bedding		Fenestral fabric
	Graded bedding		Stylolite
	Nodular diagenetic bedding		Dissolution (horse tail)
	Desiccation cracks		Fractures

Framework Grains

	Algae, undifferentiated		Skeletal fossil, undifferentiated
	Crinoid		Mollusk, undifferentiated
	Echinoderm		Ostracod
	Foraminifera		Pellet
	Intraclast		Peloid

Accessories and Hydrocarbon Shows



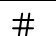




	Mica		Oil stain
	Pyrite		Dead oil
	Siliciclastic silt		Hydrocarbon odor
	Siliceous replacement		

Figure A.2: Core description key after the Shell Sample Examination Manual format.

WELL NAME: MULDROW 2			
Depth	Lithology	Bddg, Accessories	Additional Comments
5277			Scat intpar Φ , Intbd slty wkst & bd anhy, pelskel pkst lam, detr qtz slt, chal after anhy
5278			Scat intpar/mol Φ , intbd skel-pel pkst-wkst & bd anhy, skel dust, chal after anhy
5279			Scat intpar Φ , pel pkst-wkst w/intclas grnst bd, intrclst anhy cmt, chal after anhy
5280			Scat intpar/mol Φ , pel pkst grding into pel wkst, diagn lam, poss grn cpct
5281			Scat intpar/mol Φ , pel pkst grding into pel wkst, diagn lam, poss grn cpct
5282			Scat intpar/mol Φ , intbd pel-skel pkst & grn rich wkst, skel dust, disol phenomena & pos
5283			Scat intpar/mol Φ , intbd pel-skel pkst & grn rich wkst, skel dust, disol phenomena & pos
5284			Scat intpar/mol Φ , mdst- pel wkst, planar lam, nod anhy w/mud infill, pos desiccation crack, chal after anhy, frac filling anhy cmt, intprt anhy cmt/rep, grn rich lam below 5289'
5285			Scat intpar/mol Φ , mdst- pel wkst, planar lam, nod anhy w/mud infill, pos desiccation crack, chal after anhy, frac filling anhy cmt, intprt anhy cmt/rep, grn rich lam below 5289'
5286			Scat intpar/mol Φ , mdst- pel wkst, planar lam, nod anhy w/mud infill, pos desiccation crack, chal after anhy, frac filling anhy cmt, intprt anhy cmt/rep, grn rich lam below 5289'
5287			Scat intpar/mol Φ , mdst- pel wkst, planar lam, nod anhy w/mud infill, pos desiccation crack, chal after anhy, frac filling anhy cmt, intprt anhy cmt/rep, grn rich lam below 5289'
5288			Scat intpar/mol Φ , mdst- pel wkst, planar lam, nod anhy w/mud infill, pos desiccation crack, chal after anhy, frac filling anhy cmt, intprt anhy cmt/rep, grn rich lam below 5289'
5289			Scat intpar Φ , rpl wkst grad into diss cpct pkst intvl, grn cpct, chal after anhy, pos anhy filled bur below 5291', cm scale concave up current lam
5290			Scat intpar/mol Φ , grn rich wkst-pkst, grn cpct, disol ab anhy bd, chal after anhy
5291			Scat intpar Φ , pel-clas grnst/pkst grad into fen wkst, obvious intpar dolo/anhy cmt in pkst-grnst, rnd mm scale pel, pos litho & bioclasts, indst wy bdd, cm scale concave up current lam, grn cpct, chal after anhy, anhy cmt frac
5292			Obvious intpar/mol Φ , scat vug Φ , pel wkst-pkst, wy continuous-discon lam, current influenced, diag overprint, grn cpct, bur intvl
5293			Scat intpar/mol Φ , bioturbated pel wkst-pkst, diagn lam, anhy cmt/rep, l intraclas-pel pkst has obvious pel-skel mol Φ , oil strn, wy dis bdd
5294			Scat intpar/mol Φ , bioturbated pel wkst-pkst, diagn lam, anhy cmt/rep, l intraclas-pel pkst has obvious pel-skel mol Φ , oil strn, wy dis bdd
5295			Scat intpar/mol Φ , bioturbated pel wkst-pkst, diagn lam, anhy cmt/rep, l intraclas-pel pkst has obvious pel-skel mol Φ , oil strn, wy dis bdd
5296			Scat intpar/mol Φ , bioturbated pel wkst-pkst, diagn lam, anhy cmt/rep, l intraclas-pel pkst has obvious pel-skel mol Φ , oil strn, wy dis bdd
5297			Scat intpar/mol Φ , bioturbated pel wkst-pkst, diagn lam, anhy cmt/rep, l intraclas-pel pkst has obvious pel-skel mol Φ , oil strn, wy dis bdd

Figure A.3: M2 core description.

WELL NAME: MULDROW 2

Depth	Lithology	Bddg, Accessories	Additional Comments
5298		#	Obvious intpar & pel-skel mol Φ , pel pkst-grn rich wkst, C nod anhy, chal after anhy, thn
5299		#	grnst lyr w/ C intpar anhy cmt, dissol between grnst & wkst lyr, altg lyrs of cmt low Φ grnst-pkst & non-cmt high Φ pkst-wkst, poss
5300		#	
5301		#	Obvious intpar & pel/skel mold Φ in up
5302		#	pkst, scat mol Φ in wkst & l pkst, rep anhy
5303		#	Dk up pkst - obvious intpar/pel mol Φ , l lt pkst scat pel mol Φ & intpar cmt, C chalc cmt/rep,
5304		#	Obvious intpar/mol Φ , v th intv at 5303' 2" w/ pel mol/vug Φ intvl, pel wkst-pks, poss skel grns, chal cmt/rep intvl
5305		#	
5306		#	Obvious pel-skel mol & intpar Φ , alt lyrs of
5307		#	intpar cmted pkst w/scat Φ & noncmted lyrs w/obvious Φ , bitumen & pyr plugging lg vugs, bur str, indst pel grns & skel dust, indst dep fabric, anhy cmt frac, C chal cmt & rep
5308		#	
5309		#	
5310		#	
5311		#	
5312		#	Obvious skel-pel mol & intpar Φ , pel-skel pkst, undifferentiated skel frags: ech, moll, foram, bry, gn alg, & brach; anh cmted frac & mol Φ , anhy rep grns, chal rep, pos
5313		#	
5314		#	Obvious skel-pel mol Φ , arg mdst-skel wkst, thn sh lyr, pos diag in origin, ech & gm alg rich, pos spg spic below 5315'
5315		#	
5316		#	
5317		#	Obvious skel-pel mol Φ , skel-pel pkst-grn rich wkst, C anhy cmt/rep grns,
5318		#	undifferentiated skel frags: foram, moll, alg;

Figure A.3 Continued.

WELL NAME: MULDROW 2

Depth	Lithology	Bddg, Accessories	Additional Comments
5319		#	Scat pel-skel mol & intpar & vug Φ , skel dust, intpar cmt, major col change at 5319.25', R intclas ab this ctc, chal after anhy, anhy rep Obvious intpar/pel mol Φ , pel pkst-wkst, bd anhy w/pos dessication cracks, chal after Obvious pel skel mol Φ , pkst-grnst, bd anhy parallel to wvy bddg, C intpar/mol anhy cmt & anhy rep, anhy cmt frags, C forams, mill frags & pos alg, C bded nod anhy at 5324'
5320		#	
5321		#	
5322		#	
5323		#	
5324		#	

Figure A.3 Continued.

WELL NAME: MULDROW 3

Depth	Lithology	Bddg, Accessories	Additional Comments
5279		#	Scat intpar Φ , pel pkst-wkst, indst grms, C dissol & grn cmpct, anhy rep, clast erosional surf at 5280' 4"
5280		#	
5281		#	Scat intpar Φ , lam arg mdst-wkst, poss current lam, chal after anhy, col & lith change along erosional surf at 5282' 2.5", pel wkst-mdst scat pel mol Φ below surf
5282		#	
5283			Thn intraclas pkst, poss sol collapse brec Scat Φ , pel wkst-mdst, nod anhy & lam of anhy after hal?, wvy discon lam, pkst invl from 5285' 5" - 10" w/ current oriented clas & intpar anhy cmt
5284		#	
5285		#	
5286			Obvious intpar/pel mol Φ , pel-skel wkst w/ gny pkst intl, chal after anhy, C detrital qtz slt, discon wvy lams, poss diag lam, C dissol, C bur struc at 5291'
5287		#	
5288		#	
5289		#	

Figure A.4: M3 core description.

WELL NAME: MULDROW 3

Depth	Lithology	Bddg, Accessories	Additional Comments
5290		☞ # ●	
5291		⊕ # ● ☞	
5292		⊕ # ☞	Obvious pel-skel mol/intpar Φ , bioturbated pkst, chal after anhy, C anhy rep
5293		⊕ # ☞	Obvious pel mol/intpar Φ , bioturbated grn-rich wkst, indst grns, pkst in areas?, C anhy rep, anhy cmted frac, chal after anhy, poss desiccation cracks
5294		☞ # ☞	
5295		☞ # ☞	
5296		☞ # ☞	Obvious pel-skel mol/intpar & scat vug Φ , pel-skel pkst w/ altg lyrs of hi Φ & mod Φ , undifferentiated skel grns, C anhy cmt/rep, chal after anhy, intpar anhy cmt?
5297		☞ #	
5298		☞ #	
5299		☞ #	
5300		☞ #	Spty pel mol/intpar Φ , intbided pelskel wkst & pel pkst, indst pellets, nod anhy, chal after anhy, C anhy cmt/rep
5301		☞ #	
5302		☞ #	Obvious intpar/intxln & R mol Φ , wkst? & pkst? w/ indst pel grns, dolomitization precludes identification of dep tex
5303		☞ #	Obvious intpar/pelskel mol Φ , dissol w/ grn cpct, chal after anhy, anhy cmt/rep, poss lithoclast
5304		☞ #	
5305		☞ #	
5306		☞ #	5306 ' contains C pelloids, pelal grapst, skel frags of gn alg, moll?, foram
5307		☞ # ▲	Obvious intpar/skel mol Φ , bioclas detrital mound, C plty alg, pyloidal?, C crin, P foram, pel, & skel/lith clas, preferred grn orientation, C intpar/mol anhy cmt & rep
5308		☞ # ▲	
5309		☞ # ☞	Scat pel mol Φ , shly lam wkst-mdst w/ prom partially anh cmted frac, pbl sized clas w/ grapst fabric @ 5310' 11"
5310		☞ #	

Figure A.4 Continued.

WELL NAME: MULDROW 3			
Depth	Lithology	Bddg, Accessories	Additional Comments
5311		#	Scat pelskel mol Φ , P foram, spg spic & alg frags, intvl of chal cmt/rep @ 5311' 7.5", anhy, chal, & # rep, poss bur struc
5312		#	
5313		#	
5314		#	Sharp facies ctc @ 5314' 6" marked by styl
5315		#	Obvious intpar & scat vug Φ , pel pkst-grnst, C anhy rep, anhy after fen Φ ?
5316		#	Obvious pel-skel mol/intpar Φ , scat Φ in wkst, interlamated pel pkst - wkst, chal after anhy, skel grns include forams & crin
5317		#	
5318		#	
5319		#	
5320		#	Scat pel mol Φ , pel wkst-pkst?, dissol & diag lam, mic?, poss intraclas grns, # rep, erosional scour surf @ 5320' 1.5", thn shl @ 5320' 11" marks dep facies ctc
5321		#	Scat pel-skel mol Φ , wvy continuous lams, poss alg lams, mol any cmt & anhy rep
5322		#	Obvious pel-skel mol Φ , obvious anhy cmted fracs @ 5322', chal after anhy, some anhy cmt/rep
5323		#	
5324		#	Scat pel mol Φ , indst wvy lams, # rep, chal after anhy, scour surf @ 5324' 9.5"
5325		#	
5326		#	Obvious pel-skel mol Φ , scat vug Φ , grn rich wkst-pkst, C anhy cmt/rep, C intraclas grns, erosional surf @ 5327' 4"
5327		#	
5328		#	Obvious interpar Φ below erosional surf @ 5327' 4", pel pkst w/ evidence of subaerial exposure, desiccation cracks, C anhy rep,
5329		#	Scat intpar/mol Φ , bds of nod anhy ovgh, rep anhy & # follow bdding
5330		#	
5331		#	

Figure A.4 Continued.

WELL NAME: MULDROW 3

Depth	Lithology	Bddg, Accessories	Additional Comments
5332		#	Scat mol Φ , pel wkst w/ pkst lam, nod anhy, chal after anhy, rep #, wvy continuous & discon lams, rep anhy follows bdding, qtz slt
5333		#	
5334		#	
5335		#	
5336		#	Scat pel-skel mol Φ , bioturbated - churned, C qtz slt, rep anhy follows bdding
5337		#	
5338		#	Scat pel-skel mol Φ , indst pel, skel, & intrclast grns, C qtz slt

Figure A.4 Continued.

WELL NAME: MULDROW 6

Depth	Lithology	Bddg, Accessories	Additional Comments
5262			Mass gry-wh anhy w/ mdst strgr & styl at base
5263		#	Mdst-wkst w/ scat mol Φ , parallel-wvy lams, irr pkst lam, # along bddg
5264		#	
5265		#	Gm rich wkst w/ scat but obvious Φ , f skel dust, chal after anhy
5266		#	
5267		#	
5268		#	

Figure A.5: M6 core description.

WELL NAME: MULDROW 6

Depth	Lithology	Bddg, Accessories	Additional Comments
5269		#	
5270		#	Gm rich w/ scat Φ , mdy intraclas in upper 5"
5271		#	Ltl to no vis Φ , vert fracs, styl and sol swarms
5272		#	
5273			
5274		#	Scat pel mol Φ , vert fracs, styl and sol swarms, wkst/pkst lam at base
5275		#	
5276			
5277			Pkst w/ wkst lam, obvious pel-skel mol Φ , scat intpar Φ , assem of pel & skel grms, sil spg spic, anhy cmt fracs, nod anhy w/ chal after anhy
5278		#	
5279			
5280			
5281			
5282			Intbdd wkst-pkst w/ scat Φ in wkst & obvious pel-skel mol Φ in pkst, vert anhy cmt frac
5283			
5284		#	
5285		#	
5286		#	
5287		#	
5288		#	Pel pkst-gmst, poss ool/onc, major color change from tan to lr gry at 5287.5', scat intpar & vug Φ , intpar cmt, bd nod any w/ styl at base
5289			

Figure A.5 Continued.

WELL NAME: MULDROW 6

Depth	Lithology	Bddg, Accessories	Additional Comments
5290			Pel pkst w/ scat-obvious pel mol Φ , nod anhy lam, discontinuous wy lam
5291			
5292			
5293			Obvious pel-skel mol Φ , poss desiccation cracks
5294			Scat ple-skel mol Φ , anhy cmt, modly burr, diagn sol swarms
5295			
5296			
5297			Gm rich wkst-pkst w/ scat but obvious pel-skel mol Φ , sil/chal repl near 5298'
5298			

Figure A.5 Continued.

WELL NAME: MULDROW 7

Depth	Lithology	Bddg, Accessories	Additional Comments
5327			Wkst w/ pkst lam, scat skel/pel mol & intpar mol Φ , vert anhy cmt frac, microstyl, desiccation cracks & intraclas at base
5328			
5329			Scat intpar/mol Φ , sol seams & micro styl, intraclas, vert/hor fracs
5330			Scat pel mol Φ , detrital sili slt, vert anhy cmt frac, nod anhy, chal after anhy
5331			
5332			
5333			Scat pel/skel mol Φ , carb lithoclas or intraclas, anhy rep grns

Figure A.6: M7 core description.

WELL NAME: MULDROW 7

Depth	Lithology	Bddg, Accessories	Additional Comments
5334			Scat pel/skel mol Φ , irr bddg, w/ scat anhy cmt vert fracs, nod anhy, chal after anhy
5335			
5336			
5337			
5338			
5339			
5340			Grn rich wkst-pkst, scat pel/skel mol & intpar Φ , chal/# after anhy, vert anhy cmt
5341			
5342			Grn rich wkst-pkst w/ grnst lam, obvious pel/skel mol Φ , Φ more scat in grnst, chal after anhy, intpar cmt
5343			
5344			
5345			
5346			
5347			
5348			
5349			
5350			
5351			
5352			Grn rich wkst-pkst w/ C pel grns, obvious pel/skel & intpar mol Φ , anhy cmt/rep, chal after anhy

Figure A.6 Continued.

WELL NAME: MULDROW 7

Depth	Lithology	Bddg, Accessories	Additional Comments
5353		#	
5354		#	
5355		#	
5356		#	
5357		#	
5358		#	
5359		#	Skel-pel wkst w/ scat pel/skel mol Φ , anhy cmt filling mol Φ , nod anhy, chal after anhy, vert cmt frac
5360		#	
5361		#	
5362		#	Scat but obvious pel/skel mol Φ , anhy cmt filling mol Φ , nod anhy, chal spherules, vert cmt frac
5363		#	
5364		#	Dolomitization precludes determination of depositional texture
5365		#	
5366		#	Pkst w/ obvious pel/skel mol Φ , nod anhy accumulations, anhy cmt/rep, chal after anhy
5367		#	

Figure A.6 Continued.

WELL NAME: MULDROW 11			
Depth	Lithology	Bddg, Accessories	Additional Comments
5294			Scat mol Φ , mdy, wvy lam w/ intraclas intvl & desiccation features, poss bur str, anhy cmt vert frac
5295			
5296			
5297			
5298			Mdy w/ scat Φ , wvy/diagn nod lam, present qtz slt, irr grn rich lam
5299			
5300			Nod anhy accumulation w/styl, anhy cmt fen Φ , wvy lam
5301			
5302			
5303			Skel rich wkst-pkst w/ obvious mol Φ , grnst lam, anhy cmt/rep grns, nod anhy
5304			
5305			Scat but obvious pel-mol Φ , C nod & any, w/chal rep anhy margins
5306			
5307			
5308			
5309			
5310			Obvious pel/skel mol Φ , styl & wvy dis seams, hydc stain/odor, C anhy cmt & nod anhy rep, chal after anhy, vert/hor cmt frac
5311			
5312			
5313			
5314			Obvious mol Φ , nod any rep/cmt, pel dominated pkst w/vert bur struc, chal after anhy
5315			

Figure A.7: M11 core description.

WELL NAME: MULDROW 11

Depth	Lithology	Bddg, Accessories	Additional Comments
5316		#	Skel dominated pkst w/ obvious skel mol Φ, C anhy cmt/rep after skel grns, chal after anhy
5317		#	Mdy w/ scat mol Φ, wvy/diagn lam, chal & pyr after anhy, vert anhy cmt frac
5318		#	
5319		#	
5320		#	
5321		#	
5322		#	Skel invl w/scat but obvious skel mol Φ, erosional ctc between wkst/pkst, intraclas invl w/ anhy cmt fen Φ after nod anhy
5323		#	
5324		#	Scat Φ, wkst w/grn rich pkst(?) lam, indst skel/pel grns, chal after anhy
5325		#	
5326		#	
5327		#	
5328		#	Obvious mol/intpar Φ, anhy cmt/rep grns, chal after anhy
5329		#	
5330		#	Scat Φ, mdy, poss limey, blkly anhy after hal (?), styl & dissolution seams
5331		#	
5332		#	Obvious pel/skel mol Φ, anhy cmt/rep grns, chal after anhy, chal after anhy & sili rep of rk
5333		#	

Figure A.7 Continued.

WELL NAME: MULDROW 11

Depth	Lithology	Bddg, Accessories	Additional Comments
5334			Mdy pel wkst-mdst w/ scat Φ , wy & diagn lams, nod anhy rep, chal after anhy, ox hem, irr sili rep lam @ btm of 5339
5335			
5336			
5337			
5338			
5339			
5339			

Figure A.7 Continued.

WELL NAME: MULDROW 13

Depth	Lithology	Bddg, Accessories	Additional Comments
5319			Scat vug & mol Φ , limey pel wkst - pkst?, anhy rep & nod anhy, chal & # rep spg spic, insol rusty residue, anhy rep & dolo precludes identification of dep fabric
5320			
5321			Scat mol Φ , limey pel wkst - pkst?, anhy rep of grns, poss intraclas, insol residue
5322			
5323			Scat intpar/mol Φ , limey pel pkst-wkst intbd w/nod anhy bds, anhy rep, poss desiccation cracks @ 5324' 2"
5324			
5325			
5326			Scat intpar/mol Φ , pel-skel pkst, rep anhy follows bdg, skel grns include forams & crin
5327			
5328			Scat mol Φ , wkst w/ pel-skel pkst? lam, rep anhy, anhy cmted frags
5329			
5330			

Figure A.8: M13 core description.

WELL NAME: MULDROW 13			
Depth	Lithology	Bddg, Accessories	Additional Comments
5331			Obvious intpar/scat mol Φ , grn-rich wkst-pkst?, rep anhy follows lam, anhy cmted fracs, sil rep/cmt below anhy@5332' 9"
5332			
5333			
5334			N. v. p., lam mdst
5335			Scat mol Φ , intlam wkst & grn-rich wkst-pkst, poss desiccation cracks, sh lam @ 5334' 10.5", chal cmt/rep intl @ 5336' 9"
5336			
5337			
5338			Obvious intpar/mol Φ , pel pkst w/forams?, rep anhy follows lam, poss alg lams?, mdy lams in 5338-9', poss current produced, anhy cmted fracs
5339			
5340			Scat mol Φ , lam grn-rich wkst-pkst?, rep anhy/# follows lam, detrital qtz slt present, anhy cmted fracs & bur, anhy rep
5341			
5342			
5343			Scat mol/intpar Φ , grn-rich wkst-pkst?, dolo precludes definite identification of dep tex, C anhy rep, chal after any
5344			
5345			
5346			Obvious intxln/intpar Φ , wkst-pkst?, dolo precludes definite identification of dep tex, chal cmt/rep, forams & spg spic present
5347			
5348			
5349			
5350			Obvious pel/skel mol & scat intpar Φ , pkst, undifferentiated skel grns, bioturbated fabric, chal after anhy, anhy cmted fracs, forams, crin, ostr? present, blk residue poss hydc
5351			
5352			

Figure A.8 Continued.

WELL NAME: MULDROW 13

Depth	Lithology	Bddg, Accessories	Additional Comments
5353		☞ # ☉	Scat mol Φ in wkst, indst grns
5354		☞ # ☉	Obvious pel/skel mol & scat intpar Φ , pkst, C bur, chal after anhy, ostr, forams, crin, alg, & ech? present, blk residue poss
5355		☞ # ☉	Scat pel/skel mol Φ , arg wkst-mdst w/ shl lam, chal after anhy, # rep
5356		☞ # ☞	
5357		☞ #	
5358		#	Obvious skel mol & scat intpar Φ , pkst, skel grns: forams, ostr, crin, alg, ech, pelec?, bry?, & tril? present, anhy after skel grns, Φ decr as mol anhy cmt incr
5359		#	
5360		#	
5361		☞ # ☞ ☞	Ply alg rich lyr w/ mdy lam & clas, anhy cmted fracs in md clas
5362		☞ # ☞	
5363		#	
5364		☞ # ◆	Obvious skel/pel mol & scat intpar Φ , nod anhy, chal after anhy, strong hydc odor
5365		☞ # ●	
5366		☞ # ☞	Obvious skel/pel mol Φ , intlam pkst & wkst, bd anhy, scat pel mol Φ in wkst, wvy continuous lams, styl bounding anhy, chal & # after anhy, anhy rep
5367		☞ # ☞	
5368		☞ #	
5369		#	
5370		☞ # ☞	
5371		☞ #	Obvious skel/pel mol Φ , clas lamated intl w/wkst lam & anhy cmt/rep lam, C anhy cmt/rep of grns, nod anhy, anhy cmt fracs, chal after anhy
5372		☞ #	
5373		☞ # ☞	

Figure A.8 Continued.

WELL NAME: MULDROW 13

Depth	Lithology	Bddg, Accessories	Additional Comments
5374		# ⊕ ⚡	Scat-obvious skel/pel mol Φ, gm ric wkst, poss anhy rep burs, partially cmt frags, nod & rep anhy
5375		⊃ #	

Figure A.8 Continued.

WELL NAME: MULDROW 19-4

Depth	Lithology	Bddg, Accessories	Additional Comments
5269		⊃ # ●	Wkst w/ skel pkst lam, scat Φ, higher Φ in pkst, detr sili slt, anhy cmt/rep, chal after anhy, diag lam
5270		⊃ # ●	
5271		⊃	
5272		⊃ # ⊃	
5273		⊃ #	
5274		⊃ #	
5275		≡ # ● ⚡	
5276		≡ # ●	Pkst-grnst w/ gm rich wkst lam, C sili/chal rep of grns & mtrx, assem of skel grns/dust, scat skel/pel mol Φ
5277		≡ # ●	
5278		≡ #	
5279		≡ # ⊕ ⚡	Skel pkst w/ obvious skel/pel Φ, mod burr, anhy cmt of mol & vert frags, incr w/ gm content
5280		⊃ # ⊕	
5281		⊃ # ⊕	Mdy wkst w/ skel pkst lams, scat pel/skel mol Φ, diag lam, bur struc
5282		⊃ # ⊃	
5283		⊃ # ⊕	

Figure A.9: M19-4 core description.

WELL NAME: MULDROW 19-4

Depth	Lithology	Bddg, Accessories	Additional Comments
5284		#	
5285			
5286		#	
5287		#	Intvl c up from wkst to skel pkst-grnst, obvious skel/pel Φ , Φ inc w/ grn content, poss fen in grnst, mod burr, anhy cmt, chal after anhy, erosional surf at base of wkst
5288		# #	
5289		#	
5290		#	
5291		#	
5292		#	
5293		#	Intvl c up from wkst to skel pkst-grnst, obvious skel/pel Φ , Φ inc w/ grn content, anhy cmt, chal after anhy, erosional surf at top intvl, anhy at base
5294		#	
5295		#	
5296		# #	
5297		#	Mdy wkst, scat pel/skel mol Φ , indistinct lam, bur struc, anhy cmt frac, nod anhy along bddg, chal after anhy
5298		# # #	
5299		#	
5300		#	
5301		#	

Figure A.9 Continued.

WELL NAME: MULDROW 19-4

Depth	Lithology	Bddg, Accessories	Additional Comments
5302		#	Wkst-pkst w/ obvious pel/skel mol Φ , anhy cmt/rep, chal after anhy
5303		#	
5304		#	Wkst w/ pkst lam, scat pel/skel mol Φ , wvy bddg, anhy cmt, nod anhy rep, cmt vert & hor frags, chal after anhy
5305		#	

Figure A.9 Continued.

WELL NAME: MULDROW 50-1

Depth	Lithology	Bddg, Accessories	Additional Comments
5326		#	Wkst w/ scat mol Φ , grn rich in areas, wvy diag lam, vert anhy cmt frac
5327		#	
5328		#	
5329		#	
5330		#	
5331		#	
5332		#	Wkst-mdst w/ grn rich intclas lam, scat-no vis Φ , anhy cmt, chal after anhy, diag lam, vert anhy cmt frac
5333		#	
5334		#	
5335		#	
5336		#	
5337		#	
5338		#	
5339		#	

Figure A.10: M50-1 core description.

WELL NAME: MULDROW 50-1

Depth	Lithology	Bddg, Accessories	Additional Comments
5340			Wkst-pkst w/ obvious pel/skel mol Φ , anhy cmt/rep, chal after anhy, anhy cmt vert frac, bur struc
5341			
5342			
5343			
5344			
5345			Wkst w/ scat pel/skel mol Φ , dissol swarms, chal after anhy, styl
5346			
5347			
5348			Gm rich wkst-pkst w/ obvious pel/skel mol Φ , scat intpar Φ , anhy cmt/rep, loc sili rep, poss desiccation cracks at 5349', chal after anhy
5349			
5350			
5351			
5352			
5353			
5354			
5355			Wkst- mdst, ltl-no vis Φ , diag lam, chal after anhy
5356			
5357			Gm rich wkst-pkst w/ obvious pel/skel mol Φ , scat intpar Φ , anhy cmt/rep, anhy cmt vert frac, chal after anhy, intrclas at base
5358			
5359			
5360			

Figure A.10 Continued.

WELL NAME: MULDROW 50-1

Depth	Lithology	Bddg, Accessories	Additional Comments	
5361		#	Grn rich wkst-pkst w/ scat but obvious pel/skel mol Φ, anhy cmt/rep, nod anhy, chal after anhy, irr lam	
5362		#		
5363		#		
5364		#		
5365		#		
5366		#		
5367		#		
5368		#		
5369				Pkst w/ scat pel/skel mol Φ, irr sili rep lam, anhy cmt/rep, chal after anhy, intclas at base
5370		#		
5371		#		
5372		#		
5373		#		

Figure A.10 Continued.

WELL NAME: POOL 37-2

Depth	Lithology	Bddg, Accessories	Additional Comments
5286		#	Scat pel-skel mol Φ , wkst-pkst intbd w/anhy, C dessication & intclas, intclas/mol filling & rep anhy, anhy follows bddg, pos current lam, C anhy cmt vert bur at 5288.5', anhy cmted frac associated w/styl
5287		#	
5288		#	
5289		#	
5290		#	Scat pel mol Φ , wkst-grn rich wkst, pels are sml indst grns, pos pkst intvl, diag lam & dep current lam, anhy rep follows dep bddg, C anhy cmt fracs, C styl
5291		#	
5292		#	
5293		#	
5294		#	Scat pel-skel mol Φ , grn rich wkst-pkst, wh pel/clas grn intvl, indst dep fabric, chal after anhy, grn cpct
5295		#	
5296		#	Scat pelskel mol Φ , diag sol collapse brec intvl of loc pkst-wkst, skel dst in pkst
5297		#	Scat pel-skel mol Φ , grn rich wkst-pkst, indst dep fabric, chal after anhy, C nod
5298		#	Scat pelskel mol & intpar Φ , pkst-grn rich wkst, forams & skel dust, C anhy rep & cmt, chal after anhy
5299		#	
5300		#	Obvious pelskel mol & intpar Φ , pkst w/ undifferentiated skel frags, altg lyrs of hi Φ mod-poorly cmted pkst & low Φ wl cmted pkst, C anhy cmt/rep & chal after anhy, dissolution cpcted nod anhy bd at 5302.5'
5301		#	
5302		#	
5303		#	
5304		#	C-VC pelskel mol & intpar Φ , altg lyrs of hi Φ poorly cmted pkst & low Φ mod cmted pkst, skel grns: forams, pos spg spic, grn alg, & ostr/moll frags; C anhy cmted ver & hor bur at 5304', chal after anhy, C anhy cmt/rep
5305		#	
5306		#	

Figure A.11: P37-2 core description.

WELL NAME: POOL 37-2

Depth	Lithology	Bddg, Accessories	Additional Comments
5307		~ # ▲	
5308	●	~ # ✖	Obvious pelskel mol/intpar Φ , altg lyrs of pkst & grn rich wkst, skel grns: forams, ech, gn alg, ostr frags, & spg spic; chal after anhy, C anhy cmt/rep, pyr rep grns
5309	●	~ # ✖	
5310	○	✖ # ~	Scat pelskel mol & intpar Φ , skel rich intvl: ostr, alg, gast, pos pelec & ech; arg at btm
5311	●	~ #	Scat mol Φ , arg wkst & shl w/pel, gn alg, & pos ostr grns, diag lam, chal after anhy assoc w/shl
5312		~ #	
5313	●	# ⊕	Scat mol Φ , wkst-pkst w/ pel, gn alg, & pos ostr/spg spic grns, diss & grn cpct, chal after anhy, poss bur str, thn shl lam pos from diss, pyr rep grns
5314		✖ #	
5315	●	⊕ # ~	
5316	●	# ~	
5317	●	# ▲	Obvious pelskel mol & intpar Φ , pkst-wkst, skel grns: pos spg spic, ostr or moll frag, grn alg, forams; chal after anhy, pyr rep grns, C anhy cmt/rep of grns, R bit in pore
5318		#	
5319	●	# ▲ ~	
5320		~ # ~	
5321	●	~ # ~	Obvious intpar Φ , styl & intclas at 5320.6' marks erosional surf, pel pkst-grnst w/lam, pos alg lam, rep anhy pos after fen por, bd of lg nod anhy from 5321.5' - 5322.4', pos dessication cracks in anhy bd
5322	●	~ #	

Figure A.11 Continued.

WELL NAME: BEASLEY 48-4			
Depth	Lithology	Bddg, Accessories	Additional Comments
5359			LOST CORE
5360		~ # ~	Obvious pelskel mol & intpar Φ , pel pkst - wkst w/ altg lyrs of hi Φ & low Φ pkst, pos forams & skel dust, C anhy cmt/rep & chal after anhy, intraclas surf at 5359.95' bounded by styl, gm cpct & diss, localized qtz slit assoc w/ styl, rep anhy bds parallel to bdg at 5364.95'
5361		# ~	
5362		~ # ~	
5363		~ # ~	
5364		~ # ~	
5365		~ # ~	
5366		~ # ~	
5367		~ # ~	
5368		~ # ~	
5369		~ # ~	
5370			LOST CORE
5371			
5372		~ # ~	Obvious pelskel mol & intpar Φ , pkst - wkst w/ alt lyrs of dk col, hi Φ & lt col & mod-low visible Φ , anhy cmt/rep & chal after anhy, shl lams pos result of dissolution, anhy cmted fracs
5373		# ~	
5374		~ # ~	
5375		~ # ~	
5376		~ # ~	
5377		~ # ~	
5378		~ # ~	Obvious skelpel mol & R intpar Φ , gry skel pkst-wkst w/ alg, ostr, gast, & other skel grns, C dissol, anhy cmt & rep
5379		~ # ~	Obvious pel mol Φ , comly bur pelskel wkst w/ VC chal cmt & rep, anhy cmt & cmt
5380		~ # ~	

Figure A.12 : B48-4 core description.

WELL NAME: BEASLEY 48-4

Depth	Lithology	Bddg, Accessories	Additional Comments
5381		#	Obvious intpar & pelskel mol Φ , pel pkst w/ lams & poss desiccation cracks at top, any cmt & rep, poss after fen por, poss oolic & skel grns, dissol grn cpct
5382		#	
5383		#	
5384		#	
5385		#	
5386		#	Obvious intpar & pelskel mol Φ , pel pkst-grnst, altg intvls dom by mol and intpar Φ , C anhy cmt & repr, C nod anhy, poss oolic & skel grns, bded nod anhy, dissol grn
5387		#	
5388		#	
5389		#	
5390		#	
5391		#	
5392		#	
5393		#	

Figure A.12 Continued.

APPENDIX B
CORE PHOTOMICROGRAPHS

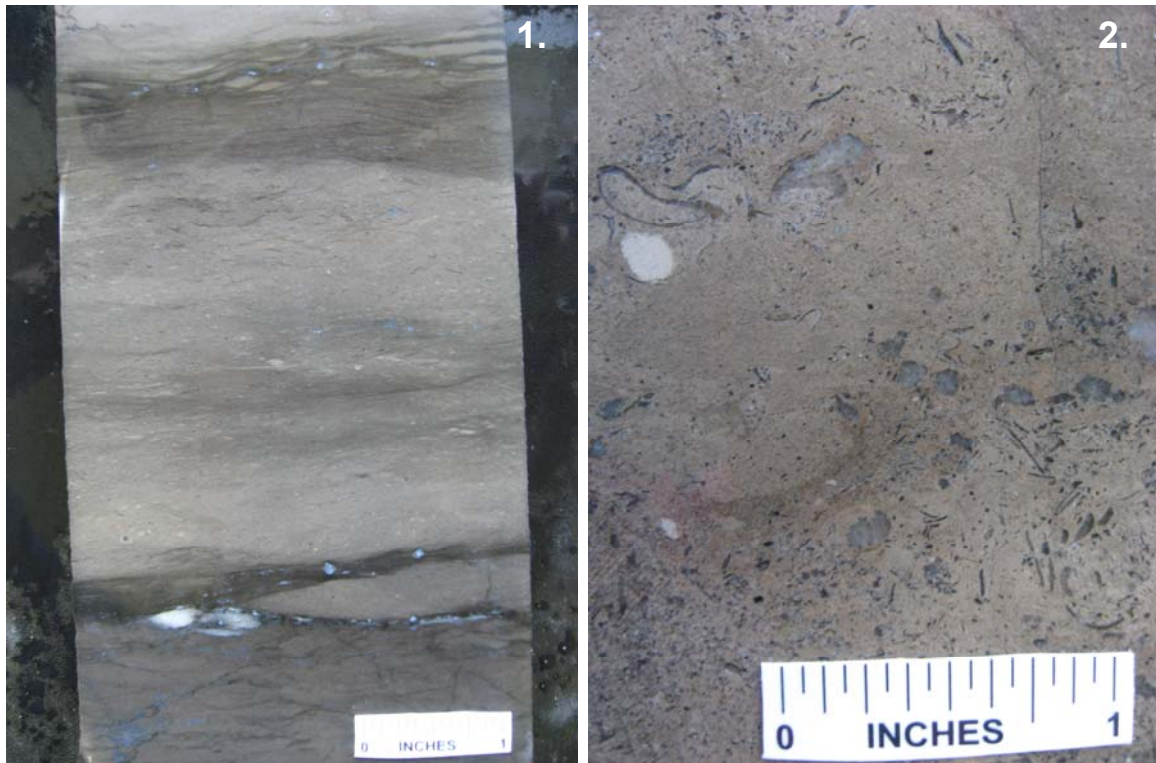


Figure B.1: Common subtidal mudstone facies with shale stringers and minor anhydrite nodules. From sample M11, 5318'.

Figure B.2: Skeletally dominated wackestone/packstone found associated with subtidal environments. Note the anhydrite replaced skeletal grains. From sample M2, 5313'.

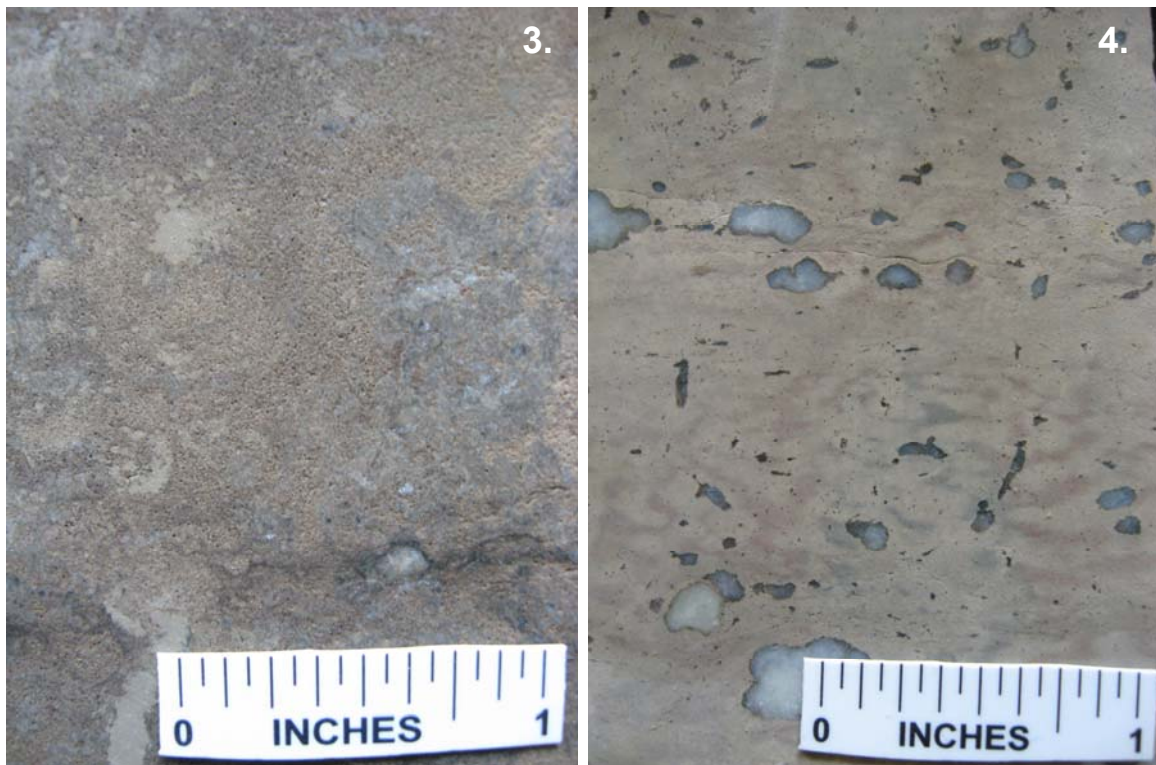


Figure B.3: Spiculiferous wackestone sub-facies from parasequence C1 accumulation. Note the circular visible porosity. Due to pore geometry, core porosity was originally identified as pel-moldic, but petrographic analysis revealed spicule-molds to be the source of porosity. From sample M7, 5350'.

Figure B.4: Bioturbated peloidal wackestone with nodular anhydrite, associated with shallow subtidal, possibly lagoonal, environments. From sample M11, 5377'.

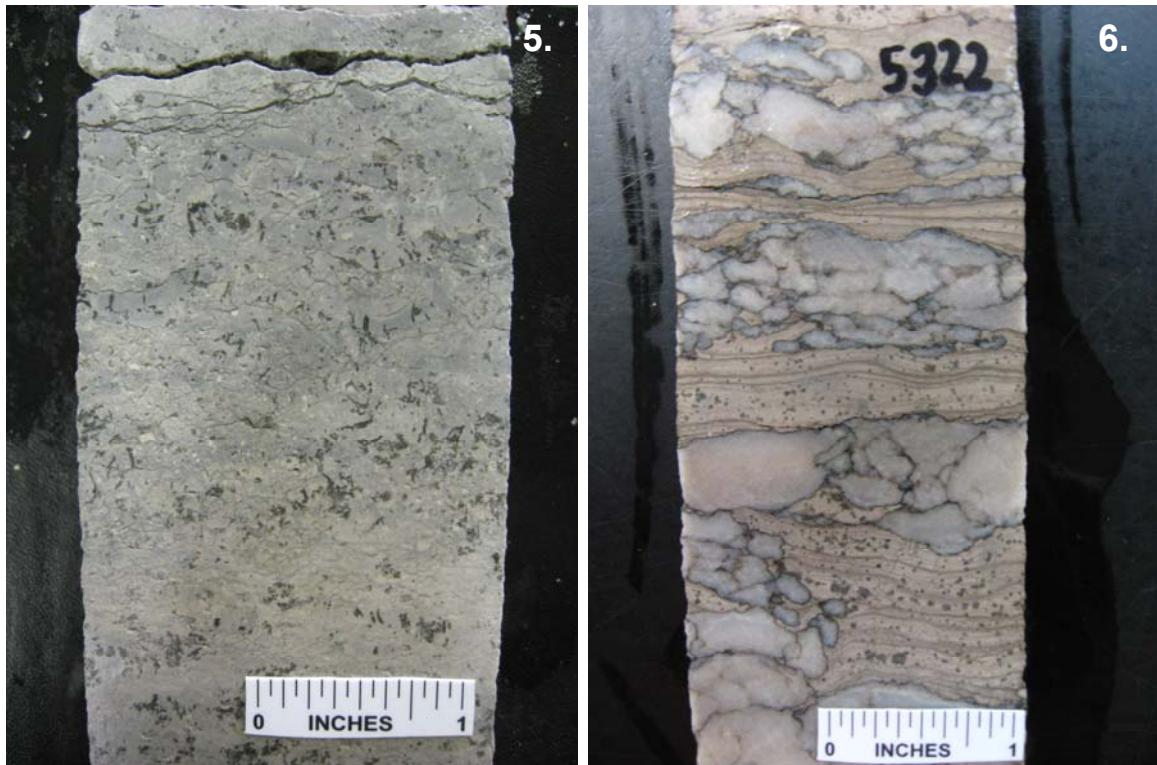


Figure B.5: Intertidal peloidal wackestone exhibiting indistinct desiccation features and flat-pebble intraclasts. Sample from P37-2 5286'.

Figure B.6: Intertidal, algal laminated mudstone facies with increasing anhydrite accumulation. Sample from M2, 5322'.

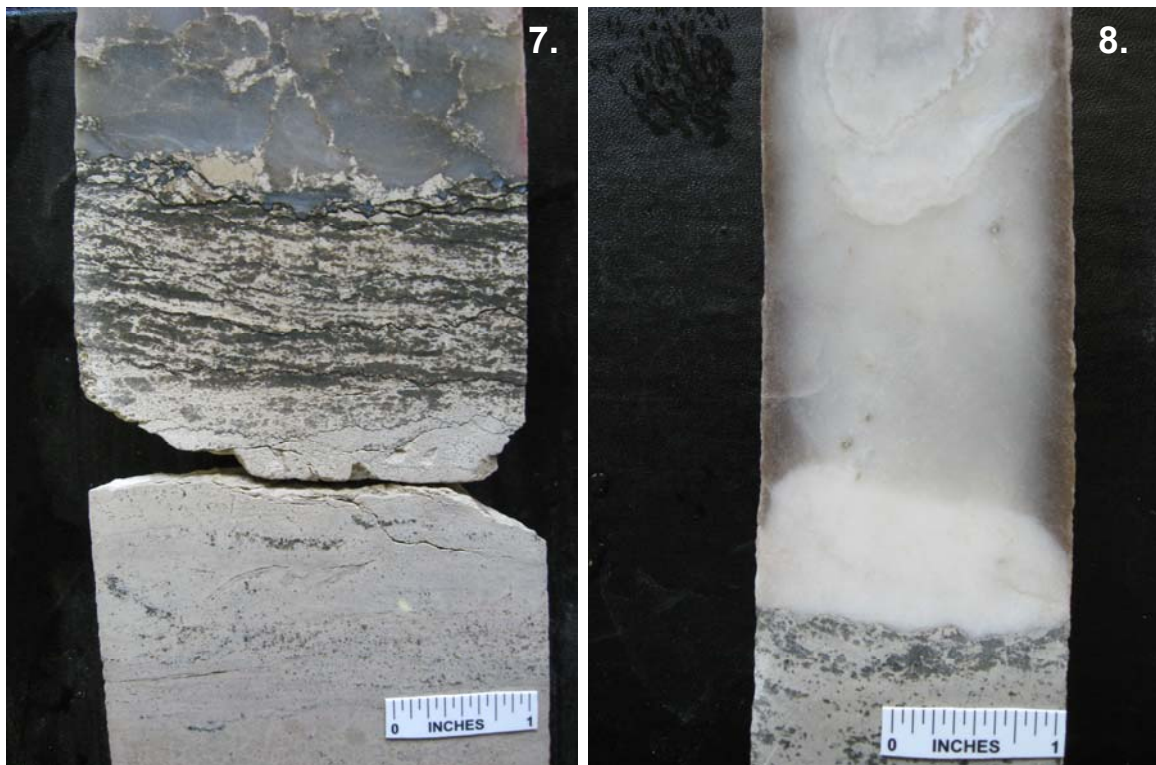


Figure B.7: Intertidal peloidal wackestone facies in contact with supratidal accumulation of anhydrite. Note anhydrite cementation of fenestrae in intertidal deposit. Sample from M11, 5300'

Figure B.8: Anhydrite of the supratidal facies. This anhydrite is the most regionally extensive accumulation in South Sunflower, extending nearly $\frac{3}{4}$ of a mile along strike from M11 to M3 and also updip to well M6. The anhydrite is found at the top of parasequence C1 and is thickest in wells M6 and M2. Sample from M6, 5262'.

APPENDIX C

THIN SECTION DESCRIPTION

Table C.1
Summarization of Thin Section Analysis

Well ID	Depth	Facies	Cycle Position	Pore Type	Core Analysis ϕ (%)	Core Analysis K (mD)
P37-2	5286	P/G	T	1Br	---	---
P37-2	5290	M	B	1Ar	---	---
P37-2	5292	W	T	1Ae	---	---
P37-2	5296	W	B	1Br	---	---
P37-2	5298	P/G	T	1Ar	3.40	0.082
P37-2	5299.9	M	T	1Ae	12.36	0.272
P37-2	5300.25	W	M-T	1Ae	15.13	1.278
P37-2	5302.3	M	M-T	1Ae	11.16	0.827
P37-2	5305	SW	M	1Ae	11.16	1.412
P37-2	5306.7	SW	M	1Be	12.16	2.074
P37-2	5310	W	M	1Ae	11.90	0.360
P37-2	5311.5	M	M	1Ar	2.86	0.123
P37-2	5315.25	M	M-B	1Ae	9.74	0.143
P37-2	5320.2	SW	B	1Br	8.80	0.551
P37-2	5320	W	B	1Br	8.80	0.551
M2	5279	P/G	T	1Br	---	---
M2	5282	W	M	1Ae	---	---
M2	5283	P/G	B	1Be	---	---
M2	5286	M	M	1Ae	---	---
M2	5289	M	T	1Ae	---	---
M2	5290	W	B	1Ae	---	---
M2	5292	W	T	1Ae	---	---
M2	5293.6	P/G	T	1Br	6.10	0.147
M2	5296.4	M	T-M	1Ae	9.06	0.881
M2	5297.7	W	M	1Ae	12.53	2.150
M2	5299.3	W	M	1Ae	7.87	1.334
M2	5302.35	SW	M	1Ae	18.63	18.131
M2	5308.25	SW	M	1Ae	17.34	3.745
M2	5313.4	P/G	M-B	1Br	7.86	1.635
M2	5316	M	B	1Ae	11.70	0.253
M2	5320.95	M	T	1Ae	10.50	0.107
M2	5324	W	T	1Ar	5.20	0.641
M3	5296	SW	M	1Ae	10.90	0.824
M3 - U	5305	W	M	1Br	9.30	2.206
M3 - L	5305	W	M	1Ae	9.30	2.206
M3	5307	P/G	M-B	1Be	6.40	0.630
M3	5313	M	B	1Ae	10.10	0.238
M3	5315	W	T	1Ae	12.10	0.038
M3	5319	M	M-B	1Ae	8.90	0.787
M3	5337	W	B (?)	1Ae	---	---

Table C.1 Continued,

Well ID	Depth	Facies	Cycle Position	Pore Type	Core Analysis ϕ (%)	Core Analysis K (mD)
M6	5277	P/G	M	1Br	6.80	1.942
M6	5283	W	M-B	1Ae	7.90	1.605
M11	5297	M	M	1Ae	---	---
M11	5313	P/G	M	1Ae	9.20	1.595
M11	5319	M	M-B	1Ae	8.30	0.048
M11	5335	W	T	1Br	8.70	0.071
M13	5350	P/G	M	1Ae	16.60	2.130
M13	5354	W	M	1Ae	14.50	1.471
M13	5365	W	B	1Ae	17.60	2.449
M19-4	5271	M	M	1Ae	---	---
M19-4	5274	W	B	1Ae	5.90	0.061
M19-4	5275	SW	T	1Ae	10.70	0.092
M19-4	5276	SW	M	1Br	5.40	0.059
M19-4	5278	M	B	1Ae	8.90	0.345
M19-4	5280	W	T	1Ae	10.40	0.109
M19-4	5282	M	M	1Ae	4.90	0.029
M19-4	5287	SW	M	1Ae	8.90	0.146
M19-4	5290	P/G	M	1Ar	8.70	0.095
M19-4	5293	W	M - B	1Ae	5.90	0.053
M19-4	5296	M	B	1Ae	8.40	0.012
M19-4	5297	M	T	1Ae	---	---
M19-4	5301	W	M	1Ar	5.30	0.027
M19-4	5303	M	B	1Ae	---	---
B48-4	5360	SW	M (?)	1Be	15.20	0.847
B48-4	5363	SW	M (?)	1Be	16.80	2.219
B48-4	5366	SW	M (?)	1Be	16.10	1.228
B48-4	5373	SW	M (?)	1Be	14.50	11.908
B48-4	5377	W	M - B	1Ae	8.60	0.073
B48-4	5381	SW	B	1Ae	16.00	1.199
B48-4	5382	M	B	1Ae	11.60	0.146
B48-4	5386	W	T	1Ae	14.00	1.099
B48-4	5390	W	T	1Ae	8.50	0.395
B48-4	5391	W	M (?)	1Ae	10.80	1.574

Muldrow 2 Thin Section Description

Sample: Muldrow 2 – 5279'

Cycle Position: Top

Depositional Characteristics

Lithofacies Type: Anhydritic Peloidal, Skeletal Dolo-Packstone

Sedimentary Structure: No Observed Structures

Framework Grains:

- Skeletal:
 - Algae – Green Present
 - Foraminifera Present
 - Sponge – Spicules Present
- Non-skeletal:
 - Peloids Common
- Detrital:
 - Siliciclastic Silt Present

Comments: Well sorted indistinct micritic peloidal grains; common anhydrite replacement of framework grains

Diagenetic Characteristics

Cementation: Anhydrite found cementing moldic pores and fractures; indistinct isopachous dolomite cement present around some peloidal grains, possibly formed before micritization of skeletal grains; present rhombic interparticle dolomite cement.

Recrystallization: Micritization of skeletal grains; neomorphism of some micritic peloidal grains

Replacement: Dolomitization; common anhydrite replacement of framework grains and matrix; replacive pyrite present

Dissolution: Partial-complete dissolution of framework grains; possible grain compaction

Stylolites: Microstylolitization present, irregular diagenetic bedding

Fractures: Discontinuous anhydrite cemented fractures

Other: NA

Porosity

Measured porosity (%) – NA

Measured permeability (mD) – NA

Ahr Genetic Pore Type: **Hybrid 1B - Reduced**

- Depositional:
 - Interparticle
 - Intraparticle
- Diagenetic:
 - Moldic
 - Intercrystalline

Comments: Depositional interparticle porosity dominates with considerable pel-skel moldic porosity from dissolution; accessory intraparticle and solution enhanced intercrystalline porosity. Considerable porosity reduction from interparticle cementation and compaction.

Remarks: Anhydritic Pel-Skel, Dolo-Packstone with indistinct micritic grains. Common anhydrite replacement of framework grains and matrix; micritic grain ghosts illustrate depositional texture.

Sample: Muldrow 2 – 5282'

Cycle Position: Middle

Depositional Characteristics

Lithofacies Type: Skeletal Dolo-Wackestone (?)

Sedimentary Structure: No Observed Structures

Framework Grains:

- Skeletal:
 - Foraminifera Present
 - Sponges – Spicules Present
- Non-skeletal:
 - Peloids Present
- Detrital:
 - Siliciclastic Silt Present

Comments: Very indistinct neomorphosed framework grains; irregular texture may be the result of compaction of a grain rich rock.

Diagenetic Characteristics

Cementation: Present anhydrite and dolomite cementation of moldic pores

Recrystallization: Neomorphism of matrix and grains

Replacement: Dolomitization, present anhydrite and possible gypsum replacement; pyritization

Dissolution: Discontinuous seams of dissolution and possible extensive grain dissolution/compaction

Stylolites: NA

Fractures: NA

Other: NA

Porosity

Measured porosity (%) – NA

Measured permeability (mD) – NA

Ahr Genetic Pore Type: **Hybrid 1Ae (?)**

- Depositional: NA
- Diagenetic:
 - Intercrystalline
 - Moldic

Comments: Solution enhanced intercrystalline and moldic porosity dominate; void spaces may be tight, separate vuggy pores or the result of anhydrite crystal plucking. Porosity may have been greatly reduced by grain compaction.

Remarks: Skeletal Dolo-Wackestone with irregular, neomorphosed texture; texture is possibly the result of extensive compaction. Framework grains are indistinct and void spaces are present. Voids may be the result of tight, vuggy pores that escaped epoxy impregnation or anhydrite crystal plucking.

Sample: Muldrow 2 – 5283'

Cycle Position: Bottom

Depositional Characteristics

Lithofacies Type: Anhydritic Peloidal Dolo-Packstone (?)

Sedimentary Structure: Diagenetic laminations

Framework Grains:

- Skeletal:
 - Foraminifera Present
 - Sponge – Spicules Present
 - Algae – Red (?) Present
- Non-skeletal:
 - Peloids Common
- Detrital:
 - Siliciclastic Silt Present

Comments: Indistinct neomorphosed and leached framework grains; diagenetic alteration and compaction makes grain identification difficult; originally a grain rich rock, probably packstone.

Diagenetic Characteristics

Cementation: Relict interparticle dolomite cement; present moldic and interparticle pore filling anhydrite and dolomite cement

Recrystallization: Neomorphism of grains

Replacement: Dolomitization; present anhydrite replacement and pyritization

Dissolution: Partial-complete grain dissolution and compaction

Stylolites: Microstylolitization

Fractures: Solution enhanced open fractures

Other: NA

Porosity

Measured porosity (%) – NA

Measured permeability (mD) – NA

Ahr Genetic Pore Type: **Hybrid 1B – Enhanced**

- Depositional:
 - Interparticle
 - Intraparticle
- Diagenetic:
 - Moldic
 - Intercrystalline
 - Fracture

Comments: Pel-moldic and solution enhanced interparticle porosity after neomorphism dominate; considerable interparticle porosity remains. Partial-complete grain dissolution and compaction have significantly altered original porosity

Remarks: Anhydritic, Peloidal Dolo-Packstone exhibiting abundant but indistinct framework grains and diagenetic laminations. Interparticle cementation, partial-complete grain dissolution, and compaction have significantly altered original porosity

Sample: Muldrow 2 – 5286'

Cycle Position: Middle

Depositional Characteristics

Lithofacies Type: Anhydritic Dolo-Mudstone

Sedimentary Structure: No Observed Structures

Framework Grains:

- Skeletal:
 - Sponge – Spicules Present
- Non-skeletal:
 - Peloids Present
- Detrital: NA

Comments: Indistinct framework grains, some of which are partially leached.

Diagenetic Characteristics

Cementation: Present anhydrite moldic cementation; majority of anhydrite is replacive

Recrystallization: NA

Replacement: Dolomitization; common anhydrite replacement throughout; present pyrite

Dissolution: Partial leaching of framework grains

Stylolites: NA

Fractures: Anhydrite cemented/replaced fracture

Other: NA

Porosity

Measured porosity (%) – NA

Measured permeability (mD) – NA

Ahr Genetic Pore Type: **Hybrid 1A - Enhanced**

- Depositional: NA
- Diagenetic:
 - Moldic
 - Intercrystalline

Comments: Present visible porosity is dominated by solution enhanced intercrystalline and skel – moldic porosity; void spaces may be tight, separate vuggy pores or the result of anhydrite crystal plucking.

Remarks: Anhydritic Dolo-Mudstone with little visible porosity and common anhydrite replacement. Void spaces may be the result of tight, vuggy pores that escaped epoxy impregnation or anhydrite crystal plucking.

Sample: Muldrow 2 – 5289'

Cycle Position: Top

Depositional Characteristics

Lithofacies Type: Skeletal Dolo-Mudstone

Sedimentary Structure: No Observed Structures

Framework Grains:

- Skeletal:
 - Sponge – Spicules Present
 - Foraminifera Present
 - Algae – Green Present
- Non-skeletal:
 - Peloids Present
- Detrital:
 - Siliciclastic Silt Present

Comments: Indistinct micritic peloidal grains and partially-completely leached skeletal grains.

Diagenetic Characteristics

Cementation: Present moldic pore filling anhydrite cement

Recrystallization: NA

Replacement: Dolomitization; present anhydrite replacement of matrix; present pyrite

Dissolution: Partial-complete dissolution of framework grains

Stylolites: NA

Fractures: Open fractures from sample preparation

Other: NA

Porosity

Measured porosity (%) – NA

Measured permeability (mD) – NA

Ahr Genetic Pore Type: **Hybrid 1A – Enhanced**

- Depositional: NA
- Diagenetic:
 - Moldic
 - Intercrystalline

Comments: Porosity dominated by skel-moldic porosity with solution enhanced intercrystalline porosity.

Remarks: Skeletal Dolo-Mudstone exhibiting moldic and intercrystalline porosity.

Sample: Muldrow 2 – 5290'

Cycle Position: Bottom

Depositional Characteristics

Lithofacies Type: Spiculiferous Peloidal Dolo-Wackestone – Mudstone

Sedimentary Structure: Interlaminated mudstone and spiculiferous, peloidal wackestone

Framework Grains:

- Skeletal:
 - Sponge – Spicules Present
- Non-skeletal:
 - Peloids Present
- Detrital: NA

Comments: Indistinct peloidal grains may be microbial in origin; spicules are partially-completely leached

Diagenetic Characteristics

Cementation: Present anhydrite and dolomite filling moldic pores

Recrystallization: Neomorphism of micrite

Replacement: Dolomitization; present anhydrite and pyrite replacement

Dissolution: Partial-complete dissolution of spicules

Stylolites: NA

Fractures: NA

Other: Residual hydrocarbon

Porosity

Measured porosity (%) – NA

Measured permeability (mD) – NA

Ahr Genetic Pore Type: **Hybrid 1A – Enhanced**

- Depositional:
 - Interparticle
- Diagenetic:
 - Moldic
 - Intercrystalline

Comments: Porosity dominated by skel-moldic porosity after spicules; accessory solution enhanced intercrystalline porosity and interparticle porosity in wackestone laminations.

Remarks: Spiculiferous Peloidal Dolo-Wackestone with mudstone laminations; wackestone exhibits indistinct peloidal grains that may be microbial in origin. Skel-moldic porosity dominates.

Sample: Muldrow 2 – 5292'

Cycle Position: Top

Depositional Characteristics

Lithofacies Type: Anhydritic, Skeletal Dolo-Wackestone

Sedimentary Structure: Anhydrite laminations

Framework Grains:

- Skeletal:
 - Sponge – Spicules Present
 - Skeletal Hash Present
 - Foraminifera Present
- Non-skeletal:
 - Peloids Present

- Detrital:
 - Siliciclastic Silt Present

Comments: Indistinct grains; skeletal hash composed of unidentified, very fine skeletal fragments.

Diagenetic Characteristics

Cementation: Present moldic pore filling anhydrite cement

Recrystallization: NA

Replacement: Dolomitization; present anhydrite and pyrite replacement; present fluorite after anhydrite

Dissolution: Partial-complete dissolution of framework grains

Stylolites: NA

Fractures: NA

Other: NA

Porosity

Measured porosity (%) – NA

Measured permeability (mD) – NA

Ahr Genetic Pore Type: **Hybrid 1A – Enhanced**

- Depositional:
 - Intraparticle
- Diagenetic:
 - Moldic
 - Intercrystalline

Comments: Porosity dominated by skel-moldic and solution enhanced intercrystalline porosity; accessory intraparticle porosity found in some skeletal grains.

Remarks: Skeletal, Anhydrite Laminated Dolo-Wackestone exhibiting partial-complete dissolution of framework grains and present fluorite replacement.

Sample: Muldrow 2 – 5293.6'

Cycle Position: Top

Depositional Characteristics

Lithofacies Type: Peloidal/Oncoidal Dolo-Grainstone

Sedimentary Structure: Preferred grain orientation

Framework Grains:

- Skeletal: NA
- Non-skeletal:
 - Peloids Abundant
 - Oncoids Common
- Detrital:
 - Siliciclastic Silt Present

Comments: Poorly sorted framework grains exhibit preferred orientation; many appear coated, possibly microbial in origin; < 1% siliciclastic silt.

Diagenetic Characteristics

Cementation: Common isopachous/interparticle dolomite cement with present interparticle anhydrite cement; present framboidal & cubic interparticle pyrite cement; present interparticle chalcedony cement.

Recrystallization: NA

Replacement: Dolomitization; present anhydrite replacement of framework grains; present replacive pyrite

Dissolution: Partial grain dissolution & grain compaction

Stylolites: NA

Fractures: NA

Other: NA

Porosity*Measured porosity (%)* – 7.1*Measured permeability (mD)* – .034*Ahr Genetic Pore Type:* **Hybrid 1B – Reduced**

- Depositional:
 - Interparticle
 - Shelter
- Diagenetic:
 - Vuggy

Comments: Porosity is dominated by poorly connected, solution enhanced interparticle and shelter pores, some forming vugs; extensive diagenetic porosity reduction from grain compaction and interparticle cementation.

Remarks: Peloidal/Oncoidal Dolo-Grainstone with common interparticle dolomite cementation. Extensive diagenetic porosity reduction from grain compaction and interparticle cementation. Porosity is dominated by poorly connected solution enhanced interparticle and shelter pores, some forming vugs.

Sample: Muldrow 2 – 5296.4'**Cycle Position: Top – Middle****Depositional Characteristics***Lithofacies Type:* Anhydritic Peloidal Dolo-Mudstone*Sedimentary Structure:* Irregular, discontinuous, laminations; possibly diagenetic*Framework Grains:*

- Skeletal:
 - Sponge – Spicules Present
- Non-skeletal:
 - Peloids Present
- Detrital:
 - Siliciclastic Silt Present

Comments: Siliceous spicules have been replaced by dolomite; indistinct micritic peloidal grains.

Diagenetic Characteristics*Cementation:* Present moldic pore filling anhydrite and dolomite cementation.*Recrystallization:* Neomorphism of micrite*Replacement:* Dolomitization; present anhydrite replacement of matrix and grains; present pyritization and possible fluorite replacement*Dissolution:* Partial dissolution of grains & grain compaction; discontinuous seams of dissolution associated with concentration of pyrite & clay (?)*Stylolites:* NA*Fractures:* NA*Other:* Residual Hydrocarbon**Porosity***Measured porosity (%)* – 8.0*Measured permeability (mD)* – .126*Ahr Genetic Pore Type:* **Hybrid 1A – Enhanced**

- Depositional: NA
- Diagenetic:
 - Intercrystalline
 - Moldic

Comments: Porosity dominated by solution enhanced intercrystalline and moldic porosity.

Remarks: Peloidal Dolo-Mudstone exhibiting irregular & discontinuous laminations, possibly diagenetic seams of dissolution. Porosity dominated by solution enhanced intercrystalline and moldic porosity.

Sample: Muldrow 2 – 5297.7'

Cycle Position: Middle

Depositional Characteristics

Lithofacies Type: Anhydritic Peloidal Spiculiferous Dolo-Wackestone

Sedimentary Structure: Wackestone-packstone with discontinuous, irregular grainstone laminations

Framework Grains:

- Skeletal:
 - Sponge – Spicules Present
- Non-skeletal:
 - Peloids Present
 - Unidentifiable Grain Common
- Detrital: NA

Comments: Moderately sorted wackestone is dominated by dolomitized spicules and indistinct peloidal grains; Grainstone laminations are composed of irregular, unidentifiable clasts, possibly composite grains.

Diagenetic Characteristics

Cementation: Present moldic and interparticle pore filling dolomite cement; present replacive interparticle and moldic pore filling anhydrite

Recrystallization: NA

Replacement: Dolomitization; present anhydrite replacement of grains and matrix; present pyrite and possible fluorite replacement

Dissolution: Dissolution of wackestone skeletal grains; possible grain compaction

Stylolites: NA

Fractures: NA

Other: Present organic material, possibly kerogen

Porosity

Measured porosity (%) – 12.6

Measured permeability (mD) – 2.040

Ahr Genetic Pore Type: **Hybrid 1A – Enhanced**

- Depositional:
 - Interparticle
- Diagenetic:
 - Moldic
 - Intercrystalline

Comments: Skel-moldic porosity dominates with considerable solution enhanced intercrystalline and interparticle porosity.

Remarks: Peloidal Spiculiferous Dolo-Wackestone with irregular, discontinuous laminations of clastic grainstone. Sample exhibits organic material, possibly kerogen, and skel-moldic porosity dominate with considerable solution enhanced intercrystalline and interparticle porosity.

Sample: Muldrow 2 – 5299.3'

Cycle Position: Middle

Depositional Characteristics

Lithofacies Type: Dolo-Mudstone - Wackestone

Sedimentary Structure: Sample contains facies contact of dolo-mudstone and a slightly more grain rich, possibly wackestone, argillaceous facies.

Framework Grains:

- Skeletal:
 - Sponge – Spicules Present
 - Foraminifera Present
- Non-skeletal:
 - Peloids Present
- Detrital:
 - Siliciclastic Silt Present

Comments: Spicules have been micritized and partially leached; indistinct micritic peloids are difficult to identify.

Diagenetic Characteristics

Cementation: Present moldic pore filling anhydrite and dolomite cement.

Recrystallization: Neomorphism of micrite

Replacement: Dolomitization; present anhydrite replacement and chalcedony replacing anhydrite; replacive pyrite

Dissolution: Partial-complete dissolution of framework grains

Stylolites: NA

Fractures: NA

Other: NA

Porosity

Measured porosity (%) – 12.5

Measured permeability (mD) – .914

Ahr Genetic Pore Type: **Hybrid 1A – Enhanced**

- Depositional: NA
- Diagenetic:
 - Moldic
 - Intercrystalline

Comments: Porosity is dominated by diagenetic solution enhanced intercrystalline porosity and skel-moldic porosity.

Remarks: Dolo-Mudstone in contact with a slight more grain rich, argillaceous wackestone facies.

Porosity is dominated by diagenetic solution enhanced intercrystalline porosity and skel-moldic porosity.

Present chalcedony replacing anhydrite.

Sample: Muldrow 2 – 5302.35'

Cycle Position: Middle

Depositional Characteristics

Lithofacies Type: Spiculiferous Dolo-Wackestone

Sedimentary Structure: No Observed Structures

Framework Grains:

- Skeletal:
 - Sponge – Spicules Common
- Non-skeletal:
 - Peloids Present
- Detrital: NA

Comments: Spicules have been micritized and partially leached; indistinct micritic peloids are difficult to identify.

- Interparticle
- Diagenetic:
 - Moldic
 - Intercrystalline

Comments: Porosity is dominated by skel-moldic porosity after sponge spicule dissolution with considerable solution enhanced intercrystalline porosity and accessory interparticle porosity

Remarks: Spiculiferous Dolo-Wackestone dominated by skel-moldic porosity with considerable solution enhanced intercrystalline porosity.

Sample: Muldrow 2 – 5313.4'

Cycle Position: Middle – Bottom

Depositional Characteristics

Lithofacies Type: Anhydritic Skeletal-Peloidal Dolo-Packstone

Sedimentary Structure: Mud filled burrow structure

Framework Grains:

- Skeletal:
 - Sponge – Spicules Common
 - Ostracods Present
 - Foraminifera Present
 - Algae Present
- Non-skeletal:
 - Peloids Present
- Detrital:
 - Siliciclastic Silt Present

Comments: Dolomitization of siliceous spicules; leaching of framework grains; anhydrite replacement/cementation of skeletal grains; undifferentiated micritic peloidal grains.

Diagenetic Characteristics

Cementation: Common interparticle & moldic pore filling anhydrite and dolomite cement; present chalcedony filling moldic pores.

Recrystallization: Neomorphism of micrite

Replacement: Dolomitization; present anhydrite replacement of framework grains & matrix; < 1% replacive pyrite

Dissolution: Partial-complete dissolution of framework grains

Stylolites: NA

Fractures: NA

Other: Residual hydrocarbon

Porosity

Measured porosity (%) – 7.6

Measured permeability (mD) – .928

Ahr Genetic Pore Type: Hybrid 1B – Reduced

- Depositional:
 - Interparticle
- Diagenetic:
 - Moldic
 - Intercrystalline

Comments: Dominated by skel-moldic porosity with considerable interparticle and accessory solution enhanced intercrystalline porosity. Considerable porosity reduction from interparticle and moldic cementation.

Remarks: Anhydritic Skeletal-Peloidal Dolo-Packstone exhibiting burrow structure; porosity is dominated by skel-moldic and considerable interparticle pores. Porosity has been reduced by interparticle and moldic cementation.

Sample: Muldrow 2 – 5316'

Cycle Position: Bottom

Depositional Characteristics

Lithofacies Type: Spiculiferous Dolo-Mudstone

Sedimentary Structure: No Observed Structures

Framework Grains:

- Skeletal:
 - Sponge – Spicules Present
- Non-skeletal: NA
- Detrital:
 - Siliciclastic Silt Present

Comments: Dissolution of siliceous sponge spicules; <1% siliciclastic silt.

Diagenetic Characteristics

Cementation: Present moldic pore filling anhydrite and rhombic dolomite cement

Recrystallization: Neomorphism of micrite

Replacement: Dolomitization; Present anhydrite replacement of mudstone matrix; Present replacive pyrite

Dissolution: Dissolution of siliceous sponge spicules and solution enhanced intercrystalline porosity

Stylolites: NA

Fractures: NA

Other: NA

Porosity

Measured porosity (%) – 11.7

Measured permeability (mD) – .253

Ahr Genetic Pore Type: **Hybrid 1A – Enhanced**

- Depositional: NA
- Diagenetic:
 - Moldic
 - Intercrystalline

Comments: Diagenetic skel moldic porosity dominates; insubstantial solution enhanced intercrystalline porosity in neomorphosed micrite; depositional mudstone preserved by skel-moldic porosity.

Remarks: Thin section depth is mismarked as MULDROW 2 - 5396; actual depth is M2 - 5316. Spiculiferous mudstone; spicules have been dissolved leaving skel-moldic porosity. < 1% of detrital siliciclastic silt is present.

Sample: Muldrow 2 – 5320.95'

Cycle Position: Bottom

Depositional Characteristics

Lithofacies Type: Dolo-Mudstone

Sedimentary Structure: Interclastic texture, possibly desiccation features from top of adjacent cycle

Framework Grains:

- Skeletal:
 - Sponge – Spicules Present
- Non-skeletal:
 - Peloids Present

- Detrital: NA

Comments: Indistinct framework grains.

Diagenetic Characteristics

Cementation: Present moldic pore filling dolomite cement.

Recrystallization: Neomorphism of micrite

Replacement: Dolomitization; present anhydrite replacing authigenic gypsum crystals; present pyrite

Dissolution: NA

Stylolites: NA

Fractures: NA

Other: NA

Porosity

Measured porosity (%) – 12.2

Measured permeability (mD) – .211

Ahr Genetic Pore Type: **Hybrid 1A – Enhanced**

- Depositional: NA
- Diagenetic:
 - Moldic
 - Intercrystalline

Comments: Present visible porosity is dominated by solution enhanced intercrystalline and moldic porosity.

Remarks: Dolo-Mudstone exhibiting interclastic desiccation features possibly from the top of the adjacent parasequence cycle; present visible porosity is dominated by solution enhanced intercrystalline and moldic porosity. Present anhydrite replacing authigenic gypsum.

Sample: Muldrow 2 – 5324'

Cycle Position: Top

Depositional Characteristics

Lithofacies Type: Anhydritic, Skeletal/Peloidal Dolo-Wackestone

Sedimentary Structure: No Observed Structures

Framework Grains:

- Skeletal:
 - Sponge – Spicules Present
 - Foraminifera Present
 - Mollusks – Unidentifiable Present
 - Gastropods Present
 - Crinoids Present
- Non-skeletal:
 - Peloids Common
- Detrital:
 - Siliciclastic Silt Present

Comments: Indistinct micritic grains; anhydrite cementation/replacement and grain dissolution make depositional fabric identifiable.

Diagenetic Characteristics

Cementation: Common anhydrite cementation of grain molds and fractures; anhydrite replacement of surrounding matrix after anhydrite cementation; present moldic pore filling dolomite cement and <1% chalcedony mold filling cement.

Recrystallization: Slight neomorphism of micritic matrix; micritization of skeletal grains

Replacement: Dolomitization; common anhydrite replacement of grains & matrix; present replacive pyrite & chalcedony

Dissolution: Complete dissolution of skeletal grains; grain compaction in upper, anhydrite poor wackestone

Stylolites: NA

Fractures: Discontinuous, vertical, anhydrite cemented fractures terminating into nodular anhydrite

Other: NA

Porosity

Measured porosity (%) – 5.2

Measured permeability (mD) – .641

Ahr Genetic Pore Type: **Hybrid 1A – Reduced**

- Depositional:
 - Interparticle
- Diagenetic:
 - Moldic
 - Intercrystalline

Comments: Diagenetic skel-pel moldic porosity dominates; relict depositional interparticle porosity is present; accessory solution enhanced intercrystalline porosity in neomorphosed micrite. Anhydrite cementation/replacement reduces porosity, but overall porosity has been enhanced by dissolution.

Remarks: Skeletal/Peloidal Dolo-Wackestone or Packstone. Micritization of framework grains and dolomitization precludes definite determination of depositional fabric.

M3 Thin Section Description

Sample: Muldrow 3 – 5296'

Cycle Position: Middle

Depositional Characteristics

Lithofacies Type: Spiculiferous Peloidal Dolo-Wackestone

Sedimentary Structure: No Structures Observed

Framework Grains:

- Skeletal:
 - Sponge – Spicules Present
 - Foraminifera Present
- Non-skeletal:
 - Peloids Present
- Detrital:
 - Siliciclastic Silt Present

Comments: Spicules have undergone partial-complete dissolution; several siliceous spicules remain; undifferentiated micritic peloids, some of which may be microbial in origin.

Diagenetic Characteristics

Cementation: Present moldic and intercrystalline pore filling anhydrite and isotropic (fluorite?) cement

Recrystallization: Neomorphism of dolo-micrite matrix

Replacement: Dolomitization; present anhydrite replacement of sample; present isotropic (fluorite?) replacement of anhydrite; present replacive pyrite

Dissolution: Extensive dissolution of sponge spicules and solution enhanced intercrystalline porosity

Stylolites: NA

Fractures: NA

Other: Unidentified, alizarin red stained, isotropic material, same material found in P37-2 5320'.

Porosity*Measured porosity (%) – 10.9**Measured permeability (mD) – .824**Ahr Genetic Pore Type: Hybrid 1A – Enhanced*

- Depositional:
 - Interparticle
- Diagenetic:
 - Moldic
 - Intercrystalline

Comments: Porosity is dominated by skel-moldic porosity after sponge spicule dissolution with considerable solution enhanced intercrystalline porosity. Some solution enhanced pores border on being vugs; accessory interparticle porosity.

Remarks: Spiculiferous Peloidal Dolo-Wackestone exhibiting extensive dissolution of sponge spicules and solution enhancement of intercrystalline porosity. Some solution enhanced pores border on being vugs.

Sample: Muldrow 3 – 5305' Upper**Cycle Position: Middle****Depositional Characteristics***Lithofacies Type: Peloidal Dolo-Wackestone**Sedimentary Structure: No Structures Observed**Framework Grains:*

- Skeletal:
 - Foraminifera Present
 - Algae – Phylloid Present
 - Undifferentiated Grains Present
- Non-skeletal:
 - Peloids Present
 - Undifferentiated Grains Present
- Detrital:
 - Siliciclastic Silt Present

Comments: Dolomitization, neomorphism and grain compaction preclude definitive identification of framework grains; undifferentiated grains may be neomorphosed peloids or skeletal grains. Algal grains have been dolomitized and highly neomorphosed.

Diagenetic Characteristics*Cementation: Present interparticle/intercrystalline dolomite and anhydrite cement**Recrystallization: Considerable neomorphism of framework grains and matrix**Replacement: Dolomitization; present anhydrite replacement; present pyrite**Dissolution: Grain compaction and possible dissolution along discontinuous micro-solution seams and stylolites**Stylolites: Pyritic stylolites found at top of sample and in the middle (separate upper 5305' description from lower 5305'); common discontinuous micro-solution seams swarming throughout upper 5305'**Fractures: NA**Other: Present organic material and unidentified alizarin red stained, isotropic material***Porosity***Measured porosity (%) – 9.3**Measured permeability (mD) – 2.206**Ahr Genetic Pore Type: Hybrid 1B – Reduced*

- Depositional:

- Interparticle
- Diagenetic:
 - Intercrystalline

Comments: Porosity is dominated by relict interparticle porosity and intercrystalline porosity after neomorphism and solution enhancement. Majority of measured porosity appears to exist in lower 5305' description. Compaction has greatly reduced original interparticle porosity.

Remarks: Peloidal Dolo-Wackestone exhibiting considerable neomorphism of framework grains and matrix; grain compaction and possible dissolution is associated with micro-solution seams swarms. Dolomitization, neomorphism and grain compaction preclude definitive identification of framework grains and depositional fabric. Due to major lithology and genetic porosity differences, the description of sample 5305' has been divided into upper and lower in relation to a major stylolite that cuts the sample.

Sample: Muldrow 3 – 5305' Lower

Cycle Position: Middle

Depositional Characteristics

Lithofacies Type: Anhydritic Skeletal Dolo-Wackestone

Sedimentary Structure: No Structures Observed

Framework Grains:

- Skeletal:
 - Sponge – Spicules Present
 - Algae – Green Present
- Non-skeletal:
 - Peloids Present
 - Pellets Present
 - Detrital: NA

Comments: Framework grains dominated by irregular molds after skeletal fragments and/or peloids; present micritic peloids some of which are probable pelletal grains.

Diagenetic Characteristics

Cementation: Common replacive/moldic pore filling anhydrite cement; present interparticle dolomite and isotropic (fluorite?) cement

Recrystallization: Considerable neomorphism of dolo-micrite matrix

Replacement: Dolomitization; present anhydrite replacement of sample; present fluorite (?) and chalcedony/gypsum replacement of anhydrite; present replacive pyrite

Dissolution: Extensive dissolution of framework grains yielding irregular moldic pores

Stylolites: Pyritic stylolite in the middle of 5305' separates upper 5305' description from lower 5305'

Fractures: Present discontinuous, vertical fractures associated with stylolite that are partially anhydrite cemented

Other: Present residual hydrocarbon in moldic pores

Porosity

Measured porosity (%) – 9.3

Measured permeability (mD) – 2.206

Ahr Genetic Pore Type: Hybrid 1A – Enhanced

- Depositional: NA
- Diagenetic:
 - Moldic
 - Intercrystalline

Comments: Porosity is dominated by irregular moldic pores and intercrystalline porosity after neomorphism and solution enhancement. Majority of measured porosity appears to exist in lower 5305' description.

Remarks: Anhydritic Skeletal Dolo-Wackestone exhibiting extensive dissolution of framework grains and considerable neomorphism of dolo-micrite matrix. Due to major lithology and genetic porosity differences, the description of sample 5305' has been divided into upper and lower in relation to a major stylolite that cuts the sample.

Sample: Muldrow 3 – 5307'

Cycle Position: Middle

Depositional Characteristics

Lithofacies Type: Anhydritic Peloidal-Algal Dolo-Packstone

Sedimentary Structure: No Structures Observed

Framework Grains:

- Skeletal:
 - Algae – Phylloid Present
 - Algae – Green Present
 - Foraminifera Present
 - Sponge – Spicules Present
 - Undifferentiated Grains Present
- Non-skeletal:
 - Peloids Present
 - Coated Grain Present
 - Undifferentiated Grains Common
- Detrital: NA

Comments: Dolomitization, neomorphism and grain compaction preclude definitive identification of framework grains; undifferentiated grains may be neomorphosed peloids or skeletal grains (echinoderm or bryozoan?). Algal grains have been dolomitized and highly neomorphosed. Peloids may be clastic or microbial in origin.

Diagenetic Characteristics

Cementation: Present interparticle/intercrystalline anhydrite and dolomite cement

Recrystallization: Considerable neomorphism of framework grains and matrix

Replacement: Dolomitization; present anhydrite replacement of framework grains and matrix

Dissolution: Solution enhanced intercrystalline porosity and possible slight dissolution along discontinuous micro-solution seams

Stylolites: Discontinuous micro-solution seams

Fractures: NA

Other: Present residual hydrocarbon and possible organic material

Porosity

Measured porosity (%) – 6.4

Measured permeability (mD) – .63

Ahr Genetic Pore Type: **Hybrid 1B – Reduced**

- Depositional:
 - Interparticle
- Diagenetic:
 - Intercrystalline

Comments: Porosity is dominated by interparticle porosity and intercrystalline porosity after neomorphism and solution enhancement. Porosity has been enhanced by neomorphism and dissolution, but overall interparticle porosity has been reduced due to anhydrite cementation.

Remarks: Anhydritic Peloidal-Algal Packstone with considerable neomorphism of framework grains and matrix. Dolomitization, neomorphism and grain compaction preclude definitive identification of framework grains and depositional fabric. Sample is possibly an algal mound deposit.

Sample: Muldrow 3 – 5313'

Cycle Position: Bottom

Depositional Characteristics

Lithofacies Type: Skeletal Mudstone

Sedimentary Structure: No Structures Observed

Framework Grains:

- Skeletal:
 - Sponge – Spicules Present
 - Foraminifera Present
 - Gastropods Present
- Non-skeletal:
 - Peloids Present
- Detrital: NA

Comments: Grains dominated by partially-completely leached spicules; peloids are undifferentiated micritic and neomorphosed dolomite peloids.

Diagenetic Characteristics

Cementation: Present moldic pore filling anhydrite and isotropic (fluorite?) cement

Recrystallization: Slight neomorphism of dolo-micrite matrix

Replacement: Dolomitization; present anhydrite replacement of grains and matrix; present replacive pyrite

Dissolution: Considerable dissolution of framework grains yielding skel-moldic pores and solution enhanced intercrystalline porosity

Stylolites: Present discontinuous micro-solution seams

Fractures: NA

Other: Possible organic material

Porosity

Measured porosity (%) – 10.1

Measured permeability (mD) – .238

Ahr Genetic Pore Type: **Hybrid 1A – Enhanced**

- Depositional: NA
- Diagenetic:
 - Moldic
 - Intercrystalline

Comments: Porosity is dominated by skel-moldic porosity after sponge spicule dissolution with considerable solution enhanced intercrystalline porosity.

Remarks: Skeletal Dolo-Mudstone exhibiting considerable dissolution of framework grains, predominantly sponge spicules, and solution enhanced intercrystalline porosity.

Sample: Muldrow 3 – 5315'

Cycle Position: Top

Depositional Characteristics

Lithofacies Type: Anhydritic Peloidal Dolo-Wackestone

Sedimentary Structure: No Structures Observed

Framework Grains:

- Skeletal:

- Sponge – Spicules Present
 - Algae – Green Present
- Non-skeletal:
 - Peloids Present
- Detrital: NA

Comments: Indistinct micritic peloidal grains are difficult to differentiate from matrix.

Diagenetic Characteristics

Cementation: Present anhydrite and isotropic (fluorite?) cementing moldic pores

Recrystallization: NA

Replacement: Common anhydrite replacement of framework grains and matrix; present replace pyrite and fluorite (?)

Dissolution: Dissolution of framework grains yielding moldic pores ; solution enhanced intercrystalline porosity

Stylolites: NA

Fractures: NA

Other: NA

Porosity

Measured porosity (%) – 12.1

Measured permeability (mD) – .038

Ahr Genetic Pore Type: **Hybrid 1A – Enhanced**

- Depositional:
 - Interparticle
- Diagenetic:
 - Moldic
 - Intercrystalline

Comments: Porosity is dominated by tight moldic porosity that resisted epoxy impregnation; considerable solution enhanced intercrystalline and interparticle porosity.

Remarks: Anhydritic Peloidal Dolo-Wackestone with indistinct peloidal grains that are difficult to distinguish from matrix. Porosity is dominated by tight moldic porosity that resisted epoxy impregnation; considerable solution enhanced intercrystalline and interparticle porosity is also present.

Sample: Muldrow 3 – 5319'

Cycle Position: Middle - Bottom

Depositional Characteristics

Lithofacies Type: Dolo-Mudstone

Sedimentary Structure: No Structures Observed

Framework Grains:

- Skeletal:
 - Sponge – Spicules Present
- Non-skeletal:
 - Peloids Present
- Detrital:
 - Siliciclastic Silt Present

Comments: Indistinct micritic peloidal grains with partially-completely leached sponge spicules.

Diagenetic Characteristics

Cementation: Present anhydrite and dolomite cementing moldic/intercrystalline pores

Recrystallization: Considerable neomorphism of dolo-micrite matrix

Replacement: Present anhydrite replacement of matrix

Dissolution: Partial-complete dissolution of spicules and solution enhanced intercrystalline porosity

Stylolites: NA

Fractures: Open discontinuous fractures are artifacts of sample preparation

Other: Residual hydrocarbon in moldic/intercrystalline pores

Porosity

Measured porosity (%) – 8.9

Measured permeability (mD) – .787

Ahr Genetic Pore Type: **Hybrid 1A – Enhanced**

- Depositional: NA
- Diagenetic:
 - Moldic
 - Intercrystalline

Comments: Porosity is dominated by skel-moldic porosity after sponge spicule dissolution with considerable solution enhanced intercrystalline porosity.

Remarks: Skeletal Dolo-Mudstone exhibiting partial-complete dissolution of framework grains, predominantly sponge spicules, and solution enhanced intercrystalline porosity.

Sample: Muldrow 3 – 5337'

Cycle Position: Bottom (?)

Depositional Characteristics

Lithofacies Type: Sandy Dolo-Wackestone

Sedimentary Structure: Silt concentrated into indistinct laminations

Framework Grains:

- Skeletal:
 - Sponge – Spicules Present
 - Foraminifera Present
- Non-skeletal:
 - Peloids Present
- Detrital:
 - Siliciclastic Silt-Very Fine Sand Common

Comments: Indistinct micritic peloidal grains and spicules, some of which are partially-completely leached. Common siliciclastic very fine sand-silt, predominantly quartz with accessory plagioclase and potassium feldspar, concentrated into indistinct laminations.

Diagenetic Characteristics

Cementation: Present moldic pore filling anhydrite, chalcedony, and isotropic (fluorite?) cement

Recrystallization: NA

Replacement: Dolomitization; present anhydrite replacement of dolo-micrite matrix

Dissolution: Partial-complete dissolution of framework grains; possibly slight dissolution/compaction along micro-solution seams

Stylolites: Discontinuous micro-solution seams

Fractures: NA

Other: NA

Porosity

Measured porosity (%) – NA

Measured permeability (mD) – NA

Ahr Genetic Pore Type: **Hybrid 1A – Enhanced**

- Depositional:
 - Interparticle
- Diagenetic:

- Moldic
- Intercrystalline

Comments: Porosity is dominated by partial-complete pel-skel molds with accessory intercrystalline and relict inter-peloidal porosity.

Remarks: Sandy Dolo-Wackestone with indistinct micritic peloidal grains and spicules that have been partially to completely leached. Common siliciclastic very fine sand-silt, predominantly quartz with accessory plagioclase and potassium feldspar, concentrated into indistinct laminations.

M6 Thin Section Description

Sample: Muldrow 6 – 5277'

Cycle Position: Middle

Depositional Characteristics

Lithofacies Type: Anhydritic Pelletal Packstone

Sedimentary Structure: No Structures Observed

Framework Grains:

- Skeletal:
 - Sponge – Spicules Present
 - Algae – Green Present
- Non-skeletal:
 - Pellets Common
- Detrital: NA

Comments: Common .2-1 mm micritic fecal pellets (average .6 mm in diameter) with moldic spiculiferous matrix.

Diagenetic Characteristics

Cementation: Common moldic pore filling/replacive anhydrite cement

Recrystallization: NA

Replacement: Dolomitization; common anhydrite replacement of matrix and framework grains; present isotropic (fluorite?) replacement; present chalcedony after anhydrite

Dissolution: Partial-complete dissolution of skeletal framework grains in matrix surrounding pellets

Stylolites: NA

Fractures: Open fracture is artifact of sample preparation

Other: Present residual hydrocarbon

Porosity

Measured porosity (%) – 6.8

Measured permeability (mD) – 1.942

Ahr Genetic Pore Type: **Hybrid 1B – Reduced**

- Depositional:
 - Interparticle
- Diagenetic:
 - Moldic
 - Intercrystalline

Comments: Porosity is dominated by skel-moldic pores found in spiculiferous matrix surrounding pelletal grains. Anhydrite cementation and replacement have greatly reduced porosity.

Remarks: Anhydritic Pelletal Dolo-Packstone with spiculiferous matrix exhibiting considerable anhydrite cementation and replacement. Porosity is dominated by skel-moldic pores after spicules in the matrix surrounding fecal pellets.

Sample: Muldrow 6 – 5283'**Cycle Position: Middle – Bottom****Depositional Characteristics**

Lithofacies Type: Anhydritic Skeletal-Pelletal Dolo-Wackestone

Sedimentary Structure: Lithofacies contact between wackestone and lower mudstone in lower portions of the sample

Framework Grains:

- Skeletal:
 - Sponge – Spicules Present
 - Algae – Green Present
- Non-skeletal:
 - Peloids Present
- Detrital:
 - Siliciclastic Silt Present

Comments: Skeletal framework grains are partially-completely leached; micritic pelletal grains average .5 mm in diameter. Present siliciclastic silt is found in lower, mudstone interval.

Diagenetic Characteristics

Cementation: Present moldic pore filling/interparticle, replacive anhydrite cement; present fluorite cement

Recrystallization: NA

Replacement: Dolomitization; common anhydrite replacement of framework grains and matrix; present chalcedony replacement of anhydrite; present replacive pyrite

Dissolution: Partial- complete dissolution of skeletal framework grains

Stylolites: Discontinuous and continuous microstylolites throughout sample

Fractures: Partially anhydrite cemented discontinuous fractures associated with stylolitization

Other: Present residual hydrocarbon

Porosity

Measured porosity (%) – 7.9

Measured permeability (mD) – 1.605

Ahr Genetic Pore Type: **Hybrid 1A – Enhanced**

- Depositional:
 - Interparticle
- Diagenetic:
 - Moldic
 - Intercrystalline

Comments: Skel-moldic porosity dominates with accessory solution enhanced intercrystalline porosity. Anhydrite cementation and replacement reduce enhanced moldic porosity.

Remarks: Anhydritic Skeletal-Pelletal Dolo-Wackestone exhibiting a lithofacies contact with a lower mudstone unit at the base of the sample. Porosity is dominated by skel-moldic pores. Overall porosity is enhanced, but has been reduced by anhydrite cementation and replacement.

M11 Thin Section Description

Sample: Muldrow 11 – 5297'

Cycle Position: Middle

Depositional Characteristics

Lithofacies Type: Dolo-Mudstone

Sedimentary Structure: Thinly bedded anhydrite

Framework Grains:

- Skeletal:
 - Foraminifera Present
- Non-skeletal:
 - Peloids Present
- Detrital:
 - Siliciclastic Silt Present

Comments: Indistinct micritic peloidal grains; some partially-completely leached; possibly wackestone.

Diagenetic Characteristics

Cementation: Present moldic/solution enhanced pore filling anhydrite, isotropic (halite?), and chalcedony cement

Recrystallization: NA

Replacement: Dolomitization; present anhydrite and halite (?) replacement of dolo-mudstone; present chalcedony after anhydrite; present pyrite

Dissolution: Partial-complete dissolution of peloids and solution enhancement of intercrystalline porosity

Stylolites: Discontinuous solution seam associated with anhydrite bed

Fractures: Vertical anhydrite cemented fractures associated with anhydrite bed; open horizontal fractures with associated “vugs” are likely artifacts of sample preparation

Other: NA

Porosity

Measured porosity (%) – NA

Measured permeability (mD) – NA

Ahr Genetic Pore Type: Hybrid 1A – Enhanced

- Depositional: NA
- Diagenetic:
 - Moldic
 - Intercrystalline

Comments: Porosity is dominated by irregular, scattered, moldic (peloidal?) porosity and solution enhanced intercrystalline porosity. Cementation reduces moldic porosity.

Remarks: Dolo-Mudstone with thinly bedded anhydrite exhibiting irregular, scattered moldic porosity and present anhydrite, halite (?), and chalcedony cement. Present siliciclastic silt-very fine sand is also found.

Sample: Muldrow 11 – 5313'

Cycle Position: Middle

Depositional Characteristics

Lithofacies Type: Anhydritic Peloidal Dolo-Packstone

Sedimentary Structure: No Structures Observed

Framework Grains:

- Skeletal:
 - Sponge – Spicules Present

- Non-skeletal:
 - Peloids Common
 - Pellets Present
- Detrital:
 - Siliciclastic Silt Present

Comments: Majority of grains are represented as irregular, probably peloidal, molds; large (.5-1 mm) micritic pelletal grains also present.

Diagenetic Characteristics

Cementation: Common anhydrite filling moldic pores

Recrystallization: Slight neomorphism of dolo-micrite matrix

Replacement: Dolomitization; Common anhydrite replacement of framework grains and matrix; replacive anhydrite nodules; present chalcedony and gypsum after anhydrite

Dissolution: Extensive grain dissolution yielding moldic pores

Stylolites: NA

Fractures: NA

Other: Residual hydrocarbon

Porosity

Measured porosity (%) – 9.2

Measured permeability (mD) – 1.595

Ahr Genetic Pore Type: **Hybrid 1A – Enhanced**

- Depositional:
 - Interparticle
- Diagenetic:
 - Moldic
 - Intercrystalline

Comments: Porosity is dominated by irregular, probably peloidal, molds; many moldic pores resisted epoxy impregnation. Accessory relict interparticle and solution enhanced intercrystalline porosity.

Remarks: Anhydritic Peloidal Dolo-Packstone exhibiting extensive framework grain dissolution and common anhydrite cementation after moldic pores. Framework grains are represented by irregular, probably peloidal molds, many of which resisted epoxy impregnation. Sample also contains present large (.5-1 mm) pelletal grains and replacive anhydrite nodules.

Sample: Muldrow 11 – 5319'

Cycle Position: Middle – Bottom

Depositional Characteristics

Lithofacies Type: Dolo-Mudstone

Sedimentary Structure: Thinly bedded – laminated pyritic and organic rich shale (possibly diagenetic solution seam)

Framework Grains:

- Skeletal: NA
- Non-skeletal:
 - Peloids Present
- Detrital:
 - Siliciclastic Silt Present
 - Mica Present

Comments: Indistinct neomorphosed grains; siliciclastic silt and mica concentrated in shale.

Diagenetic Characteristics

Cementation: Present replacive anhydrite cement

Recrystallization: Considerable neomorphism of mudstone

Replacement: Dolomitization; present anhydrite replacement of sample; present pyrite

Dissolution: Solution enhanced intercrystalline pores and possibly pel-molds (?)

Stylolites: Shale laminations may be the result of extensive dissolution/compaction along solution seam swarm

Fractures: NA

Other: NA

Porosity

Measured porosity (%) – 8.3

Measured permeability (mD) – .048

Ahr Genetic Pore Type: **Hybrid 1A – Enhanced**

- Depositional: NA
- Diagenetic:
 - Intercrystalline
 - Moldic

Comments: Porosity is dominated by intercrystalline porosity, primarily after solution enhancement, with possible pel-moldic porosity.

Remarks: Dolo-Mudstone with thinly bedded-laminated “shale”. Shale is possibly the result of extensive compaction/dissolution due to solution seams. Insoluble organics, pyrite, and siliciclastic silt are found concentrated within “shale” supporting this theory.

Sample: Muldrow 11 – 5335’

Cycle Position: Top

Depositional Characteristics

Lithofacies Type: Peloidal Dolo -Wackestone

Sedimentary Structure: Clotted, possibly microbial fabric; possible desiccation features

Framework Grains:

- Skeletal:
 - Foraminifera Present
 - Algae – Green Present
 - Gastropod Present
 - Sponge – Spicules Present
- Non-skeletal:
 - Peloids Common
- Detrital:
 - Siliciclastic Silt Present

Comments: Indistinct micritic peloids grains are difficult to distinguish from matrix; clotted fabric may be the result of peloidal clasts created by desiccation.

Diagenetic Characteristics

Cementation: Common interparticle/moldic porosity and fracture filling anhydrite; present halite (?) cementing interparticle/moldic pores and fractures

Recrystallization: NA

Replacement: Dolomitization; common anhydrite/halite (?) replacement

Dissolution: Considerable dissolution and grain compaction associated with stylolites

Stylolites: Stylolitization throughout sample yielding dissolution/compaction of grains

Fractures: Common discontinuous fractures throughout sample; fractures are typically anhydrite/halite (?) cemented and associated with stylolites; some fractures remain partially-completely open

Other: NA

Porosity*Measured porosity (%)* – 8.7*Measured permeability (mD)* – .071*Ahr Genetic Pore Type:* **Hybrid 1B – Reduced**

- Depositional:
 - Interparticle
 - Intraparticle
- Diagenetic:
 - Moldic
 - Intercrystalline

Comments: Porosity is dominated by relict interparticle and intercrystalline porosity; present intraparticle and moldic porosity also exists. Porosity has been greatly reduced by dissolution/compaction associated with stylolitization and common cementation/replacement by anhydrite and halite (?)

Remarks: Anhydritic Peloidal Dolo-Wackestone exhibiting clotted (possibly microbial) fabric and possibly desiccation features. Peloidal grains and clotted “clasts” are indistinct and difficult to differentiate from matrix. Sample is highly cemented by anhydrite/halite (?) and has undergone dissolution/compaction from stylolitization.

M13 Thin Section Description

Sample: Muldrow 13 – 5350’**Cycle Position: Middle****Depositional Characteristics***Lithofacies Type:* Peloidal-Skeletal Dolo-Packstone*Sedimentary Structure:* No Structures Observed*Framework Grains:*

- Skeletal:

○ Algae – Undifferentiated	Present
○ Sponge – Spicules	Present
○ Foraminifera	Present
- Non-skeletal:

○ Peloids	Present
-----------	---------
- Detrital:

○ Siliciclastic Silt	Present
----------------------	---------

Comments: Indistinct micritic grains, possibly algal in origin; present micritic and moldic peloidal grains and spicule molds.

Diagenetic Characteristics*Cementation:* Present moldic pore filling/replacive anhydrite cement*Recrystallization:* Slight neomorphism of dolo-micrite*Replacement:* Dolomitization; present anhydrite replacement of framework grains and dolo-micrite matrix*Dissolution:* Partial-complete dissolution of framework grains*Stylolites:* NA*Fractures:* NA*Other:* Present residual hydrocarbon and organic material**Porosity***Measured porosity (%)* – 16.6*Measured permeability (mD)* – 2.13*Ahr Genetic Pore Type:* **Hybrid 1A – Enhanced**

- Depositional:

- Interparticle
- Diagenetic:
 - Moldic
 - Intercrystalline

Comments: Porosity dominated by undifferentiated moldic pores with considerable solution enhanced intercrystalline porosity and accessory interparticle.

Remarks: Peloidal-Skeletal Dolo-Packstone with undifferentiated moldic pores, possibly after peloidal or algal grains. Dissolution makes definitive identification of grains difficult.

Sample: Muldrow 13 – 5354'

Cycle Position: Middle

Depositional Characteristics

Lithofacies Type: Skeletal-Peloidal Dolo-Wackestone

Sedimentary Structure: No Structures Observed

Framework Grains:

- Skeletal:
 - Algae – Green Present
 - Sponge – Spicules Present
 - Ostracods Present
 - Foraminifera Present
- Non-skeletal:
 - Peloids Present
- Detrital:
 - Siliciclastic Silt Present

Comments: Indistinct micritic framework grains; many have been partially-completely leached and cemented.

Diagenetic Characteristics

Cementation: Present moldic pore filling anhydrite, chalcedony, and fluorite cement

Recrystallization: Slight neomorphism of dolo-micrite matrix

Replacement: Dolomitization; present anhydrite replacement

Dissolution: Partial-complete dissolution of framework grains

Stylolites: NA

Fractures: NA

Other: Considerable residual hydrocarbon and organic material

Porosity

Measured porosity (%) – 14.5

Measured permeability (mD) – 1.471

Ahr Genetic Pore Type: **Hybrid 1A – Enhanced**

- Depositional: NA
- Diagenetic:
 - Moldic
 - Intercrystalline

Comments: Skel-pel moldic porosity dominates with considerable solution enhanced intercrystalline porosity.

Remarks: Skeletal-Peloidal Dolo-Wackestone with indistinct framework grains, many of which have been partially to completely leached. Considerable hydrocarbon and organic material are found in sample.

Sample: Muldrow 13 – 5365'**Cycle Position: Bottom****Depositional Characteristics**

Lithofacies Type: Peloidal Dolo-Wackestone – Mudstone

Sedimentary Structure: Indistinct laminations after changing grain/mud ratio and porosity differences

Framework Grains:

- Skeletal:
 - Sponge – Spicules Present
- Non-skeletal:
 - Peloids Present
- Detrital:
 - Siliciclastic Silt Present

Comments: Indistinct micritic peloidal grains.

Diagenetic Characteristics

Cementation: Present moldic pore filling/replacive anhydrite and chalcedony cement

Recrystallization: Slight neomorphism of dolo-micrite in some laminations

Replacement: Dolomitization; present anhydrite and chalcedony replacement

Dissolution: Partial-complete dissolution of some framework grains; solution enhancement of intercrystalline porosity; some vuggy pores after dissolution

Stylolites: Discontinuous solution seams/microstylolites throughout sample

Fractures: NA

Other: Present residual hydrocarbon

Porosity

Measured porosity (%) – 17.6

Measured permeability (mD) – 2.449

Ahr Genetic Pore Type: **Hybrid 1A – Enhanced**

- Depositional:
 - Interparticle
- Diagenetic:
 - Moldic
 - Intercrystalline
 - Vug – Separate

Comments: Porosity is dominated by interparticle and moldic pores in more grain rich wackestone laminations; considerable solution enhanced intercrystalline porosity is found throughout sample; diagenetically enhanced vuggy pores are also found within an anhydrite rich, muddy lamination. Certain laminations are 1Be genetic pore type, but overall sample is 1Ae

Remarks: Peloidal Dolo-Wackestone exhibiting indistinct laminations with variable porosity trends. Grain rich laminations are dominated by interparticle and moldic porosity. Considerable solution enhanced intercrystalline porosity is found throughout sample.

M19-4 Thin Section Description

Sample: Muldrow 19-4_5271'

Cycle Position: Middle

Depositional Characteristics

Lithofacies Type: Anhydritic Dolo-Mudstone

Sedimentary Structure: No Structures Observed

Framework Grains:

- Skeletal:
 - Undifferentiated Dust Present
- Non-skeletal:
 - Peloids Present
- Detrital: NA

Comments: Indistinct micritic peloidal grain; mudstone may have originally been peloidal rich rock.

Diagenetic Characteristics

Cementation: Common replacive anhydrite cement with present replacive and moldic/interparticle pore filling isotropic (halite?) cement; present chalcedony filling moldic pores

Recrystallization: NA

Replacement: Dolomitization; common anhydrite after dolomite matrix; present isotropic mineral (halite?) after anhydrite/dolomite; pyritization

Dissolution: Solution enhanced intercrystalline and skel-moldic porosity

Stylolites: NA

Fractures: NA

Other: NA

Porosity

Measured porosity (%) – NA

Measured permeability (mD) – NA

Ahr Genetic Pore Type: **Hybrid 1A – Enhanced**

- Depositional:
 - Possibly Interparticle
- Diagenetic:
 - Moldic
 - Intercrystalline

Comments: Porosity dominated by solution enhanced moldic and intercrystalline porosity; possibly considerable interparticle porosity between indistinct micritic peloidal grains.

Remarks: Anhydritic Dolo-Mudstone with indistinct micritic peloidal grains; sample was possibly a peloidal, grain supported rock that underwent considerable compaction. Exhibits solution enhanced moldic and intercrystalline porosity; considerable porosity may be relict interparticle porosity between indistinct micritic peloidal grains.

Sample: Muldrow 19-4_5274'

Cycle Position: Bottom

Depositional Characteristics

Lithofacies Type: Peloidal Dolo-Wackestone

Sedimentary Structure: Possible desiccation features

Framework Grains:

- Skeletal:
 - Sponge – Spicules Present
 - Algae – Green Present

- Non-skeletal:
 - Peloids Present
- Detrital:
 - Siliciclastic Silt Present

Comments: Indistinct micritic peloidal grains and present skeletal hash; skeletal grains are partially-completely leached

Diagenetic Characteristics

Cementation: Present moldic pore filling anhydrite with accessory chalcedony, dolomite, and isotropic (probably halite) cement

Recrystallization: Slight neomorphism of micrite matrix

Replacement: Dolomitization; present anhydrite and isotropic mineral (halite?) after dolomite; pyritization

Dissolution: Partial-complete dissolution of skeletal framework grains

Stylolites: NA

Fractures: NA

Other: NA

Porosity

Measured porosity (%) – 5.9

Measured permeability (mD) – .061

Ahr Genetic Pore Type: **Hybrid 1A – Enhanced**

- Depositional:
 - Interparticle
- Diagenetic:
 - Moldic
 - Intercrystalline

Comments: Porosity dominated by skel-moldic porosity accessory solution enhanced intercrystalline porosity and relict interparticle porosity in wackestone.

Remarks: Peloidal Dolo-Wackestone dominated by skel-moldic porosity and indistinct micritic peloidal grains. Possibly a desiccated wackestone with mudstone infill.

Sample: Muldrow 19-4 _5275'

Cycle Position: Top

Depositional Characteristics

Lithofacies Type: Spiculiferous Dolo-Wackestone – Mudstone

Sedimentary Structure: Inclined, interlaminated mudstone and wackestone intervals

Framework Grains:

- Skeletal:
 - Sponge – Spicules Common
 - Algae – Green Present
- Non-skeletal:
 - Peloids Present
- Detrital: NA

Comments: Framework grains dominated by sponge spicules, most of which have been partially-completely leached and present micritic peloidal grains.

Diagenetic Characteristics

Cementation: Present anhydrite and chalcedony filling skel-moldic pores

Recrystallization: Slight neomorphism of micrite

Replacement: Dolomitization; present anhydrite and chalcedony replacement of dolomite matrix; pyritization

Dissolution: Partial-complete dissolution of siliceous sponge spicules

Stylolites: NA

Fractures: Vertical, discontinuous dolomite/anhydrite cemented fracture is present; open fractures appear to be the result of sample preparation

Other: Residual hydrocarbon

Porosity

Measured porosity (%) – 10.7

Measured permeability (mD) – .092

Ahr Genetic Pore Type: **Hybrid 1A – Enhanced**

- Depositional: NA
- Diagenetic:
 - Moldic
 - Intercrystalline

Comments: Porosity dominated by skel-moldic pores after partial-complete dissolution of sponge spicules; accessory solution enhanced intercrystalline porosity.

Remarks: Interlaminated Spiculiferous Dolo-Wackestone – Mudstone exhibiting inclined laminations and common sponge spicules. Porosity dominated by skel-moldic porosity after partial-complete dissolution of sponge spicules.

Sample: Muldrow 19-4_5276'

Cycle Position: Middle

Depositional Characteristics

Lithofacies Type: Siliceous Spiculiferous Dolo-Wackestone

Sedimentary Structure: Alternating diagenetic laminations of low and high chalcedony replacement

Framework Grains:

- Skeletal:

○ Sponge – Spicules	Common
○ Algae – Green	Present
○ Foraminifera	Present
- Non-skeletal:

○ Peloids	Present
-----------	---------
- Detrital:

○ Glauconite	Present
--------------	---------

Comments: Framework grains are dominated by siliceous sponge spicules.

Diagenetic Characteristics

Cementation: Common replacive and moldic pore filling chalcedony/siliceous cement; present anhydrite and dolomite moldic pore filling cement;

Recrystallization: Slight neomorphism of micrite matrix

Replacement: Common chert/chalcedony replacement of dolo-matrix; dolomitization and pyritization

Dissolution: present partial-complete dissolution of skeletal grains

Stylolites: NA

Fractures: Prominent open fracture is the result of sample preparation

Other: NA

Porosity

Measured porosity (%) – 5.4

Measured permeability (mD) – .059

Ahr Genetic Pore Type: **Hybrid 1B – Reduced**

- Depositional:
 - Interparticle

- Diagenetic:
 - Moldic
 - Intercrystalline

Comments: Porosity dominated by relict skel-moldic, interparticle, and intercrystalline porosity; overall porosity has been greatly reduced by common chalcedony/chert cementation and replacement.

Remarks: Siliceous Spiculiferous Dolo-Wackestone with present detrital glauconite; porosity has been greatly reduced by common chalcedony/chert cementation and replacement.

Sample: Muldrow 19-4_5278'

Cycle Position: Bottom

Depositional Characteristics

Lithofacies Type: Spiculiferous Mudstone

Sedimentary Structure: Indistinct, continuous and parallel laminations defined by slight differences in mud/grain ratio

Framework Grains:

- Skeletal:
 - Sponge – Spicules Present
 - Foraminifera Present
- Non-skeletal:
 - Peloids Present
- Detrital:
 - Siliciclastic Silt Present

Comments: Partially-completely leached sponge spicules dominate.

Diagenetic Characteristics

Cementation: Present moldic pore filling and replacive anhydrite cement

Recrystallization: Neomorphism of dolo-micrite matrix

Replacement: Dolomitization; Present anhydrite after dolo-matrix and present chalcedony after anhydrite

Dissolution: Partial-complete dissolution of sponge spicules

Stylolites: NA

Fractures: NA

Other: Residual hydrocarbon in moldic pores

Porosity

Measured porosity (%) – 8.9

Measured permeability (mD) – .345

Ahr Genetic Pore Type: **Hybrid 1A – Enhanced**

- Depositional: NA
- Diagenetic:
 - Moldic
 - Intercrystalline

Comments: Porosity is dominated by skel-moldic porosity after spicule dissolution with accessory solution enhanced intercrystalline porosity.

Remarks: Spiculiferous Dolo-Mudstone with indistinct continuous, parallel laminations. Porosity is dominated by skel-moldic porosity after spicule dissolution.

Sample: Muldrow 19-4_5280'

Cycle Position: Top

Depositional Characteristics

Lithofacies Type: Anhydritic Skeletal Dolo-Wackestone/Mudstone

Sedimentary Structure: Possible burrow structure

Framework Grains:

- Skeletal:
 - Algae – Green Present
 - Bivalve – Undifferentiated Present
 - Foraminifera Present
 - Sponge – Spicules Present
- Non-skeletal:
 - Peloids Present
- Detrital:
 - Siliciclastic Silt Present

Comments: Indistinct framework grains are highlighted by anhydrite replacement and concentrated in lower portion of thin section.

Diagenetic Characteristics

Cementation: Common replacive/moldic pore filling anhydrite cement

Recrystallization: Slight neomorphism of dolo-micrite

Replacement: Dolomitization; common anhydrite replacement; present chalcedony after anhydrite

Dissolution: Present partial-complete grain dissolution

Stylolites: NA

Fractures: NA

Other: Residual hydrocarbon throughout sample

Porosity

Measured porosity (%) – 10.4

Measured permeability (mD) – .109

Ahr Genetic Pore Type: **Hybrid 1A – Enhanced**

- Depositional: NA
- Diagenetic:
 - Moldic
 - Intercrystalline

Comments: Porosity dominated by moldic and solution enhanced intercrystalline porosity; porosity has undergone considerable reduction from anhydrite cementation/replacement.

Remarks: Anhydritic Skeletal Dolo-Wackestone with interfingering of mudstone and possible burrow structure. Indistinct framework grains are highlighted by anhydrite cementation/replacement.

Sample: Muldrow 19-4_5282'

Cycle Position: Middle

Depositional Characteristics

Lithofacies Type: Dolo-Mudstone

Sedimentary Structure: No Structures Observed

Framework Grains:

- Skeletal:
 - Sponge – Spicules Present
- Non-skeletal:
 - Peloids Present
- Detrital: NA

Comments: Very few indistinct sponge spicules and micritic peloids; some spicules have been leached.

Diagenetic Characteristics

Cementation: Present anhydrite cementing prominent fracture and present moldic pores; present moldic pore filling chalcedony

Recrystallization: NA

Replacement: Present anhydrite replacement

Dissolution: Present leached skeletal grains and solution enhanced intercrystalline porosity

Stylolites: NA

Fractures: Two discontinuous, vertical anhydrite cemented fractures

Other: Residual hydrocarbon

Porosity

Measured porosity (%) – 4.9

Measured permeability (mD) – .029

Ahr Genetic Pore Type: **Hybrid 1A – Enhanced**

- Depositional: NA
- Diagenetic:
 - Moldic
 - Intercrystalline

Comments: Porosity is dominated by skel-moldic and solution enhanced intercrystalline porosity.

Remarks: Dolo-Mudstone with two prominent discontinuous, vertical, anhydrite cemented fractures. Contains very little visible porosity which is dominated by skel-moldic and solution enhanced intercrystalline porosity.

Sample: Muldrow 19-4_5287'

Cycle Position: Middle

Depositional Characteristics

Lithofacies Type: Anhydritic Spiculiferous Dolo-Wackestone

Sedimentary Structure: No Structures Observed

Framework Grains:

- Skeletal:
 - Sponge – Spicules Common
- Non-skeletal:
 - Peloids Present
- Detrital: NA

Comments: Partially-completely leached sponge spicules with indistinct peloidal (pelletal?) grains; many spicules have been cemented/replaced by anhydrite.

Diagenetic Characteristics

Cementation: Common replacive/moldic pore filling anhydrite cement.

Recrystallization: Neomorphism of dolo-micrite matrix

Replacement: Dolomitization; present anhydrite replacement with present chalcedony after anhydrite

Dissolution: Partially-completely leached sponge spicules

Stylolites: NA

Fractures: NA

Other: NA

Porosity

Measured porosity (%) – 8.9

Measured permeability (mD) – .146

Ahr Genetic Pore Type: **Hybrid 1A – Enhanced**

- Depositional: NA
- Diagenetic:
 - Moldic

- Intercrystalline

Comments: Porosity is dominated by skel-moldic porosity after partial-complete dissolution of sponge spicules; accessory solution enhanced intercrystalline porosity. Anhydrite cementation has considerably reduced moldic porosity.

Remarks: Anhydritic Spiculiferous Dolo-Wackestone exhibiting skel-moldic porosity after partial-complete dissolution of sponge spicules.

Sample: Muldrow 19-4_5290'

Cycle Position: Middle

Depositional Characteristics

Lithofacies Type: Anhydritic Peloidal Dolo-Packstone

Sedimentary Structure: No Structures Observed

Framework Grains:

- Skeletal:
 - Foraminifera Present
- Non-skeletal:
 - Peloids Abundant
- Detrital: NA

Comments: Abundant undifferentiated micritic peloidal grains; some are possibly microbial in origin.

Diagenetic Characteristics

Cementation: Common interparticle anhydrite/gypsum cement; present relict interparticle/isopachous dolomite cement

Recrystallization: NA

Replacement: Dolomitization; Common anhydrite after framework grains; present gypsum (?) after anhydrite; present pyrite

Dissolution: Present solution enhancement of interparticle pores

Stylolites: NA

Fractures: NA

Other: NA

Porosity

Measured porosity (%) – 8.7

Measured permeability (mD) – .095

Ahr Genetic Pore Type: **Hybrid 1A – Reduced**

- Depositional:
 - Interparticle
- Diagenetic:
 - Intercrystalline

Comments: Porosity is dominated by interparticle porosity, some of which has undergone solution enhancement; anhydrite cementation/replacement and dolomite cementation has reduced initial interparticle porosity.

Remarks: Anhydritic Peloidal Dolo-Packstone exhibits common anhydrite cementation/replacement with present relict interparticle dolomite cementation. Interparticle porosity dominates with some solution enhancement, but cementation has reduced initial interparticle porosity.

Sample: Muldrow 19-4_5293'

Cycle Position: Middle – Bottom

Depositional Characteristics

Lithofacies Type: Anhydritic Pel-Skel Dolo-Wackestone

Sedimentary Structure: No Structures Observed

Framework Grains:

- Skeletal:
 - Undifferentiated Fragments Present
 - Sponge – Spicules Present
- Non-skeletal:
 - Peloids Common
- Detrital: NA

Comments: Grains dominated by undifferentiated peloidal grains some of which are micritic, moldic, or anhydrite replaced; present skeletal fragments have also undergone dissolution and anhydrite cementation/replacement.

Diagenetic Characteristics

Cementation: Common replacive/moldic pore filling anhydrite cement

Recrystallization: Slight neomorphism of dolo-micrite matrix

Replacement: Dolomitization; common anhydrite replacement; present replacive pyrite

Dissolution: Partial-complete dissolution of undifferentiated skeletal and peloidal grains

Stylolites: NA

Fractures: NA

Other: NA

Porosity

Measured porosity (%) – 5.9

Measured permeability (mD) – .053

Ahr Genetic Pore Type: **Hybrid 1A – Enhanced**

- Depositional: NA
- Diagenetic:
 - Moldic
 - Intercrystalline

Comments: Porosity dominated by pel-skel moldic porosity with accessory solution enhanced intercrystalline porosity

Remarks: Anhydritic Pel-Skel Dolo-Wackestone exhibiting common anhydrite cementation/replacement. Porosity is dominated by molds after undifferentiated skeletal and peloidal grains.

Sample: Muldrow 19-4_5296'

Cycle Position: Bottom

Depositional Characteristics

Lithofacies Type: Anhydritic Peloidal Mudstone

Sedimentary Structure: No Structures Observed

Framework Grains:

- Skeletal:
 - Sponge – Spicules Present
- Non-skeletal:
 - Peloids Present
- Detrital:
 - Siliciclastic Silt Present

Comments: Indistinct micritic peloidal grains, some of which are neomorphosed, are difficult to distinguish from dolo-micrite matrix (possibly a wackestone); indistinct partially leached sponge spicules scattered in matrix; possibly large skeletal fragments replaced by anhydrite.

Diagenetic Characteristics

Cementation: Common replacive/moldic pore filling anhydrite cement

Recrystallization: Slight neomorphism of dolo-matrix and some framework grains

Replacement: Dolomitization; Common anhydrite replacement of matrix and framework grains; present replacive pyrite

Dissolution: Partial-complete dissolution and possible compaction of some framework grains; solution enhanced intercrystalline porosity

Stylolites: NA

Fractures: NA

Other: NA

Porosity

Measured porosity (%) – 8.4

Measured permeability (mD) – .012

Ahr Genetic Pore Type: **Hybrid 1A – Enhanced**

- Depositional:
 - Interparticle
- Diagenetic:
 - Moldic
 - Intercrystalline

Comments: Porosity is dominated by undifferentiated moldic and solution enhanced intercrystalline porosity; some pores may be interparticle after indistinct micritic peloidal grains.

Remarks: Anhydritic Peloidal Dolo-Mudstone with indistinct micritic peloidal grains; sample is possibly a wackestone due to unidentified, neomorphosed peloids. Porosity appears to be dominated by undifferentiated moldic porosity and solution enhanced intercrystalline porosity, but some pores may be interparticle after indistinct, unidentified peloidal grains.

Sample: Muldrow 19-4_5297'**Cycle Position: Top****Depositional Characteristics**

Lithofacies Type: Mudstone

Sedimentary Structure: Indistinct laminations defined by porosity differences; siliciclastic silt rich laminations; silt concentration is likely due to dissolution along microstylolites not depositional mechanisms

Framework Grains:

- Skeletal: NA
- Non-skeletal:
 - Peloids Present
- Detrital:
 - Siliciclastic Silt Present
 - Mica – Muscovite Present

Comments: Present indistinct peloidal grains some of which have undergone partial-complete dissolution.

Diagenetic Characteristics

Cementation: Present moldic and intercrystalline anhydrite cementation

Recrystallization: NA

Replacement: Present anhydrite replacement of dolo-micrite matrix; present replacive pyrite

Dissolution: Probable dissolution along microstylolites resulting in concentration of siliciclastic silt

Stylolites: Present continuous microstylolites

Fractures: Discontinuous open fractures are likely artifacts of sample preparation

Other: NA

Porosity*Measured porosity (%) – NA**Measured permeability (mD) – NA**Ahr Genetic Pore Type: Hybrid 1A – Enhanced*

- Depositional: NA
- Diagenetic:
 - Moldic
 - Intercrystalline

Comments: Porosity is dominated by present pel-moldic and solution enhanced intercrystalline porosity. Porosity seems to be concentrated in slightly more grain rich mudstone laminations.

Remarks: Dolo-Mudstone with indistinct laminations defined by porosity differences and grain distribution. Laminations of siliciclastic silt also occur, probably as a result of dissolution concentration along microstylolites. Porosity is dominated by pel-moldic and solution enhanced intercrystalline porosity and is concentrated in slightly more grain rich mudstone laminations.

Sample: Muldrow 19-4_5301'**Cycle Position: Middle****Depositional Characteristics***Lithofacies Type: Anhydritic Pel-Skel Dolo-Wackestone**Sedimentary Structure: No Structures Observed**Framework Grains:*

- Skeletal:
 - Sponge – Spicules Present
 - Undifferentiated Fragments Present
- Non-skeletal:
 - Peloids Present
- Detrital:
 - Siliciclastic Silt Present

Comments: Grains dominated by undifferentiated peloidal grains (micritic, moldic, and anhydrite replaced); present skeletal fragments have also undergone dissolution and anhydrite cementation/replacement.

Diagenetic Characteristics*Cementation: Common replacive/moldic pore filling anhydrite cement**Recrystallization: Slight neomorphism of dolo-micrite matrix**Replacement: Abundant anhydrite replacement/cementation of skeletal grains and matrix**Dissolution: Partial-complete dissolution of framework grains and solution enhanced intercrystalline porosity**Stylolites: NA**Fractures: NA**Other: Present residual hydrocarbon***Porosity***Measured porosity (%) – 5.3**Measured permeability (mD) – .027**Ahr Genetic Pore Type: Hybrid 1A – Reduced*

- Depositional:
 - Interparticle
- Diagenetic:
 - Moldic
 - Intercrystalline

Comments: Porosity is dominated by pel-skel moldic and solution enhanced intercrystalline porosity with accessory interparticle porosity. Anhydrite cementation/replacement has greatly reduced porosity.

Remarks: Anhydritic Pel-Skel Dolo-Wackestone with extensive anhydrite cementation and replacement. Anhydrite precludes definitive determination of depositional fabric and has greatly reduced porosity.

Sample: Muldrow 19-4_5303'

Cycle Position: Bottom

Depositional Characteristics

Lithofacies Type: Dolo-Mudstone

Sedimentary Structure: No Structures Observed

Framework Grains:

- Skeletal:
 - Sponge – Spicules Present
- Non-skeletal:
 - Peloids Present
- Detrital: NA

Comments: Partially-completely leached sponge dolomitized sponge spicules; indistinct neomorphosed micritic peloids are difficult to distinguish from matrix.

Diagenetic Characteristics

Cementation: Present anhydrite cementation of skel-moldic porosity

Recrystallization: Slight neomorphism of dolo-micrite matrix

Replacement: Dolomitization; present anhydrite and pyrite replacement

Dissolution: Partial-complete dissolution of sponge spicules; possible dissolution along microstylolite swarm

Stylolites: Swarm of discontinuous microstylolites

Fractures: NA

Other: NA

Porosity

Measured porosity (%) – NA

Measured permeability (mD) – NA

Ahr Genetic Pore Type: **Hybrid 1A – Enhanced**

- Depositional: NA
- Diagenetic:
 - Moldic
 - Intercrystalline

Comments: Porosity is dominated by skel-moldic porosity after partial-complete dissolution of sponge spicules with accessory solution enhanced intercrystalline porosity.

Remarks: Dolo-Mudstone with scattered skel-moldic porosity after partially-complete dissolution of sponge spicules.

P37-2 Thin Section Description

Sample: Pool 37-2_5286'

Cycle Position: Top

Depositional Characteristics

Lithofacies Type: Limey Anhydritic Peloidal Dolo-Packstone

Sedimentary Structure: Desiccation cracks in peloidal packstone with dolo-mud infill; micaceous shale laminations

Framework Grains:

- Skeletal: NA
- Non-skeletal:
 - Peloids Abundant
- Detrital: NA

Comments: Undifferentiated micritic peloidal grains; some may be pelletal or skeletal in origin.

Diagenetic Characteristics

Cementation: Present moldic and interparticle pore filling anhydrite cement; present interparticle and moldic pore filling rhombic dolomite cement.

Recrystallization: NA

Replacement: Partial dolomitization; present anhydrite replacement; present replacive pyrite & fluorite

Dissolution: Dissolution and possible compaction along microstylolites

Stylolites: Microstylolitization associated with shale and replacive pyrite

Fractures: Present partially-completely anhydrite cemented fractures; open fractures along shale laminae appear to be artifacts of sample prep

Other: NA

Porosity

Measured porosity (%) – NA

Measured permeability (mD) – NA

Ahr Genetic Pore Type: **Hybrid 1B – Reduced**

- Depositional:
 - Interparticle
- Diagenetic:
 - Intercrystalline
 - Vuggy

Comments: Porosity dominated by solution enhanced interparticle, vuggy porosity; insubstantial solution enhanced intercrystalline porosity; most interparticle and vuggy pores are so tight that there was no epoxy impregnation. Porosity greatly reduced by cementation and compaction along stylolites.

Remarks: Limey, Anhydritic, Peloidal, Dolo-Packstone that exhibits clear desiccation features and dolomite mud infilling cracks. Present but tight interparticle/vuggy porosity resisted epoxy impregnation.

Sample: Pool 37-2_5290'

Cycle Position: Bottom

Depositional Characteristics

Lithofacies Type: Dolo-Mudstone

Sedimentary Structure: Indistinct, wavy, discontinuous laminations

Framework Grains:

- Skeletal: NA
- Non-skeletal:
 - Peloids Present

- Detrital:
 - Siliciclastic Silt Present

Comments: Wavy nature of bedding may be the result of indistinct micritic grains aligned with depositional bedding

Diagenetic Characteristics

Cementation: Anhydrite cement/replacement; possibly after crystal moldic porosity from dissolution of rhombic dolomite or halite.

Recrystallization: NA

Replacement: Partial dolomitization; present anhydrite replacement

Dissolution: Possible dissolution along pyrite prone laminations

Stylolites: NA

Fractures: NA

Other: NA

Porosity

Measured porosity (%) – NA

Measured permeability (mD) – NA

Ahr Genetic Pore Type: **Hybrid 1A – Reduced**

- Depositional: NA
- Diagenetic:
 - Intercrystalline

Comments: Insubstantial solution enhanced intercrystalline porosity in neomorphosed micrite. < 1% visible porosity.

Remarks: Limey Dolo-Mudstone with discontinuous wavy laminations. Wavy nature may be the result of very indistinct micritic framework grains. < 1% visible porosity. Anhydrite cementation/replacement possibly after crystal molds.

Sample: Pool 37-2_5292'

Cycle Position: Top

Depositional Characteristics

Lithofacies Type: Anhydritic Peloidal Dolo-Wackestone

Sedimentary Structure: No Observed Structures

Framework Grains:

- Skeletal:
 - Algae – Green Present
 - Foraminifera Present
- Non-skeletal:
 - Peloids Common
- Detrital:
 - Siliciclastic Silt Present
 - Mica Present

Comments: Micritic peloidal and skeletal grains; partial dissolution of some framework grains.

Diagenetic Characteristics

Cementation: Fracture filling and interparticle/moldic pore filling anhydrite cement.

Recrystallization: NA

Replacement: Dolomitization; present anhydrite replacement of framework grains & matrix; present gypsum (?) replacement of anhydrite

Dissolution: Dissolution associated with microstylolites; partial dissolution of some framework grains

Stylolites: Microstylolitization

Fractures: Partially-completely cemented discontinuous fractures associated with microstylolites
Other: NA

Porosity

Measured porosity (%) – NA

Measured permeability (mD) – NA

Ahr Genetic Pore Type: **Hybrid 1A – Enhanced**

- Depositional:
 - Interparticle
 - Intraparticle
- Diagenetic:
 - Moldic
 - Intercrystalline

Comments: Pel-skel moldic porosity dominates with considerable solution enhanced intercrystalline porosity; insubstantial interparticle and intraparticle porosity.

Remarks: Anhydritic Dolo-Wackestone dominated by pel-skel moldic porosity. Present anhydrite replacement followed by replacive gypsum. Present detrital siliciclastic silt and mica.

Sample: Pool 37-2_5296'

Cycle Position: Bottom

Depositional Characteristics

Lithofacies Type: Anhydritic Peloidal Dolo-Wackestone

Sedimentary Structure: Possible collapse structure; common neomorphosed intraclasts

Framework Grains:

- Skeletal:
 - Foraminifera Present
 - Echinoderms Present
- Non-skeletal:
 - Peloids Common
- Detrital:
 - Siliciclastic Silt Present

Comments: Indistinct micritic framework grains in rock matrix; neomorphism of intraclasts precludes determination of their original depositional fabric

Diagenetic Characteristics

Cementation: Interparticle & isopachous dolomite cement; present interparticle/moldic pore filling anhydrite cement; majority of anhydrite appears replacive.

Recrystallization: Neomorphism of micrite; intraclasts are neomorphosed

Replacement: Present anhydrite replacement of framework grains and matrix

Dissolution: Solution enhanced porosity from neomorphism; dissolution of some framework grains; possible grain compaction

Stylolites: NA

Fractures: NA

Other: NA

Porosity

Measured porosity (%) – NA

Measured permeability (mD) – NA

Ahr Genetic Pore Type: **Hybrid 1B – Reduced**

- Depositional:
 - Interparticle
- Diagenetic:

- Moldic
- Intercrystalline

Comments: Pel-skel moldic porosity in intraclasts dominates with considerable interparticle porosity in wackestone; solution enhanced intercrystalline porosity from neomorphism. Compaction has reduced original porosity.

Remarks: Anhydritic Peloidal Dolo-Wackestone, possibly packstone. Intraclastic fabric possibly due to collapse feature. Porosity is dominated by interparticle & pel-moldic as well as solution enhanced intercrystalline porosity from neomorphism.

Sample: Pool 37-2_5298'

Cycle Position: Top

Depositional Characteristics

Lithofacies Type: Anhydritic Peloidal Dolo-Packstone

Sedimentary Structure: Possible burrow structures

Framework Grains:

- Skeletal:
 - Foraminifera Present
 - Algae – Phylloid Present
 - Algae – Red (?) Present
 - Unidentified Skeletal Fragments Present
- Non-skeletal:
 - Peloids Abundant
 - Coated Grains Common
- Detrital: NA

Comments: Undifferentiated peloidal grains may be microbial or pelletal in origin; present phylloid algae; common anhydrite replacement of grains

Diagenetic Characteristics

Cementation: Relict interparticle dolomite cement; common replacive interparticle anhydrite cement

Recrystallization: NA

Replacement: Common anhydrite replacement of framework grains and matrix; present pyrite and gypsum replacement

Dissolution: Possible grain dissolution and compaction

Stylolites: Discontinuous seams of dissolution

Fractures: Partially anhydrite cemented fractures

Other: NA

Porosity

Measured porosity (%) – 3.4

Measured permeability (mD) – .082

Ahr Genetic Pore Type: Hybrid 1A – Reduced

- Depositional:
 - Interparticle
 - Intraparticle
- Diagenetic:
 - Moldic
 - Intercrystalline

Comments: Relict interparticle porosity dominates with considerable solution enhanced moldic and intercrystalline porosity.

Remarks: Anhydritic Peloidal Dolo-Packstone with possible burrow structure and common anhydrite replacement of framework grains and matrix.

Sample: Pool 37-2_5299.9'

Cycle Position: Top

Depositional Characteristics

Lithofacies Type: Anhydritic Dolo-Mudstone

Sedimentary Structure: Interlaminated dolo-mudstone & peloidal wackestone

Framework Grains:

- Skeletal:
 - Sponge – spicules Present
- Non-skeletal:
 - Peloids Present
- Detrital:
 - Siliciclastic Silt Present

Comments: indistinct micritic peloidal grains & dolomite replaced sponge spicules; thickness of the thin section makes grain determination difficult.

Diagenetic Characteristics

Cementation: Present interparticle/moldic pore filling anhydrite and rhombic dolomite cement

Recrystallization: NA

Replacement: Dolomitization of matrix & framework grains; common blocky anhydrite replacement; present replacive pyrite

Dissolution: Possible grain dissolution & compaction in wackestone laminations

Stylolites: NA

Fractures: NA

Other: Residual hydrocarbon

Porosity

Measured porosity (%) – 9.8

Measured permeability (mD) – .1

Ahr Genetic Pore Type: **Hybrid 1A – Enhanced**

- Depositional: NA
- Diagenetic:
 - Moldic
 - Intercrystalline

Comments: Little visible porosity; skel-moldic & solution enhanced intercrystalline porosity dominate.

Remarks: Interlaminated Anhydritic Dolo-Mudstone - Wackestone with common anhydrite replacement. Indistinct micritic framework grains have possibly undergone compaction. Very little visible porosity; skel-moldic & solution enhanced intercrystalline porosity dominate.

Sample: Pool 37-2_5300.25'

Cycle Position: Middle – Top

Depositional Characteristics

Lithofacies Type: Peloidal -Spiculiferous Dolo-Wackestone

Sedimentary Structure: No Observed Structures

Framework Grains:

- Skeletal:
 - Sponge – spicules Present
- Non-skeletal:

- Peloids Present
- Pellets Present
- Detrital:
 - Siliciclastic Silt Present

Comments: Neomorphosed dolomitized spicules and micritic peloids, possibly fecal pellets; gray concentration of sponge spicules represent sponge bodies.

Diagenetic Characteristics

Cementation: Present interparticle and moldic pore filling anhydrite and rhombic dolomite cement

Recrystallization: NA

Replacement: Dolomitization; present anhydrite replacement; present pyrite replacement

Dissolution: Possible grain dissolution/compaction

Stylolites: NA

Fractures: NA

Other: NA

Porosity

Measured porosity (%) – 15.9

Measured permeability (mD) – 1.87

Ahr Genetic Pore Type: **Hybrid 1A – Enhanced**

- Depositional:
 - Interparticle
- Diagenetic:
 - Moldic
 - Intercrystalline

Comments: Moldic porosity after sponge spicules dominates with solution enhanced intercrystalline and accessory interparticle porosity.

Remarks: Dolo-Wackestone with present peloidal & skeletal grains. Interparticle porosity dominates as well as solution enhanced moldic and intercrystalline.

Sample: Pool 37-2_5302.3'

Cycle Position: Middle - Top

Depositional Characteristics

Lithofacies Type: Anhydritic Dolo-Mudstone

Sedimentary Structure: No Observed Structures

Framework Grains:

- Skeletal:
 - Sponge – spicules Present
- Non-skeletal:
 - Peloids Present

Comments: Argillaceous peloidal grains; some are possibly the result of grain dissolution/compaction, not depositional grain fabric; possible micritized foraminifera; single observed siliceous sponge spicule.

Diagenetic Characteristics

Cementation: Present interparticle/moldic pore filling anhydrite and dolomite cement; majority of anhydrite appears to be replacive.

Recrystallization: NA

Replacement: Dolomitization; common anhydrite replacement of framework grains & matrix; present pyritization

Dissolution: Possible grain dissolution/compaction

Stylolites: NA

Fractures: NA

Other: NA

Porosity

Measured porosity (%) – 10.8

Measured permeability (mD) – .563

Ahr Genetic Pore Type: **Hybrid 1A – Enhanced**

- Depositional:
 - Interparticle
- Diagenetic:
 - Intercrystalline
 - Moldic

Comments: Solution enhanced moldic and intercrystalline porosity dominates.

Remarks: Anhydritic Dolo-Mudstone with unusual argillaceous grains(?) and solution enhanced intercrystalline porosity. "Grains" probably composed organics and/or clay minerals. Common anhydrite replacement.

Sample: Pool 37-2_5305

Cycle Position: Middle

Depositional Characteristics

Lithofacies Type: Spiculiferous Dolo-Wackestone

Sedimentary Structure: No Observed Structures

Framework Grains:

- Skeletal:
 - Sponge – spicules Present
 - Ostracods Present
- Non-skeletal:
 - Peloids Present
- Detrital:
 - Siliciclastic Silt Present

Comments: Partial to complete dolomitization and subsequent dissolution of sponge spicules; possible ostracod fragments and indistinct neomorphosed peloids.

Diagenetic Characteristics

Cementation: Present moldic pore filling anhydrite and dolomite cement.

Recrystallization: NA

Replacement: Dolomitization of framework grains and matrix; present anhydrite replacement; pyritization

Dissolution: Possible dissolution along pyritic microstylolites

Stylolites: Microstylolitization

Fractures: NA

Other: NA

Porosity

Measured porosity (%) – 14.7

Measured permeability (mD) – .399

Ahr Genetic Pore Type: **Hybrid 1A – Enhanced**

- Depositional: NA
- Diagenetic:
 - Skel - Moldic
 - Intercrystalline

Comments: Diagenetic skel-moldic porosity after sponge spicule dissolution dominates with accessory solution enhanced intercrystalline and borderline vuggy porosity.

Remarks: Spiculiferous Dolo-Wackestone exhibiting primarily diagenetic skel-moldic porosity. Sample exhibits partial-complete dolomitization of siliceous sponge spicules and subsequent dissolution of grains.

Sample: Pool 37-2_5306.7'

Cycle Position: Middle

Depositional Characteristics

Lithofacies Type: Anhydritic Spiculiferous Dolo-Wackestone

Sedimentary Structure: No Observed Structures

Framework Grains:

- Skeletal:
 - Sponge – spicules Present
 - Ostracods Present
- Non-skeletal:
 - Peloids Present
- Detrital:
 - Siliciclastic Silt Present

Comments: Peloidal grains are indistinct due to dolomitization & neomorphism; possible ostracod, gastropod, & algae fragments; well sorted.

Diagenetic Characteristics

Cementation: Common interparticle and moldic pore filling anhydrite cement; present finely crystalline pore filling dolomite cementation.

Recrystallization: Neomorphism of matrix & framework grains

Replacement: Dolomitization; anhydrite replacement of dolomite; present pyrite replacement

Dissolution: Dissolution of framework grains yielding moldic pores

Stylolites: NA

Fractures: NA

Other: Residual hydrocarbon

Porosity

Measured porosity (%) – 13.3

Measured permeability (mD) – 3.66

Ahr Genetic Pore Type: **Hybrid 1A – Enhanced**

- Depositional:
 - Interparticle
- Diagenetic:
 - Moldic
 - Intercrystalline

Comments: Porosity is dominated by skel-pel moldic and relict depositional interparticle porosity; sample also exhibits accessory solution enhanced intercrystalline porosity from neomorphism and solution enhancement.

Remarks: Anhydritic Spiculiferous Dolo-Wackestone exhibiting extensive neomorphism which makes framework grains indistinct. Depositional interparticle porosity dominates with present moldic porosity.

Sample: Pool 37-2_5310'

Cycle Position: Middle

Depositional Characteristics

Lithofacies Type: Anhydritic Skeletal Dolo-Wackestone

Sedimentary Structure: Wackestone and mudstone lithofacies contact at base of sample

Framework Grains:

- Skeletal:
 - Algae – Green Present
 - Echinoderms Present
 - Ostracods Present
 - Undifferentiated Bivalves Present
 - Gastropods Present
 - Sponge – Spicules Present
- Non-skeletal:
 - Peloids Present
- Detrital: NA

Comments: Skeletal fragments exhibiting partial-complete dissolution and anhydrite cementation dominate; present micritic peloids, possibly pellets, are also found. Present siliciclastic silt found in mudstone.

Diagenetic Characteristics

Cementation: Common moldic pore filling anhydrite cement with present chalcedony/dolomite filling pores

Recrystallization: Slight neomorphism of dolo-micrite matrix

Replacement: Present anhydrite replacing framework grains and dolo-matrix

Dissolution: Partial-complete dissolution of framework grains and solution enhancement of intercrystalline porosity

Stylolites: NA

Fractures: NA

Other: Residual hydrocarbon in large pores

Porosity

Measured porosity (%) – 11.9

Measured permeability (mD) – .360

Ahr Genetic Pore Type: **Hybrid 1A – Enhanced**

- Depositional:
 - Interparticle
- Diagenetic:
 - Moldic
 - Intercrystalline

Comments: Porosity is dominated by moldic pores after partial-complete dissolution of skeletal framework grains and exhibits considerable solution enhanced intercrystalline pores; present interparticle porosity is also found. Anhydrite cementation reduces moldic porosity.

Remarks: Anhydritic Skeletal Dolo-Wackestone exhibiting a mudstone lithofacies at the base of the sample. Porosity is dominated by moldic pores after partial-complete dissolution of skeletal framework grains.

Sample: Pool 37-2_5311.5'

Cycle Position: Middle

Depositional Characteristics

Lithofacies Type: Dolo-Mudstone

Sedimentary Structure: Possible argillaceous lamination

Framework Grains:

- Skeletal: NA
- Non-skeletal: NA
- Detrital:

- Siliciclastic Silt Present

Comments: Possible, indistinct neomorphosed framework grains.

Diagenetic Characteristics

Cementation: Present intercrystalline pore filling anhydrite & rhombic dolomite cement.

Recrystallization: Neomorphism of micrite

Replacement: Dolomitization; present anhydrite replacement; pyritization

Dissolution: Possible dissolution along discontinuous pyritic seams

Stylolites: NA

Fractures: Open fractures are artifacts of sample preparation

Other: Residual hydrocarbon

Porosity

Measured porosity (%) – 2.9

Measured permeability (mD) – .583

Ahr Genetic Pore Type: **Hybrid 1A – Reduced**

- Depositional: NA
- Diagenetic:
 - Intercrystalline

Comments: Minimal solution enhanced intercrystalline porosity in micritic matrix; porosity has been greatly reduced by neomorphism.

Remarks: Sample failed during HPMI test. Porosity and permeability values are taken from core measurements.

Sample: Pool 37-2_ 5315.25'

Cycle Position: Middle - Bottom

Depositional Characteristics

Lithofacies Type: Dolo-Mudstone

Sedimentary Structure: No Observed Structures

Framework Grains:

- Skeletal:
 - Sponge – spicules Present
 - Ostracods Present
- Non-skeletal: NA
- Detrital: NA
- Comments: Skeletal grains have been partially - completely leached; well sorted.

Diagenetic Characteristics

Cementation: Present moldic pore filling anhydrite cement; possible dolomite cement.

Recrystallization: Neomorphism of micrite

Replacement: Dolomitization; present anhydrite replacement; present pyrite replacement

Dissolution: Partial - complete dissolution of sponge spicules

Stylolites: NA

Fractures: NA

Other: NA

Porosity

Measured porosity (%) – 13.6

Measured permeability (mD) – 0.565

Ahr Genetic Pore Type: **Hybrid 1A – Enhanced**

- Depositional: NA
- Diagenetic:

- Moldic
- Intercrystalline

Comments: Porosity dominated by skel-moldic porosity with accessory solution enhanced intercrystalline porosity.

Remarks: Spiculiferous Dolo-Mudstone exhibiting skel-moldic porosity and present anhydrite/pyrite replacement.

Sample: Pool 37-2_5320.2'

Cycle Position: Bottom

Depositional Characteristics

Lithofacies Type: Anhydritic Spiculiferous Dolo-Wackestone

Sedimentary Structure: Burrow structure

Framework Grains:

- Skeletal:
 - Sponge – Spicules Common
 - Algae – Green Present
 - Gastropods Present
- Non-skeletal:
 - Peloids Present
- Detrital: NA

Comments: Grains have undergone dolomitization, partial - complete dissolution, and subsequent cementation/replacement by anhydrite.

Diagenetic Characteristics

Cementation: Common moldic pore filling anhydrite; present dolomite cement

Recrystallization: Neomorphism of micrite

Replacement: Dolomitization; common anhydrite replacement of framework grains and matrix; present pyrite replacement

Dissolution: Partial - complete dissolution of framework grains

Stylolites: NA

Fractures: NA

Other: Present organic material

Porosity

Measured porosity (%) – 9.9

Measured permeability (mD) – 1.0

Ahr Genetic Pore Type: Hybrid 1B – Reduced

Depositional:

- Interparticle
- Diagenetic:
 - Moldic
 - Intercrystalline

Comments: Porosity is dominated by skel-moldic porosity with considerable interparticle porosity and accessory solution enhanced intercrystalline porosity.

Remarks: Burrowed Anhydritic, Spiculiferous Dolo-Wackestone exhibiting skel-moldic porosity.

Sample: Pool 37-2_5320

Cycle Position: Bottom

Depositional Characteristics

Lithofacies Type: Anhydritic Peloidal Dolo-Wackestone

Sedimentary Structure: Facies contact at stylolite

Framework Grains:

- Skeletal:
 - Sponge – Spicules Present
- Non-skeletal:
 - Peloids Present
- Detrital: NA

Comments: Indistinct micritic peloids and clastic grains.

Diagenetic Characteristics

Cementation: Present interparticle pore filling rhombic dolomite and replace moldic/fracture filling anhydrite cement

Recrystallization: Neomorphism of wackestone above stylolite

Replacement: Common anhydrite replacement; common chalcedony replacement of anhydrite above stylolite

Dissolution: Dissolution and compaction of grains

Stylolites: Prominent stylolite containing unidentified isotropic material, possibly organic; associated microstylolites

Fractures: Present discontinuous anhydrite cemented fractures below stylolite

Other: NA

Porosity

Measured porosity (%) – 8.8

Measured permeability (mD) – .551

Ahr Genetic Pore Type: **Hybrid 1B – Reduced**

- Depositional:
 - Interparticle
- Diagenetic:
 - Moldic
 - Intercrystalline

Comments: Solution enhanced skel-pel moldic and intercrystalline porosity dominates; considerable porosity reduction from cementation and compaction.

Remarks: Highly diagenetic Anhydritic Peloidal Dolo-Wackestone exhibiting common anhydrite/chalcedony replacement and stylolitization. Wackestone above stylolite is neomorphosed and contains common chalcedony replacement of anhydrite and wackestone below stylolite appears micritized and contains common anhydrite replacement and fracturing but little-no chalcedony. Unusual, possibly organic, isotropic material is found contained in the stylolite.

B48-4 Thin Section Description

Sample: Beasley 48-4_5360'

Cycle Position: Middle (?)

Depositional Characteristics

Lithofacies Type: Spiculiferous Dolo-Wackestone

Sedimentary Structure: Contains mudstone laminations above stylolite and peloidal packstone laminations below stylolite

Framework Grains:

- Skeletal:
 - Sponge – Spicules Common
- Non-skeletal:
 - Peloids Present
- Detrital:
 - Siliciclastic Silt Present

Comments: Common spicule molds throughout sample; undifferentiated peloids are concentrated into packstone laminations and may be microbial in origin.

Diagenetic Characteristics

Cementation: Present moldic and interparticle pore filling anhydrite cement

Recrystallization: Neomorphism of micrite

Replacement: Dolomitization; present anhydrite replacement after cementation

Dissolution: Complete dissolution of siliceous spicules; dissolution/compaction of grains associated with stylolite

Stylolites: Present stylolites and discontinuous solution seams cutting sample

Fractures: Discontinuous open fractures are artifacts of sample preparation

Other: NA

Porosity

Measured porosity (%) – 15.2

Measured permeability (mD) – .847

Ahr Genetic Pore Type: **Hybrid 1B – Enhanced**

- Depositional:
 - Interparticle
- Diagenetic:
 - Moldic
 - Intercrystalline

Comments: Porosity is dominated by skel-moldic porosity after spicule dissolution; accessory interparticle porosity found in packstone laminations and solution enhanced intercrystalline porosity.

Remarks: Spiculiferous Dolo-Wackestone exhibiting mudstone laminations above stylolite and peloidal packstone laminations below stylolite. Grain dissolution and possible compaction along stylolite. Skel-moldic porosity after spicule dissolution dominates.

Sample: Beasley 48-4_5363'

Cycle Position: Middle (?)

Depositional Characteristics

Lithofacies Type: Spiculiferous Dolo-Wackestone

Sedimentary Structure: Discontinuous, irregular, spiculiferous peloidal wackestone laminations

Framework Grains:

- Skeletal:
 - Sponge – Spicules Common

- Non-skeletal:
 - Peloids Present
 - Pellets Present
- Detrital:
 - Siliciclastic Silt Present

Comments: Common spicule molds throughout sample; undifferentiated micritic peloids and pellets.

Diagenetic Characteristics

Cementation: Present moldic pore filling anhydrite cement

Recrystallization: Neomorphism of micrite

Replacement: Dolomitization; present anhydrite replacement of grains and matrix; present chalcedony after anhydrite

Dissolution: Complete dissolution of siliceous spicules

Stylolites: NA

Fractures: NA

Other: NA

Porosity

Measured porosity (%) – 16.8

Measured permeability (mD) – 2.219

Ahr Genetic Pore Type: **Hybrid 1B – Enhanced**

- Depositional:
 - Interparticle
- Diagenetic:
 - Moldic
 - Intercrystalline

Comments: Porosity is dominated by skel-moldic porosity after spicule dissolution and solution enhanced intercrystalline porosity; accessory interparticle porosity.

Remarks: Spiculiferous Dolo-Wackestone exhibiting discontinuous, irregular, spiculiferous peloidal wackestone laminations. Skel-moldic porosity after spicule dissolution dominates.

Sample: Beasley 48-4_5366'

Cycle Position: Middle (?)

Depositional Characteristics

Lithofacies Type: Spiculiferous Dolo-Wackestone

Sedimentary Structure: No Structure Observed

Framework Grains:

- Skeletal:
 - Sponge – Spicules Common
- Non-skeletal:
 - Peloids Present
- Detrital:
 - Siliciclastic Silt Present

Comments: Common spicule molds throughout sample; undifferentiated micritic peloids.

Diagenetic Characteristics

Cementation: Present moldic pore filling anhydrite cement

Recrystallization: Neomorphism of micrite

Replacement: Present anhydrite replacement of grains and matrix

Dissolution: Complete dissolution of siliceous spicules

Stylolites: Discontinuous stylolite at top of sample

Fractures: NA

Other: Present organic material

Porosity

Measured porosity (%) – 16.1

Measured permeability (mD) – 1.228

Ahr Genetic Pore Type: **Hybrid 1B – Enhanced**

- Depositional:
 - Interparticle
- Diagenetic:
 - Moldic
 - Intercrystalline

Comments: Porosity is dominated by skel-moldic porosity after spicule dissolution and solution enhanced intercrystalline porosity; accessory interparticle porosity.

Remarks: Spiculiferous Dolo-Wackestone dominated by skel-moldic porosity after spicule dissolution.

Sample: Beasley 48-4_5373'

Cycle Position: Middle (?)

Depositional Characteristics

Lithofacies Type: Spiculiferous Dolo-Wackestone

Sedimentary Structure: Bladed anhydrite nodule is possibly after a burrow structure.

Framework Grains:

- Skeletal:
 - Sponge – Spicules Common
- Non-skeletal:
 - Peloids Present
- Detrital:
 - Siliciclastic Silt Present

Comments: spicule molds throughout sample; undifferentiated micritic peloids, possibly pelletal.

Diagenetic Characteristics

Cementation: Present skel-moldic pore filling anhydrite and chalcedony cement

Recrystallization: Neomorphism of micrite

Replacement: Dolomitization; present anhydrite replacement of grains and matrix; present siliceous, chalcedony replacement of anhydrite and dolomite matrix; pyritization

Dissolution: Complete dissolution of siliceous spicules; areas of possible compaction

Stylolites: NA

Fractures: NA

Other: Present organic material and residual hydrocarbon in pores

Porosity

Measured porosity (%) – 14.5

Measured permeability (mD) – 11.908

Ahr Genetic Pore Type: **Hybrid 1B – Enhanced**

- Depositional:
 - Interparticle
- Diagenetic:
 - Moldic
 - Intercrystalline

Comments: Porosity is dominated by skel-moldic porosity after spicule dissolution and solution enhanced intercrystalline porosity; accessory interparticle porosity.

Remarks: Spiculiferous Dolo-Wackestone dominated by skel-moldic porosity after spicule dissolution. Present siliceous chalcedony cementation and replacement with present organic material/residual hydrocarbon.

Sample: Beasley 48-4_5377'

Cycle Position: Middle - Bottom

Depositional Characteristics

Lithofacies Type: Skeletal Wackestone

Sedimentary Structure: No Observed Structures

Framework Grains:

- Skeletal:
 - Sponge – Spicules Present
 - Algae – Green Present
 - Bivalve – Unidentified Present
 - Foraminifera Present
 - Gastropod Present
- Non-skeletal:
 - Peloids Present
- Detrital: NA

Comments: Present spicule molds throughout sample with indistinct micritic algal and bivalve grains; bivalves are possible pelecypods. Very indistinct peloidal grains.

Diagenetic Characteristics

Cementation: Present anhydrite and dolomite filling skel-moldic pores; present chalcedony cement

Recrystallization: Neomorphism of matrix and framework grains

Replacement: Dolomitization; present anhydrite after dolomite and gypsum; present chalcedony after anhydrite

Dissolution: Dissolution of skeletal framework grains; compaction/dissolution along stylolites

Stylolites: Continuous stylolite and multiple discontinuous microstylolites cutting sample

Fractures: Discontinuous open and partially anhydrite cemented fractures originating from stylolite

Other: Residual hydrocarbon and present organic material; unidentified isotropic material, same material found in P37-2 5320'.

Porosity

Measured porosity (%) – .073

Measured permeability (mD) – 8.6

Ahr Genetic Pore Type: Hybrid 1A - Enhanced

- Depositional:
 - Intraparticle
- Diagenetic:
 - Moldic
 - Intercrystalline

Comments: Dominated by skel-moldic porosity with accessory solution enhanced intercrystalline and intraparticle porosity; possible porosity reduction by compaction associated with stylolites.

Remarks: Grain rich Skeletal Wackestone with indistinct micritic skeletal grains and skel-molds. Sample exhibits dissolution of skeletal grains and possible compaction/dissolution along stylolites. Fracturing is found associated with stylolitization.

Sample: Beasley 48-4_5381'

Cycle Position: Bottom

Depositional Characteristics

Lithofacies Type: Spiculiferous Dolo-Wackestone

Sedimentary Structure: Churned, bioturbated fabric

Framework Grains:

- Skeletal:
 - Sponge – Spicules Present
 - Algae – Green Present
- Non-skeletal:
 - Peloids Present
- Detrital:
 - Siliciclastic Silt Present

Comments: Partially-completely leached spicules with present siliceous spicules; indistinct micritic peloidal grains and limey intraclastic grains.

Diagenetic Characteristics

Cementation: Present anhydrite and dolomite filling skel-moldic pores; present chalcedony cement

Recrystallization: Neomorphism of matrix and framework grains

Replacement: Dolomitization; present anhydrite replacement

Dissolution: Dissolution of skeletal framework grains

Stylolites: NA

Fractures: NA

Other: Residual hydrocarbon and present organic material; unidentified isotropic material, same material found in P37-2 5320'.

Porosity

Measured porosity (%) – 16.0

Measured permeability (mD) – 1.199

Ahr Genetic Pore Type: **Hybrid 1A – Enhanced**

- Depositional: NA
- Diagenetic:
 - Moldic
 - Intercrystalline

Comments: Porosity is dominated by skel-moldic porosity after spicule dissolution and solution enhanced intercrystalline porosity

Remarks: Bioturbated Spiculiferous Dolo-Wackestone dominated by skel-moldic porosity after spicule dissolution. Present siliceous chalcedony cementation and replacement with present organic material/residual hydrocarbon. Sample contains unidentified isotropic material, same material found in P37-2 5320' and previous B48-4 sample.

Sample: Beasley 48-4_5382'

Cycle Position: Bottom

Depositional Characteristics

Lithofacies Type: Dolo-Mudstone

Sedimentary Structure: No Structures Observed

Framework Grains:

- Skeletal:
 - Foraminifera Present
 - Sponge – Spicules Present
 - Algae – Green Present
- Non-skeletal:
 - Peloids Present

- Detrital: NA

Comments: Indistinct micritic framework grains, some are partially – completely leached.

Diagenetic Characteristics

Cementation: Present indistinct dolomite cementation and moldic pore filling anhydrite cement

Recrystallization: NA

Replacement: Dolomitization; present anhydrite replacement; present chalcedony and fluorite replacement

Dissolution: Partial to complete grain dissolution; possible dissolution associated with pyrite

Stylolites: NA

Fractures: NA

Other: NA

Porosity

Measured porosity (%) – 11.6

Measured permeability (mD) – .146

Ahr Genetic Pore Type: **Hybrid 1A – Enhanced**

- Depositional:
 - Interparticle
 - Intraparticle
- Diagenetic:
 - Moldic
 - Intercrystalline

Comments: Porosity dominated by skel/pel moldic with considerable solution enhanced intercrystalline porosity; accessory interparticle and skeletal intraparticle porosity.

Remarks: Dolo-Mudstone with indistinct micritic framework grains; present anhydrite replacement with present chalcedony and fluorite cement/replacement. Skel-pel moldic porosity dominates with considerable solution enhanced intercrystalline porosity.

Sample: B48-4_5386'

Cycle Position: Top

Depositional Characteristics

Lithofacies Type: Peloidal Dolo-Wackestone

Sedimentary Structure: No Structures Observed

Framework Grains:

- Skeletal:

○ Algae – Phylloid (?)	Present
○ Foraminifera	Present
○ Gastropod	Present
○ Sponge – Spicules	Present
- Non-skeletal:

○ Peloids	Present
-----------	---------
- Detrital: NA

Comments: Undifferentiated micritic peloidal grains; indistinct micritic skeletal grains.

Diagenetic Characteristics

Cementation: Present relict isopachous dolomite cement; present anhydrite cement

Recrystallization: Neomorphism of micrite

Replacement: Dolomitization; present anhydrite replacement of grains and matrix

Dissolution: Partial-complete grain dissolution; likely grain dissolution and compaction along discontinuous solution seams

Stylolites: Discontinuous solution seams/horsetails

Fractures: NA

Other: Possible organic material

Porosity

Measured porosity (%) – 14.0

Measured permeability (mD) – 1.099

Ahr Genetic Pore Type: **Hybrid 1A – Enhanced**

- Depositional:
 - Interparticle
- Diagenetic:
 - Moldic
 - Intercrystalline

Comments: Porosity dominated by pel/skel moldic and interparticle porosity with considerable solution enhanced intercrystalline porosity. Porosity enhancement by dissolution and reduction by compaction.

Remarks: Dolo-Mudstone with micritic peloidal grains and present skeletal grains. Partial-complete grain dissolution with likely grain dissolution and compaction along discontinuous solution seams. Porosity dominated by pel/skel moldic and interparticle porosity with considerable solution enhanced intercrystalline porosity.

Sample: B48-4_5390'

Cycle Position: Top

Depositional Characteristics

Lithofacies Type: Anhydritic Dolo-Wackestone

Sedimentary Structure: No Structures Observed

Framework Grains:

- Skeletal:
 - Sponge – Spicules Present
 - Foraminifera Present
- Non-skeletal:
 - Peloids Common
- Detrital: NA

Comments: Indistinct micritic peloidal and skeletal grains; grain boundaries illustrated by anhydrite replacement and grain dissolution.

Diagenetic Characteristics

Cementation: Common replaceive, moldic pore filling anhydrite cementation

Recrystallization: Micritization of framework grains

Replacement: Common anhydrite replacement; present chalcedony replacement

Dissolution: Partial-complete dissolution of framework grains

Stylolites: Small continuous stylolite at bottom of sample

Fractures: NA

Other: NA

Porosity

Measured porosity (%) – 8.5

Measured permeability (mD) – .395

Ahr Genetic Pore Type: **Hybrid 1A – Enhanced**

- Depositional:
 - Interparticle
- Diagenetic:
 - Moldic
 - Intercrystalline

Comments: Porosity dominated by pel/skel moldic with considerable solution enhanced intercrystalline porosity; accessory interparticle porosity. Porosity enhancement by grain dissolution but reduced by anhydrite cementation.

Remarks: Grain rich Anhydritic Pel-Skel Dolo-Wackestone exhibiting partial-complete dissolution of indistinct framework grains and common subsequent cementation/replacement by anhydrite. Possibly originally a packstone.

Sample: B48-4_5391'

Cycle Position: Middle (?)

Depositional Characteristics

Lithofacies Type: Anhydritic Peloidal Dolo-Wackestone

Sedimentary Structure: No Structures Observed

Framework Grains:

- Skeletal:
 - Sponge – Spicules Present
- Non-skeletal:
 - Peloids Present
- Detrital: NA

Comments: Micritic peloidal grains with present partially-completely leached spicules.

Diagenetic Characteristics

Cementation: Present replacive, moldic pore filling anhydrite cement

Recrystallization: NA

Replacement: Dolomitization; common anhydrite replacement of grains and matrix

Dissolution: Partial-complete dissolution of framework grains; possible compaction along solution seams

Stylolites: Discontinuous wavy solution seams

Fractures: NA

Other: NA

Porosity

Measured porosity (%) – 10.8

Measured permeability (mD) – 1.574

Ahr Genetic Pore Type: **Hybrid 1A – Enhanced**

- Depositional:
 - Interparticle
- Diagenetic:
 - Moldic
 - Intercrystalline

Comments: Porosity dominated by pel/skel moldic with considerable solution enhanced intercrystalline porosity; accessory interparticle porosity. Porosity enhancement by grain dissolution but reduced by anhydrite cementation.

Remarks: Anhydritic Peloidal Dolo-Wackestone exhibiting partial-complete dissolution of framework grains and common subsequent cementation/replacement by anhydrite.

APPENDIX D
THIN SECTION PHOTOMICROGRAPHS

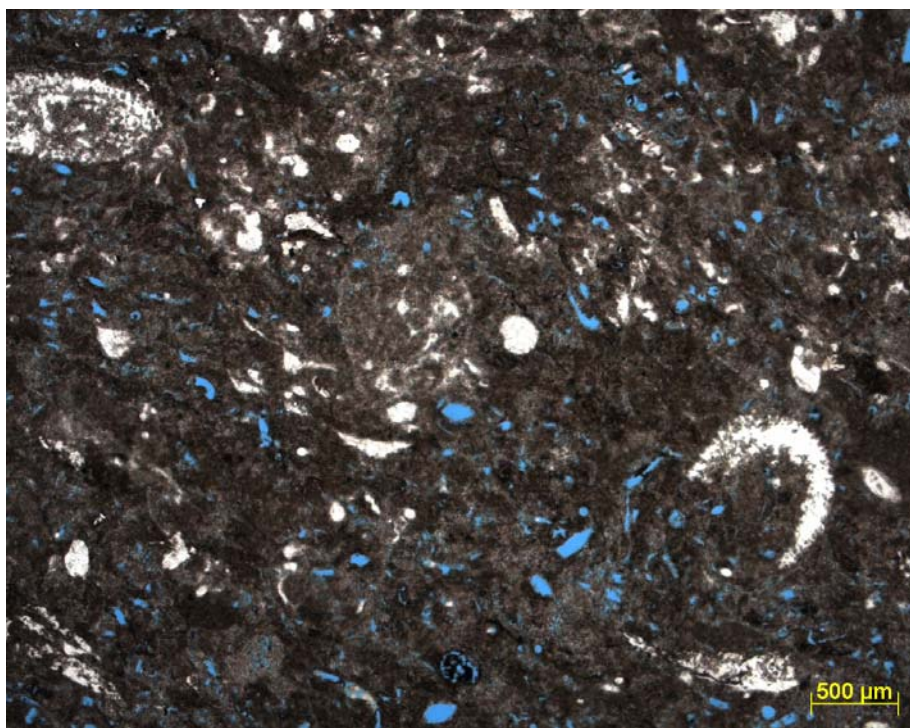


Figure D.1: Skeletal – Example of skeletal-peloidal wackestone facies exhibiting H1-Ae porosity. Sample M13, 5354'.



Figure D.2: Spiculiferous wackestone sub-facies exhibiting H1-Be porosity. Sample B48-8, 5373'.



Figure D.3: Mudstone facies with shaley stringers; exhibits H1-Ae porosity. Sample M11, 5319'.

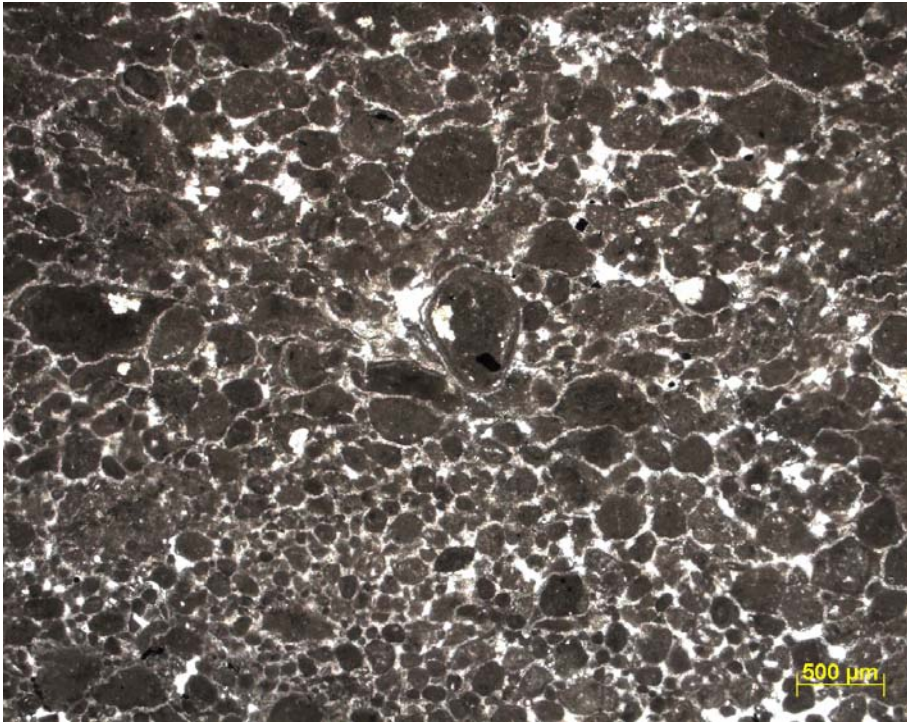


Figure D.4: Peloidal-oncoidal grainstone (P/G facies); exhibits HI-Br porosity from mechanical grain compaction. Sample M2, 5293.6'.

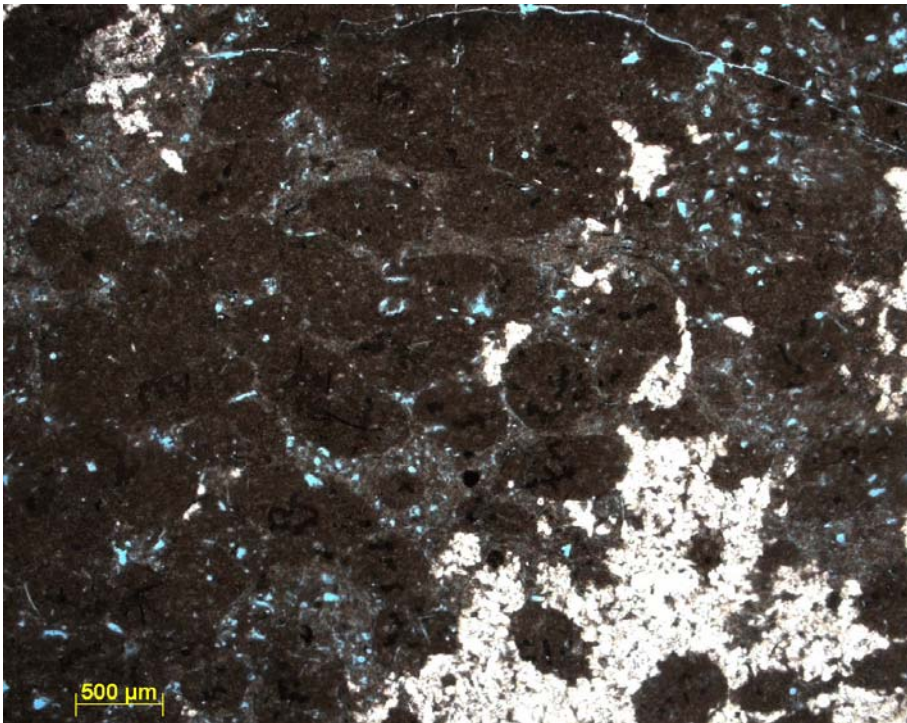


Figure D.5: Pelletal-peloidal packstone (P/G facies) associated with intertidal environment; HI-Br porosity after compaction and replacement. Sample M6, 5277'.

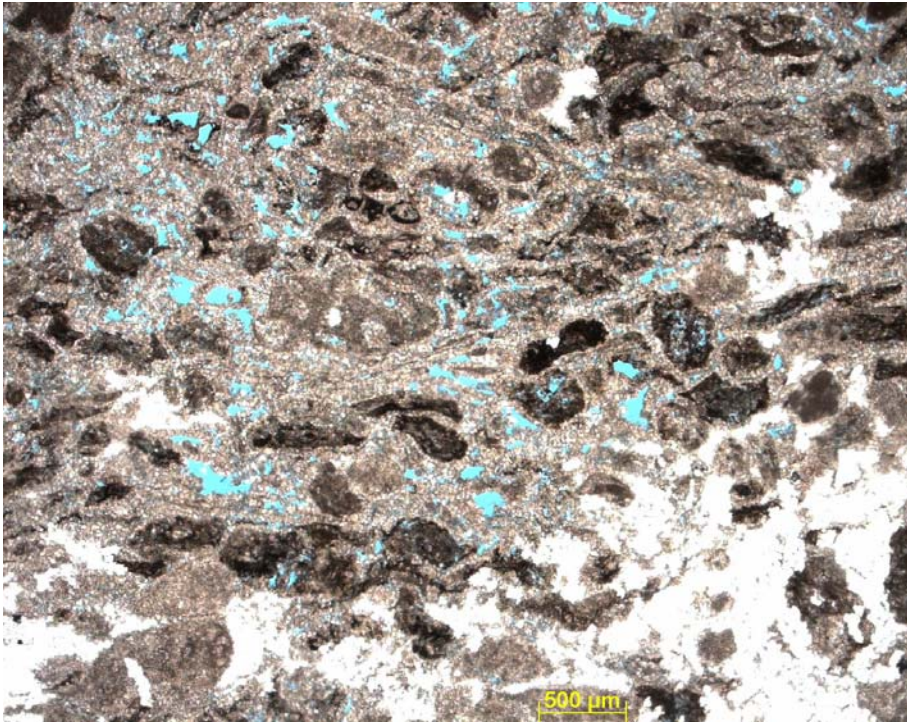


Figure D.6: Algal-peloidal packstone (P/G facies). Despite anhydrite, sample exhibits HI-Be porosity after extensive dolomitization and dissolution. Sample M3, 5307'.

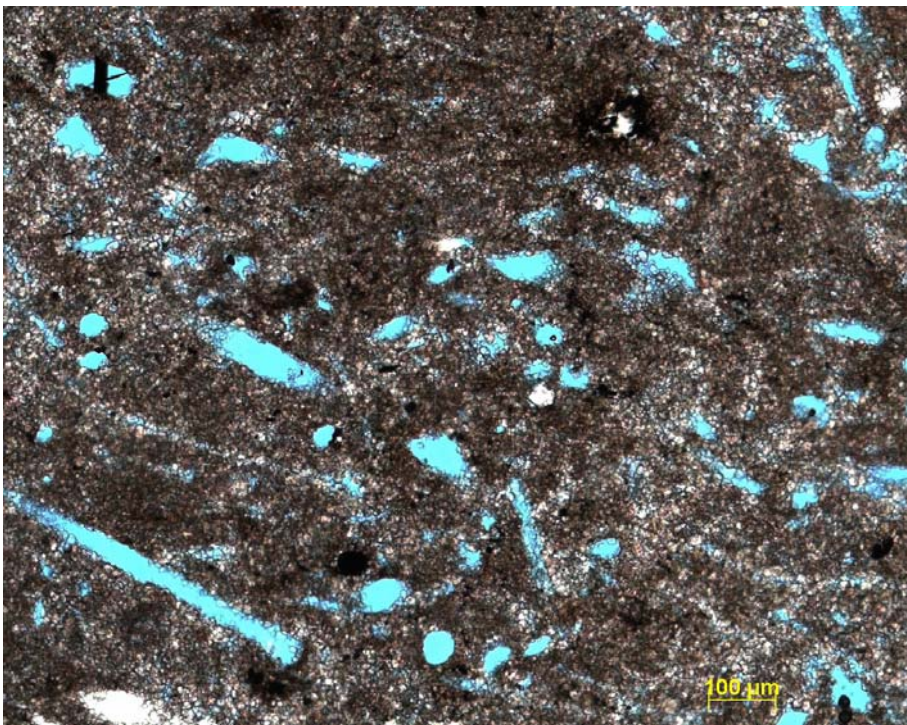


Figure D.7: Spiculiferous wackestone sub-facies exhibiting HI-Ae, skel-moldic porosity. Sample B48-4, 5381'.

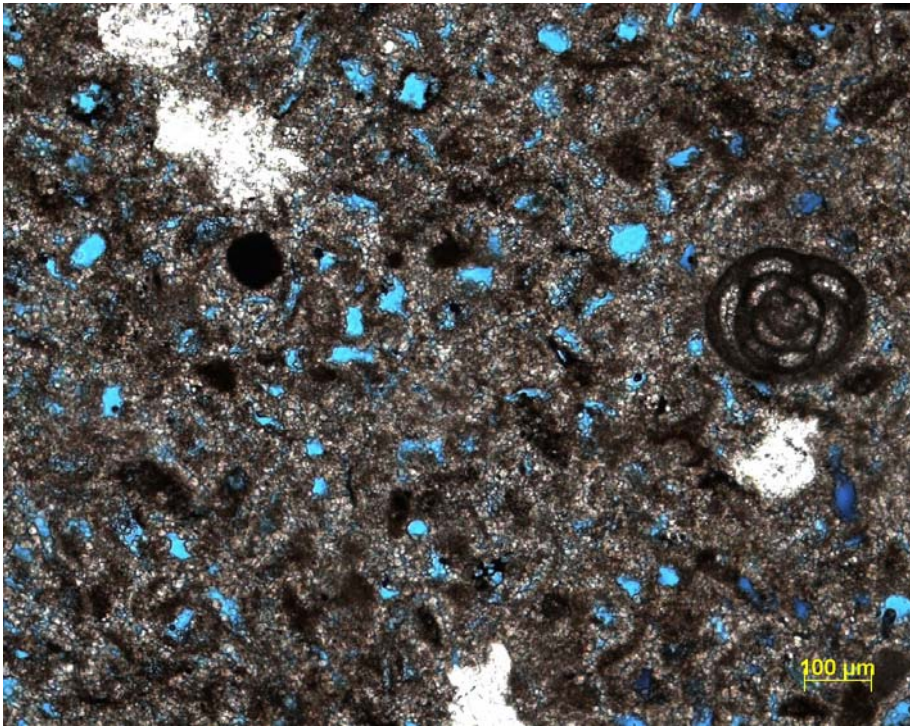


Figure D.8: Peloidal-skeletal wackestone (W facies) illustrating HI-Ae porosity. Sample M13, 5305'.

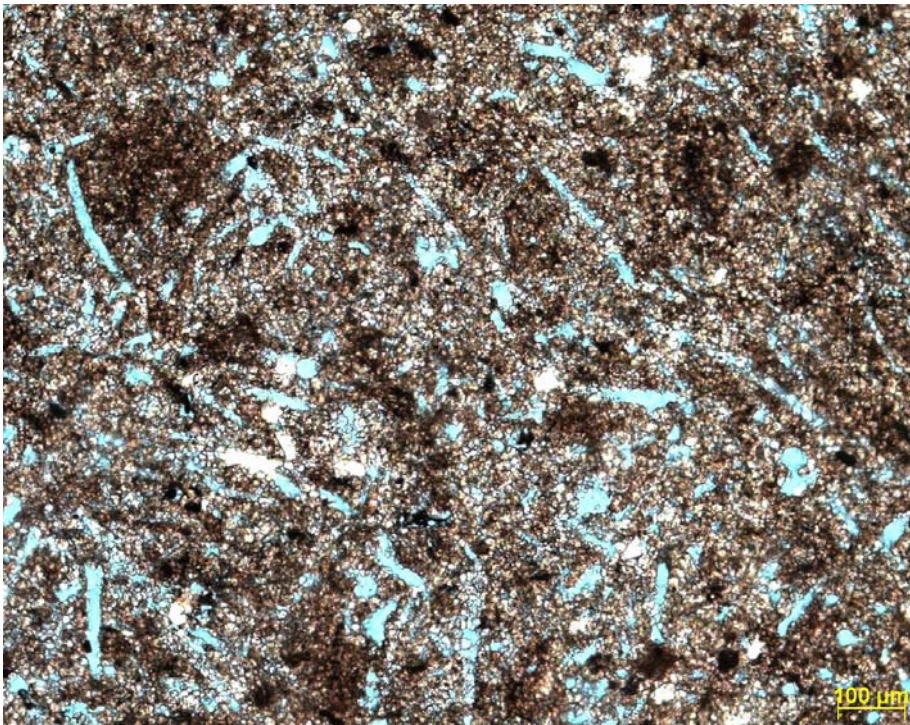


Figure D.9: Spiculiferous wackestone sub-facies exhibiting HI-Be porosity. Sample B48-8, 5373'.

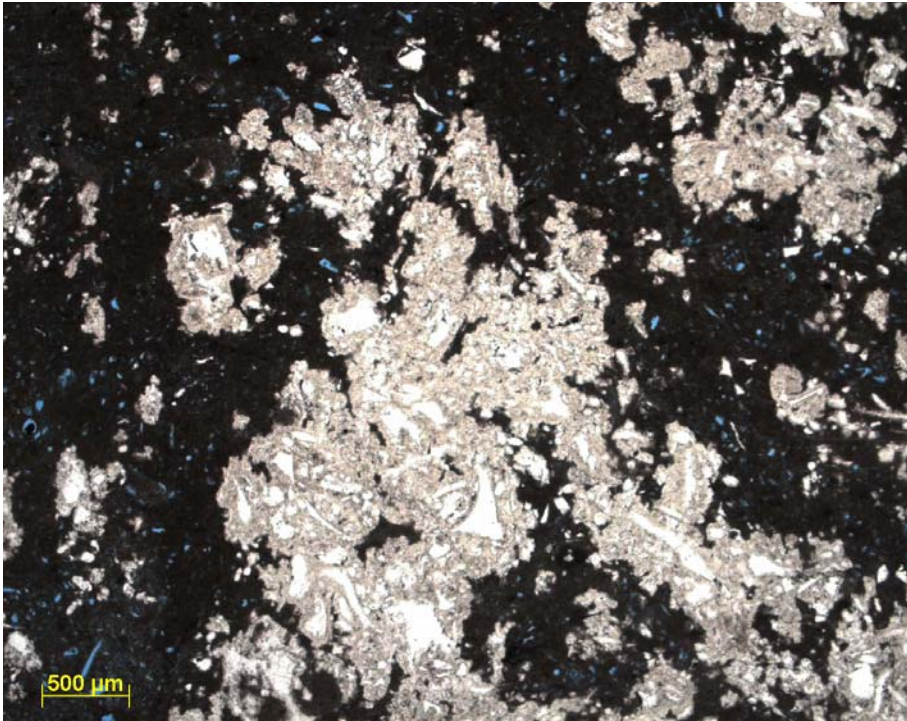


Figure D.10: Skeletal-peloidal wackestone (W facies) illustrating HI-Ar porosity after anhydrite replacement and cementation. Sample M2, 5324'.

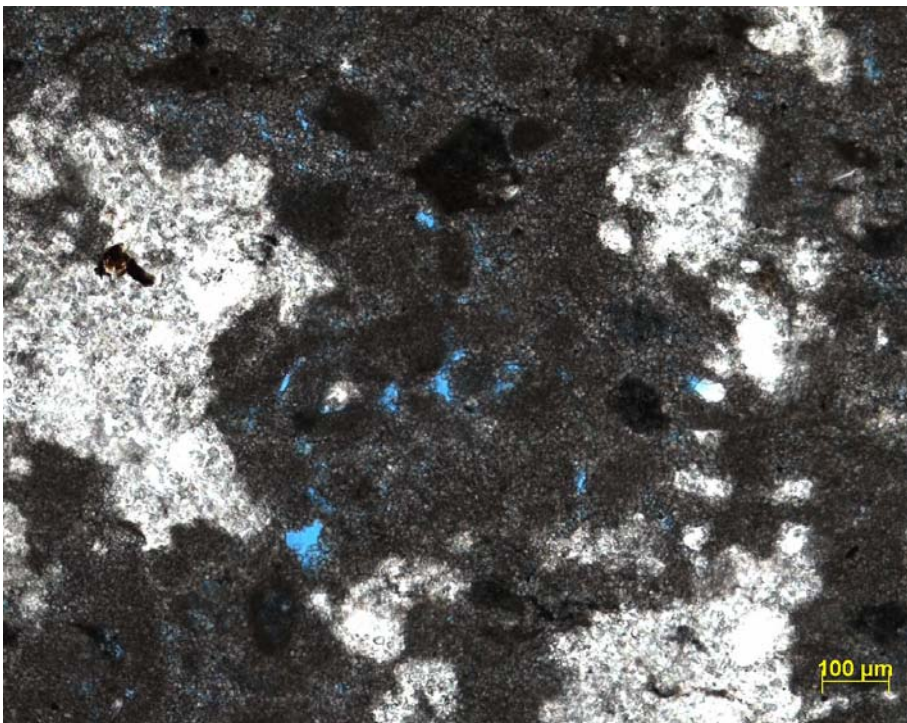


Figure D.11: Wackestone facies with indistinct micritic peloidal grains; displays HI-Ar porosity after anhydrite replacement/cementation. Sample M19-4, 5301'.



Figure D.12: Packstone facies with unidentifiable peloidal grains; displays H1-Br porosity after mechanical grain compaction. Sample M3, 5305.

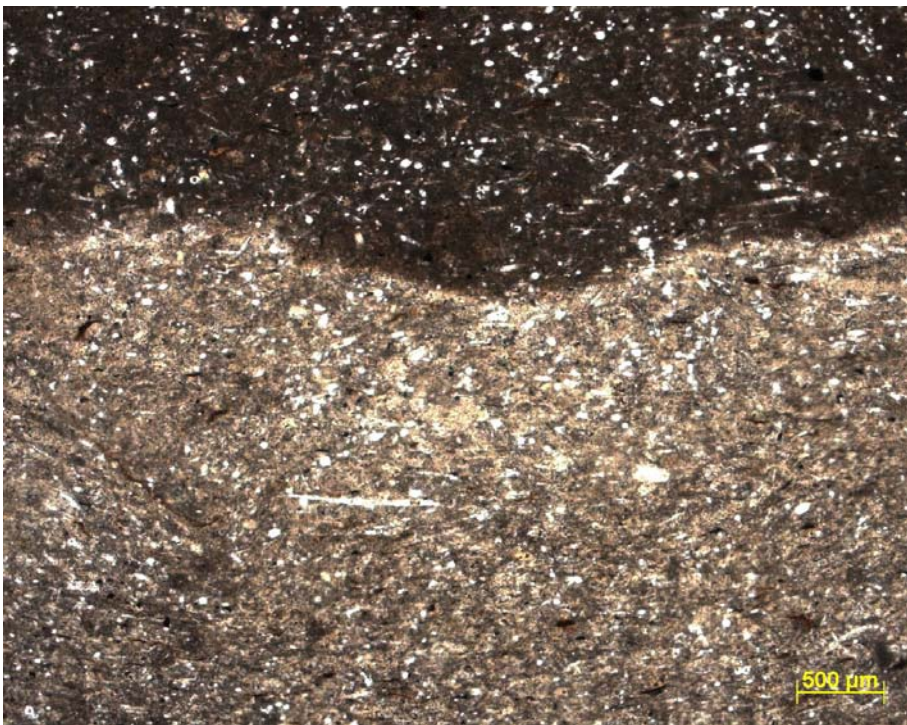


Figure D.13: Spiculiferous wackestone sub-facies; lower, light colored interval exhibits extensive siliceous replacement and H1-Cr porosity. Sample M19-4, 5276'.

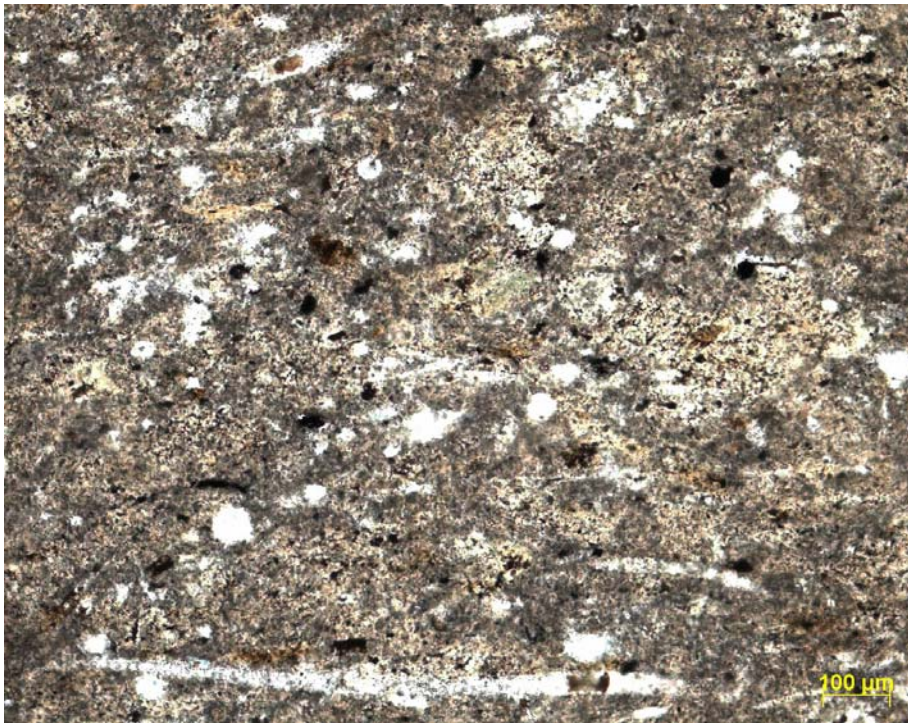


Figure D.14: Siliceous replacement extends beyond grain boundaries into surrounding matrix severing facies/porosity relationship. H1-Cr porosity. Sample M19-4, 5276'.

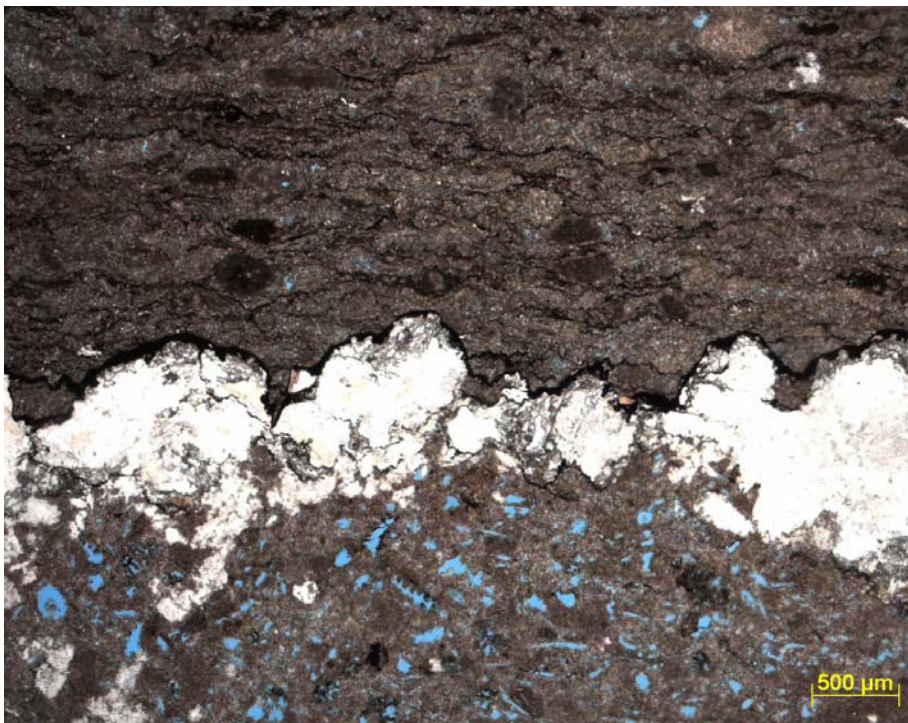


Figure D.15: Sample M3, 5305' illustrates stylolitic contact between H1-Br porosity (upper) after compaction and H1-Ae porosity (lower) after dissolution.



Figure D.16: Siliciclastic silty wackestone from M3, 5337'. Possible marker bed below Sunflower pay.

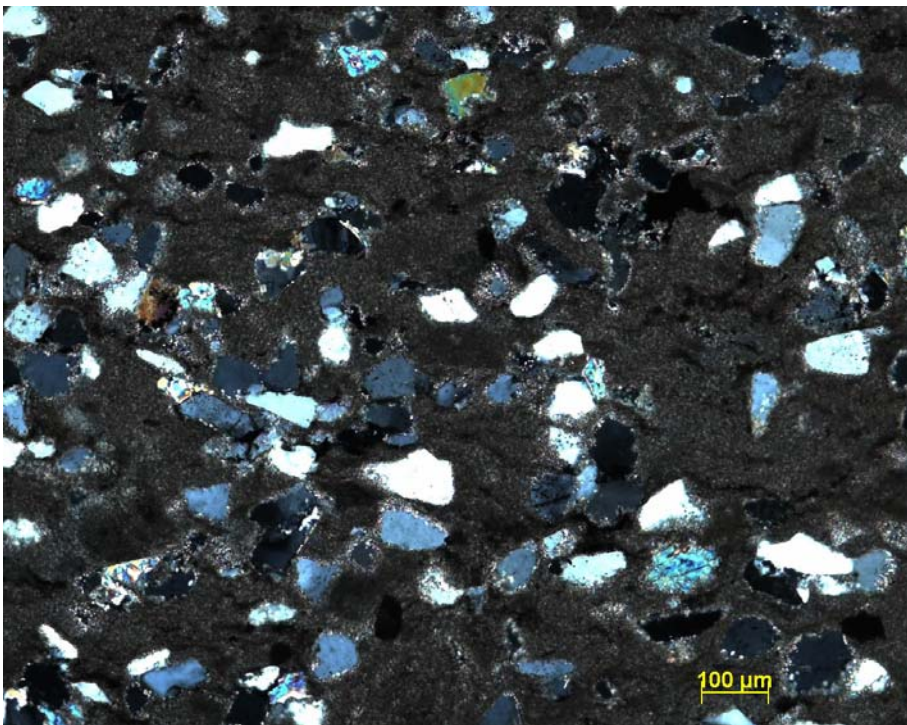


Figure D.17: Siliciclastic silty wackestone from M3, 5337' under cross-polarized light.

VITA

Name: Aubrey Humbolt

Address: 13980 S. 4210 Rd.
Claremore, OK 74017

Email Address: aubreys@tamu.edu

Education: B.S., Geology, Oklahoma State University, 2006
M.S., Geology, Texas A&M University, 2008

Professional Affiliations: American Association of Petroleum Geologists
Geological Society of America

Professional Experience: ConocoPhillips, Bartlesville, OK – Assistant Geologist
Green Country Petrophysics, Bartlesville, OK – Contractor
Texland Petroleum, Fort Worth, TX – Contractor
Devon Energy, Oklahoma City, OK – Geologist